Comparative Embryology of Arctoperlaria (Insecta: Plecoptera)

January 2019

Shodo MTOW

Comparative Embryology of Arctoperlaria (Insecta: Plecoptera)

A Dissertation Submitted to

the Graduate School of Life and Environmental Sciences,

the University of Tsukuba

in Partial Fulfillment of the Requirements

for the Degree of Doctor of Philosophy in Science

(Doctoral Program in Biological Sciences)

Shodo MTOW

CONTENTS

ABSTRACT

Plecoptera is one of the most controversial groups in reconstruction of interordinal relationships of insects. Aiming at 1) the detailed description of the embryonic development of Plecoptera, and 2) the reconstruction of the groundplan and phylogeny of Plecoptera and Polyneoptera, the comprehensive comparative embryological study of Plecoptera was conducted, using nine arctoperlarian stoneflies from nine families, i.e., Scopuridae, Taeniopterygidae, Leuctridae, Capniidae, and Nemouridae of Euholognatha, and Perlidae, Chloroperlidae, Perlodidae, and Peltoperlidae of Systellognatha.

The egg structure and embryonic development of nine arctoperlarian plecopterans were examined and described with spherical reference to *Scopura montana* (Scopuridae). Euholognatha has eggs characterized by a thin, transparent chorion, while the eggs of Systellognatha are characterized by a collar and anchor plate at the posterior pole. These features represent an apomorphic groundplan for each group.

The embryos are formed by the concentration of blastoderm cells toward the posterior pole of the egg. Soon after the formation of the embryo, amnioserosal folds are formed and fused with each other, resulting in a ball-shaped “embryo-amnion composite” that is a potential autapomorphy of Plecoptera. As an embryological autapomorphy of Polyneoptera, embryo elongation occurs on the egg surface, supporting the affiliation of Plecoptera to Polyneoptera. After its elongation on the egg surface, the embryo sinks into the yolk with its cephalic and caudal ends remaining on the egg surface. This unique embryonic posture may be regarded as an apomorphic groundplan of Plecoptera.

The serosa converges beneath the embryo to form a thickened serosa, comprising cells in a radial arrangement, in association with the formation of the amnioserosal fold. The thickened serosa then deposits the thickened serosal cuticle, consisting of four layers differing in fine structure and electron density. These serosal derivatives may also be regarded as an embryological autapomorphy of Plecoptera.

Arctoperlarian plecopterans perform three types of katatrepsis: 1) the first type, in which the embryo's anteroposterior and dorsoventral axes change in reverse during katatrepsis, is found in Capniidae, Nemouridae, Perlidae, Chloroperlidae, and Perlodidae, and this sharing is symplesiomorphic; 2) the second one, in which the embryo's axes are not changed during katatrepsis, is found in Scopuridae, Taeniopterygidae, and Leuctridae, and this may be regarded as synapomorphic to them; 3) the third one, in which the embryo rotates around its anteroposterior axis by 90° during katatrepsis as known for Pteronarcyidae, is found in Peltoperlidae, and this type may be synapomorphic to these two families.

INTRODUCTION

Hexapoda are the most diverse group among the organisms which have ever appeared in the 3-billion-year history of life on Earth, and the most prevailed animals on land, accounting for three quarters of all animal in species (Grimaldi and Engel, 2005). Hexapoda or Insecta s. lat. are divided into Protura, Collembola, Diplura, and Insecta s. str. or Ectognatha, which comprise Archaeognatha and Dicondylia (= Zygentoma + Pterygota). Wing-acquired insects or Pterygota represent more than 99% of all known insect species, and they consist of two monophyletic groups based on the functional structure of the wings: Palaeoptera, which have not yet developed the ability to fold the wings back over the abdomen, and Neoptera, which have acquired the mechanism to fold the wings on their abdomen at resting. Neoptera amount to 99% in number of species in Pterygota, and are divided into three major lineages: Polyneoptera, derived from the early explosive radiation of Neoptera, Acercaria (= Paraneoptera excluding Zoraptera), which are specialized in total lacking of cerci, and Holometabola, which are characterized by holometabolous metamorphosis.

Polyneoptera comprise ten lower neopteran orders, including the Plecoptera, Dermaptera, Embioptera, Phasmatodea, Orthoptera, Zoraptera, Grylloblattodea, Mantophasmatodea, Mantodea, and Blattodea s. lat. (= “Blattaria” + Isoptera). However, phylogenetic relationships among these orders have been much disputed over, and problems persist in the higher-level phylogeny of insects (Fig. 1) (e.g., Kristensen, 1975, 1991; Boudreaux, 1979; Hennig, 1981; Klass, 2009; Beutel et al., 2013, 2017; Kjer et al., 2016). In addition, the monophyly of Polyneoptera has been debated over for a long time, but it was recently supported based on morphological and embryological studies (e.g.,

Yoshizawa, 2011; Mashimo et al., 2014; Wipfler et al., 2015, Fig. 1B) and molecular data (e.g., Ishiwata et al., 2011, Fig. 1D; Song et al., 2016); Misof et al. (2014) conducted a large-scale phylogenomic analysis based on transcriptomes of 1,478 genes, and provided a strong support for monophyletic Polyneoptera (Fig. 1E), which was collaborated by the latest phylogenomic study focused on polyneopteran insects (Wipfler et al., 2019). Phylogenetic positions of Zoraptera and Dermaptera, both of which has long been under debate (see Klass, 2003, 2009; Beutel and Weide, 2005), were reliably placed in the monophyletic Polyneoptera (e.g., Ishiwata et al., 2011; Yoshizawa, 2011; Mashimo et al., 2014; Misof et al., 2014). In spite of recent challenges from various disciplines, phylogenetic relationships within Polyneoptera remain still far apart from consensus (see Beutel et al., 2013).

Plecoptera or stoneflies, of which affiliation to Polyneoptera seems currently established, represent an order with approximately 3,700 described species including fossil species distributed over all continents except Antarctica (DeWalt et al., 2015). Nymphs are almost exclusively aquatic and can be found mainly in cold, well-oxygenated running waters. Stoneflies are important components of clean streams, and they are often used as bioindicators (Fochetti and Tierno de Figueroa, 2008). The relationships between family group taxa within Plecoptera, comprising 16 families, have been widely accepted based on the two-suborder concept: the suborder Antarctoperlaria is found only in the Southern Hemisphere and contains four families, whereas the suborder Arctoperlaria, primarily inhabiting the Northern Hemisphere, is comped of two subgroups, Systellognatha and Euholognatha, each containing six families (Zwick, 2000; Beutel et al., 2014; DeWalt et al., 2019). Recent molecular phylogenetic analyses support the monophyly of each suborder and each arctoperlarian subgroup (Terry, 2004; Kjer et al.,

2006; McCulloch et al., 2016). However, in contrast to Antarctoperlaria, the monophyly of Arctoperlaria is only supported by morphological characters related to the complex mate-finding syndrome “drumming,” which is shared by all families of this group (with the exception of the Scopuridae) (Zwick, 1973, 2000).

The systematic position of Plecoptera, which are mostly defined by plesiomorphic features, has been highly controversial in the Neoptera (Zwick, 2009). Various hypotheses have been proposed for the phylogenetic position of Plecoptera including sistergroup relations to the remaining neopterans (e.g., Kristensen, 1975, 1991; Beutel and Gorb, 2006, Fig. 1A; Klug and Klass, 2007; Zwick, 2009), to the remaining polyneopterans (Paurometabola or Pliconeoptera including Zoraptera, cf. Wipfler et al., 2015, Fig. 1B) (Fausto et al., 2001; Beutel et al., 2014) and even to Paraneoptera s. lat. (= Acercaria + Zoraptera) + Holometabola (Ross, 1955, Fig. 1C; Hamilton, 1972). As the candidates of plecopteran sistergroup, Hennig (1981) suggested the remining polyneopterans, or alternatively Paraneoptera s. lat. + Holometabola, with no convincing support for either view provided. Recent comparative morphologies, molecular phylogenetics, and combined analyses have proposed different polyneopteran orders or assemblages as the sister group of Plecoptera, including the “Dermaptera” (Ishiwata et al., 2011, Fig. 1D), “Embioptera” (Kukalová-Peck, 2008), “Orthoptera” (Kômoto et al., 2012), “Zoraptera” (Matsumura et al., 2015), “Zoraptera + Dermaptera” (Terry and Whiting, 2005), “Zoraptera + Embioptera” (Grimaldi and Engel, 2005), “Chimaeraptera (= Xenonomia = Grylloblattodea + Mantophasmatodea)” (Blanke et al., 2012), “Orthoptera + Chimaeraptera + Eukinolabia (= Embioptera + Phasmatodea) ＋ Dictyoptera (= Mantodea + Blattodea)” (Misof et al., 2014, Fig. 1E). However, these recent changes were not always based on new evidence for Plecoptera itself, but

Plecoptera was only shoved around as other taxa were studied and views of their interrelations changed (Zwick, 2009).

A comparative embryological approach can be a potential source of deep phylogenetic information that can help to resolve these debates for the following reasons: 1) the comparative embryology can critically evaluate the homology of given features following and comparing their morphogenetic processes (e.g., Mashimo and Machida, 2017); 2) it can introduce the features which only appear during the embryonic period to the phylogenetic reconstruction (e.g., Machida, 2006; Fujita and Machida, 2017); and 3) it enables more reliable reconstruction of the groundplan of given groups and/or features because it can refer to the primary state which has suffered from little modification (e.g., Mashimo et al., 2014). In the past few decades, Machida and his colleagues have been vigorously provided embryological studies, which have provided us with novel embryological knowledge on hexapods and enable us to reconstruct their groundplan and phylogeny. For example, 1) the embryological information was provided concerning the orders/suborders on which embryological knowledge had been totally lacking, e.g., Protura (Machida and Takahashi, 2003; Fukui and Machida, 2006), Zoraptera (Mashimo et al., 2014), Mantophasmatodea (Machida et al., 2004), Raphidioptera (Tsutsumi and Machida, 2006), and coleopteran suborders Archostemata and Myxophaga (Kojima et al., in prep.); 2) the evolution of Hexapoda was discussed from the comparative embryological perspective, based on the successional changes of functional specialization between the embryo proper and embryonic membranes (e.g., Machida et al., 1994a, 2002; Machida and Ando, 1998; Ikeda and Machida, 2001; Fukui and Machida, 2006; Machida, 2006, 2009; Masumoto and Machida, 2006; Sekiya and Machida, 2009; Tomizuka and Machida, 2015) and the critical examination of cephalic construction in Hexapoda (e.g.,

Ikeda and Machida, 1998; Fukui and Machida, 2009; Sekiya and Machida, 2011; Blanke and Machida, 2016; Tomizuka and Machida, 2017); 3) a reliable phylogeny formulated as "Ellipura (= Protura + Collembola) + Cercophora [= Diplura + Ectognatha (= Archaeognatha + Zygentoma + Pterygota)] was presented, which is congruent with the comprehensive, large-scale transcriptome-based phylogenomics (Misof et al., 2014), dismissing not only Hennig's "Entognatha-Ectognatha System" (Hennig, 1981) formulated as "Entognatha (= Ellipura + Diplura) + Ectognatha" but "Nonoculata (= Protura + Diplura)" hypothesis proposed from molecular phylogenetic studies (e.g., Luan et al., 2005); and 4) as for Polyneoptera, of which monophyly had been often disputed (see above), the comparative embryology first suggested the two potential morphological autapomorphies of Polyneoptera, i.e., i) the formation of embryo by the fusion of paired regions with higher cellular density in blastoderm, and ii) immersion of the embryo into the yolk after its full elongation on the egg surface (Mashimo et al., 2014: see also Uchifune and Machida, 2005; Jintsu, 2010; Shimizu, 2013; Fujita and Machida, 2017; Fukui et al., 2018), to advocate the monophyletic Polyneoptera.

The earliest embryological study on Plecoptera was made by Miller (1939, 1940) using a systellognathan *Pteronarcys proteus* Newman, 1838 of Pteronarcyidae. He examined and described its embryonic development in detail, focusing on the early development, embryonic membranes, yolk cells, and morphogenesis of several organs. Khoo (1968a,b) studied the egg diapause of a systellognathan *Diura bicaudata* (Linnaeus, 1758) of Perlodidae, and a euholognathan *Brachyptera risi* (Morton, 1896) of Taeniopterygidae with a brief note of embryogenesis. Detailed studies using a systellognathan *Kamimuria tibialis* (Pictet, 1841) of Perlidae have been conducted by Kishimoto and Ando (1985, 1986) and Kishimoto (1986, 1987) including the early

development, general embryogenesis, and organogenesis of alimentary canal and nerves system. Thereafter, a brief report on the blastokinesis of several arctoperlarian embryos by Kishimoto (1997a) and a note on the egg swelling during embryogenesis in some euholognathan Leuctridae and Nemouridae by Zwick (1999) appeared. Recently, the sub-lethal effects of water temperature on egg development was investigated in several aquatic insects including euholognathan Notonemouridae (Ross-Gillespie et al., 2018). In spite of these contributions, however, our knowledge of the embryonic development of Plecoptera remains rather insufficient and fragmented: although several detailed studies exist in the arctoperlarian subgroup Systellognatha, these come from only two of six families: *Pt. proteus* of Pteronarcyidae by Miller (1939, 1940) and *K. tibialis* of Perlidae by Kishimoto and Ando (1985, 1986) and Kishimoto (1986, 1987); little data exist on the development of other systellognathan families and Euholognatha (e.g., Khoo, 1968a,b; Kishimoto, 1997a). In addition, embryological information on Antarctoperlaria is entirely lacking. Thus, the comparative embryological studies covering families as much representatives as possible are strongly desired.

Given this background, I have undertaken a comparative embryological study of Plecoptera, covering all the nine Japanese arctoperlarian families (Kawai, 1967; Shimizu et al., 2005): five families of the infraorder Euholognatha, i.e., Scopuridae, Taeniopterygidae, Leuctridae, Capniidae, and Nemouridae; four families of the infraorder Systellognatha, i.e., Perlidae, Chloroperlidae, Perlodidae, and Peltoperlidae. The purposes of the present study are: 1) to describe the egg structure and embryonic development in nine plecopteran families, 2) comparing the results with previous works to reconstruct the groundplan of Plecoptera and Polyneoptera, 3) to discuss the

interfamily relationships in Arctoperlaria, and 4) to provide a new, sound basis contributing to solving the phylogenetic issues concerning Plecoptera and Polyneoptera.

MATERIALS AND METHODS

1. Materials

Adults of nine arctoperlarian stoneflies from the nine families (Table 1) were collected in 2014 to 2017 around the streams in Sugadaira Kogen, Ueda, Nagano, Japan, i.e., Daimyojin-zawa, Kara-sawa, and Naka-no-sawa. As for *Scopura montana*, late instar larvae were reared and raised to adults *en masse* in plastic cases (167 mm × 117 mm × 58 mm) containing stones and a layer of water and fed with fallen leaves.

Females after mating were kept separately in plastic cases (68 mm × 39 mm × 15 mm) containing tissue paper under controlled temperature (Table 1), and fed on fruits (apple or persimmon) and commercial food for insects (Mushi-jelly, Mitani, Ibaraki, Japan) and fish (TetraFin, Spectrum Brands Japan, Yokohama, Japan, or Koi-no-sato, Japan Pet Food, Tokyo, Japan). The eggs deposited by females were incubated in plastic cases (36 mm × 36 mm × 14 mm) filled with water under controlled temperature (Table 1).

2. Fixation

Prior to fixation, eggs were soaked in commercial bleach (Kitchen Bleach S, Mitsuei, Fukushima, Japan) for several seconds and cleaned using a small brush to remove the gelatinous layer that covered them. The eggs were rinsed in Ephrussi-Beadle's solution (0.75% NaCl, 0.035% KCl, 0.021% $CaCl_2$) containing detergent (0.1% Triton X-100), punctured with a fine needle, fixed with either Kahle's fixative (ethyl alcohol : formalin : acetic acid : distilled water = 15 : 6 : 2 : 30) or FAA (ethyl alcohol : formalin : acetic acid = 15 : 5 : 1) for 24 h, and stored in 80% ethyl alcohol at

room temperature or Karnovsky's fixative [2% paraformaldehyde and 2.5% glutaraldehyde in 0.1 M HCl-sodium cacodylate buffer, pH 7.2 (SCB)] for 24 h and stored in SCB at 4°C.

3. External morphology

The fixed eggs were stained with DAPI (4',6-diamidino-2-phenylindole dihydrochloride) solution diluted to 10 μg/l with PBS (18.6 mM $NaH_2PO_4 \cdot H_2O$, 84.1 mM $NaH_2PO_4 \cdot 2H_2O$, 1.75 M NaCl, pH 7.4) at 4°C for 20 min to several days depending on specimens. The eggs stained with DAPI were observed under a fluorescence stereomicroscope (MZ FL III + FluoCombi, Leica, Heerbrugg, Switzerland) with UV excitation at 360 nm. Systellognatha eggs, which have a tough chorion layer, were dechorionated with a fine needle and fine forceps prior to staining.

For scanning electron microscopy (SEM), eggs and embryos dissected out of the fixed eggs using fine forceps in distilled water were postfixed with 1% OsO_4 for 1 h. They were dehydrated in a graded ethanol series, dried either with a critical point dryer (Samdri-PVT-3D, tousimis, Rockville, USA) or naturally dried with HMDS (1,1,1,3,3,3-Hexamethyldisilazane) as described by Faull and Williams (2016), coated with gold, and then observed under an SEM (SM-300, TOPCON, Tokyo, Japan) at an acceleration voltage of 15 kV.

Dissected embryos and *Apteroperla tikumana* eggs, which are prone to distortion in the course of processing due to their softness, were observed using the nano-suit method, as described by Takaku et al. (2013) and Fujita et al. (2016). They were soaked in 1% polyoxyethylene sorbitan monolaurate (Tween 20) solution for 1 h, blotted briefly

on dry filter paper to remove excess solution, mounted on a stab, and observed with the SEM at an acceleration voltage of 5 kV.

The embryonic cuticle secreted at later developmental stages over the entire surface of the embryo is often swollen and separated from the embryo or wrinkled. In coated specimens this impedes accurate observation of the surface of the embryo in the usual high-vacuum SEM mode (Machida, 2000). To surmount the problem, non-coated embryos were observed using a low-vacuum SEM (SM-300 Wet-4, TOPCON, Tokyo, Japan) at 13 Pa at an acceleration voltage of 15 kV.

To record blastokinesis, eggs were observed alive using a time-lapse VTR system (CK-2 or CK-40, inverted microscope, Olympus, Tokyo, Japan; TSN401A, CCD color camera, Elmo, Nagoya, Japan; Live capture 2, web camera system, downloaded from http://www2.wisnet.ne.jp/~daddy).

4. Histology

The eggs fixed with Kahle's fixative were dehydrated in a graded ethanol series and embedded in a methacrylate resin (Technovit 7100, Kulzer, Wehrheim, Germany) in accordance with Machida et al. (1994a,b). Semithin sections at a thickness of 2 μm were cut using a semithin microtome (H-1500, Bio-Rad, Hercules, USA), equipped with a tungsten carbide knife (Superhard Knife, Meiwafosis, Tokyo, Japan). Sections were stained with 0.5% Delafield's hematoxylin for 12 h, 0.5% eosin G for 1 h and 0.5% fast green FCF 100% ethanol for 1 min, and observed with a biological microscope (Optiphoto-2, Nikon, Tokyo, Japan) and captured with a CCD camera (DS-Fi2, Nikon, Tokyo, Japan).

The eggs fixed with Karnovsky's fixative were then post-fixed with 1% OsO_4 for 1 h, dehydrated in a graded ethanol series, and embedded in an epoxy resin (Agar Low Viscosity Resin Kit, Agar Scientific, Essex, UK). Serial, semi-thin sectioning at a thickness of 0.75 μm was performed, using a ultramicrotome (MT-XL, RMC, Arizona, USA) equipped with a diamond knife (Histo Jumbo, DiATOME, Nidau, Switzerland), according to methods described by Blumer et al. (2002). The sections were then stained using 0.1% toluidine blue O solution and observed under the Nikon Optiphot-2 microscope and captured with the Nikon DS-Fi2 CCD camera.

5. Transmission electron microscopy

For transmission electron microscopy (TEM), the eggs embedded in the above-mentioned epoxy resin were processed with the RMC MT-XL ultramicrotome, equipped with a diamond knife (Histoknife, Drukker, Cuijk, Netherlands), into 75-nm thick sections. The sections were then stained with platinum blue (TI Blue, Nisshin EM, Tokyo, Japan, Inaga et al., 2007) and lead citrate (Venable and Coggeshall, 1965) and observed with a transmission electron microscope (HT7700, Hitachi, Tokyo, Japan) at an acceleration voltage of 80 kV.

RESULTS

The orientation of the insect eggs is defined according to the embryo just before hatching (Wheeler, 1893). When applying this definition to plecopterans we encounter a serious problem. As generally found in hemimetabolan insects, i.e., Palaeoptera, Polyneoptera, and Acercaria, usually in plecopterans, 1) the embryo forms at the posterior pole of the egg or the ventral side near the posterior pole; 2) in the course of anatrepsis, the embryo substantially elongates with its posterior end ahead, resulting in its ventral side facing the dorsal side of the egg and the embryo's anteroposterior axis reversed, i.e., both the anteroposterior and dorsoventral axes of the embryo become opposed to those of the egg; 3) katatrepsis then occurs, and the embryo appears again on the egg surface, shifting its position to the ventral side of the egg, and its anteroposterior axis is reversed, i.e., both the anteroposterior and dorsoventral axes of the embryo correspond again to those of the egg (see Anderson, 1972; Mashimo et al., 2014). This type of blastokinesis was revealed to occur in a large proportion of the plecopterans examined in the present study such as *Apteroperla tikumana* (Capniidae) (Figs. 37, 55: see also 1.4.). However, an aberrant form of katatrepsis, in which the embryo maintained unchanged positions of the anteroposterior and dorsoventral axes, was found to be performed in a small proportion of the plecopterans examined such as *Scopura montana* (Scopuridae) (Figs. 4, 55: see also 1.1.). In these plecopterans, the embryo reaches hatching, with its anteroposterior and dorsoventral axes opposed to those of other plecopterans. Simply following to the general definition of the orientation of eggs by Wheeler (1893), we would have to describe, for example, that in these plecopterans the embryo forms at the *anterior* pole of the egg, which would thus differ from other plecopterans. To avoid such a problem in orientation,

in the present study I define the orientation of the egg in Plecoptera as follows: 1) the posterior is where the embryo forms, and the anterior is its opposite; 2) the dorsal is where the embryo exists just before katatrepsis, and the ventral is the opposite.

In what follows, I describe the egg structure and an outline of embryonic development in one species from each of nine arctoperlarian families. As for the embryonic development, first I made a detailed description on *S. montana* with special reference to external morphology, dividing it into 12 stages following Kishimoto and Ando (1985), and then I gave descriptions for other species, focusing on the differences from *S. montana* and/or other species.

1. Eggs and embryonic development of Euholognatha

1.1 *Scopura montana* (Scopuridae)

1.1.1 Egg

Eggs are spheroidal with long and short diameters of 330–400 μm and 300–330 μm, respectively (Fig. 2A). They are ivory in color because the yellowish yolk is visible through the transparent egg membranes. The surface is surrounded by a sticky coat. The egg membranes are composed of three layers: the exochorion, the endochorion, and the thin vitelline membrane (Figs. 2B, 3A, B). The exochorion, representing a less electron-dense layer with a thickness of 0.5–1 μm (Fig. 3A), often peels off during embryonic development due to its fragility. The exochorion of the anterior third of the egg contains a weak, polygonal pattern, which forms several rosettes around the anterior pole of the egg (Fig. 2C): at the center of each rosette, a micropyle of ca. 2 μm in diameter opens, and the micropyles are arranged roughly in circle (Fig. 2C, D). The endochorion's outer surface is furnished with rod-like materials, approximately 1–2 μm in length and 0.4–0.5 μm in

height, and numerous small hemispherical protuberances with a diameter of 100 nm and a height of 75 nm (Figs. 2B, 3A, B). The endochorion is divided into endochorion 1 (Ench1) and endochorion 2 (Ench2), each containing two sublayers (Fig. 3B). The outer layer of the endochorion (i.e., the endochorion 2) comprises a 0.3–0.4 μm thick layer (Ench2-II) of high electron density and a 100-nm thick layer (Ench2-I) of low electron density. The inner layer of endochorion (i.e., the endochorion 1) is subdivided into a less electron-dense layer of approximately 0.5-μm thickness (Ench1-II) and a more electron-dense layer of approximately 100-nm thickness (Ench1-I). The vitelline membrane is a high electron-dense layer and fairly thin at approximately 10-nm thickness (Fig. 3A, B).

1.1.2 Embryonic Development

The egg period is 75–85 days at 8°C.

A series of embryonic development is shown in Figures 4 and 5.

Stage 1

The cleavage nuclei arrive at the egg surface (Fig. 6A, G), and a unicellular blastoderm forms (Fig. 6B, H). Soon after completion of blastoderm formation, the embryonic and extraembryonic areas are differentiated. The former forms at the posterior pole of the egg and is more densely cellulated than the latter (Fig. 6C, I), and the nuclei of the former are smaller and more crowded than those of the latter (Fig. 6D, E, J, K). The embryonic area is differentiated into a discoid germ disc about 100 μm in diameter, and the extraembryonic area is the serosa (Figs. 4A, 5A, 6F, L).

Stage 2

The amnion is produced from the margin of the germ disc or embryo, keeping step with the convergence of the serosa beneath the embryo (Fig. 7A). During this process, the amnion forms the amnioserosal fold along with the serosa, and anatrepsis starts. The amnioserosal fold, of which formation is more progressive in the posterior region of the embryo than in the anterior, extends beneath the embryo (Figs. 7B–D, 8A, B, 9A, B). Finally, the amnioserosal folds fuse with each other, and the amniotic pore becomes closed (Figs. 8C, 9C, D). After the fusion of the amnioserosal folds, the embryo is elliptical, with long and short diameters approximately 120 μm and 85 μm, respectively (Fig. 7D), but then becomes circular about 110 μm in diameter (Figs. 4B, 5B), and the outer and inner constituents of the folds, the serosa and amnion, detach from each other (Fig. 8C). The amnion then covers the embryo's venter and, together with the embryo, forms a compressed, ball-shaped "embryo-amnion composite" (Figs. 8C, 10A, C; see also Fig. 11A).

The condensed serosa beneath the embryo and the embryo-amnion composite further converge, resulting in a "thickened serosa" formation (Fig. 10A, C). Initially, the thickened serosa is composed of a simple condensation of serosal cells (Fig. 10A); however, they gradually assume a radial cell arrangement (Fig. 10C; see also Fig. 11A). At about the same time the thickened serosa starts to form, an electron-dense cuticular layer termed "serosal cuticle 1," which is approximately 1 μm-thick, is secreted from the microvilli of the serosal cells. When the secretion begins, the cuticular layer is discontinuously demonstrated (Fig. 10B), but soon after, the serosal cuticle 1 is completed as a continuous layer (Fig. 10D).

Stage 3

The embryo elongates approximately to 185 μm in length along the posterior egg surface (Figs. 4C, 5C). The protocephalon and protocorm differentiate, and the embryo assumes a pear-shape (Fig. 5C). As a result of fusion of amnioserosal folds, the egg surface is entirely covered with the serosa.

During Stage 3, the serosa further converges beneath the embryo, and the thickened serosa enlarges and takes on its definitive configuration (Fig. 11A–C). It is shaped like a compressed hemisphere, approximately 20 μm in height and 60–100 μm in diameter, and is composed of approximately 20 thickened serosal cells arranged radially. Each of these thickened serosal cells is columnar, with long and short diameters of approximately 30 μm and 10 μm, respectively (Fig. 11A–C). The cytoplasm in the apical (i.e., the direction facing the egg surface) part of the thickened serosa contains numerous granules of approximately 100 nm in diameter and intermediate electron density (Fig. 12A). A secretion showing a similar electron density to these granules then appears in the interspace between the microvilli. A cuticular layer of similar electron density, named "serosal cuticle 2," is then deposited beneath the serosal cuticle 1. Accordingly, these granules and the secretion are the precursors of serosal cuticle 2 (Fig. 12B).

Stage 4

The embryo elongates posterior to approximately 350 μm along the egg surface, attaining more than one-third of the egg circumference (Fig. 4D). The protocephalon grows wider into the form of a head lobe (Fig. 5D). Segmentation starts at this stage (not distinctly shown in figures).

During Stage 4, a cuticle layer that is less electron-dense than serosal cuticle 2, termed “serosal cuticle 3,” is then secreted (Fig. 13). This cuticle layer is demonstrated as toluidine-philic under light microscopy (see Fig. 19A, B). Numerous vertical striations, distinguishable by their higher electron density, run inside serosal cuticles 2 and 3 (Fig. 13).

Stage 5

The embryo elongates posteriorly with its caudal region ahead, and its anteroposterior axis is reversed (Fig. 4E). The thoracic to anterior abdominal region sinks into the yolk with the cephalic and posterior abdominal regions remaining on the egg surface (Figs. 4E, 5E). The embryo then assumes an S-shape. Segmentation proceeds towards the posterior, and appendages develop in the differentiated segments. The stomodaeum appears at the center of the head (Figs. 5E, 14). In the mandibular, maxillary, labial, and thoracic segments, the appendages differentiate, but in the intercalary segment appendages do not develop (Fig. 14). The neural groove appears as a continuous median groove in the ventral surface of the embryo (Fig. 14).

Stage 6

The embryo grows and further sinks into the yolk (Fig. 4F). Segmentation and appendage formation continue to proceed. The clypeolabrum appears as a single swelling anterior to the stomodaeum (Figs. 5F, 15B, C). The antennal, maxillary, labial and thoracic appendages elongate as lateral swellings (Fig. 15A–C). The mandibular appendages are less developed and shorter than the other appendages (Fig. 15C). At the caudal end of the embryo the proctodaeum invaginates (Fig. 15A).

During Stages 5 and 6, a cuticular layer with even less electron density than that of serosal cuticle 3, termed “serosal cuticle 4,” is heavily secreted (Fig. 16B). Serosal cuticle 4 is comprised of an outer fibrous part (SeCt4-I) and an inner lamellar one (SeCt4-II). This process completes a remarkably thickened (approximately 20 μm) cuticular structure (i.e., serosal cuticles 1, 2, 3, and 4) beneath the embryo (Fig. 16A).

The serosal cuticle, secreted by the region other than the thickened serosa, is very thin, i.e., 2–3 μm in thickness, and its layered construction is obscured. In this region, although the serosal cuticles 1 and 4 can be discerned, the serosal cuticles 2 and 3 are difficult to distinguish (Fig. 16A, C): these cuticles may be highly reduced or lacking.

Stage 7

The embryo grows in the yolk, attaining its maximum length (Figs. 4G, 5G). Antennal flagellum elongates medially (Fig. 17C, D). The maxillary, labial, and thoracic appendages divide themselves into the proximal coxopodite and distal telopodite, whereas the mandibles remain short (Fig. 17A, B). In the maxillary and labial appendages, the telopodites develop into palps, and their endites are enlarged, and the maxillary endites differentiate into two parts, the mesal lacinia and lateral galea (Fig. 17D). The thoracic appendages elongate posteriorly.

During Stage 7, the thickened serosa that acquired its definitive form in Stage 3, and accomplished the secretion of the serosal cuticles in Stage 6, begins degenerating. The radial cell arrangement of the thickened serosa then becomes loose and obscured (Fig. 19A–D). Many mitochondria are found in the cytoplasm close to the apical surface of the thickened serosa (Fig. 18A). The microvilli on that apical surface are rapidly

thinned and also begin to degenerate (Fig. 18A). During this process, the interspace between the microvilli becomes electron lucent (asterisks in Fig. 18A).

As the radial cell arrangement of the thickened serosa becomes looser, the contact point of the serosa and the thickened serosa shifts from the original ventral side of the thickened serosa (Figs. 18B, 19A, B) to the dorsal side (Fig. 19C, D).

Stage 8

The embryo develops further, with the abdomen enlarged in the yolk, and the head moving close to the egg surface (Figs. 4H, 5H). Antennal flagellum further elongates (Fig. 20C). In the maxillary and labial appendages, the palps are enlarged and the labial endites differentiate into two parts, the mesal glossa and lateral paraglossa (Fig. 20C). The labial appendages of both sides begin to move toward the median line (Fig. 20C, D). Thoracic appendages further elongate: coxopodites divide into two parts, the proximal subcoxa and the distal coxa, and telopodites differentiate into the trochanter, femur, tibia, tarsus and pretarsus (Fig. 20A, B). The first abdominal appendages or pleuropodia, which are divided into the proximal coxopodite and distal telopodite, are well developed, showing glandular appearance in section (Figs. 20A, B, 21). Cerci are differentiated as distinct paired appendages of 11th abdominal segment (Fig. 20A, D).

In early Stage 8, the contact point of the serosa and the thickened serosa shifts up to the central part of the thickened serosa dorsum. The serosa then breaks off contact with the thickened serosa and again fuses with the amnion, resulting in the recovery of the amnioserosal fold. The thickened serosa is then left behind on the thickened serosal cuticle until its degeneration (Fig. 19E, F).

In late Stage 8, the thickened serosa disintegrates (Fig. 22A). The serosal cells liberated from the disintegrated thickened serosa begin to float between the serosal cuticle and the serosa (Fig. 22A).

Stage 9

In this stage, katatrepsis occurs. The amnioserosal fold ruptures around the region where the amniotic pore closed, and the embryo appears again on the egg surface (Figs. 4I, 5I, 22B). The serosa migrates toward the ventral region of the egg and condenses to form the secondary dorsal organ. The amnion spreads over the area the serosa had occupied, functioning as the provisional dorsal closure (Figs. 4I, 5I, 22B). The embryo does not change its position during katatrepsis, and its positioning during intertrepsis on the dorsal side of the egg is maintained, with its head kept at the posterior pole of the egg. As a result, the anteroposterior and dorsoventral axes of the embryo remain opposite to those of the egg, and the embryo reaches hatching keeping this orientation (Figs. 4I–L, 22A, B, 54A–C). The labial appendages of both sides further move medially (Fig. 23A, C, D). Pro- and mesothoracic telopodites begin to elongate medially, whereas metathoracic telopodites still elongate posteriorly (Fig. 23A–C). The abdominal area begins to bend and elongate anteriorly. In the 11th abdominal segment, the Y-shape opening of proctodaeum surrounded with a supraanal lobe and a pair of subanal lobes can be seen (Fig. 23C).

The serosal cells liberated from the thickened serosa are still found between the serosal cuticle and the embryo or amnion (Fig. 22B).

Stage 10

The embryo further grows and the definitive dorsal closure proceeds from the posterior (Figs. 4J, 5J). The secondary dorsal organ enlarges. The clypeolabrum differentiates into the clypeus and labrum (Fig. 24D). The frons becomes distinct (Fig. 24D). The antennal flagellum further elongates (Fig. 24C). The metathoracic telopodites begin to elongate toward the median line, and a pretarsus with bifurcated unguis is clearly distinguished (Fig. 24A, B). The abdomen further elongates anteriorly, and the caudal end of the embryo reaches the labrum (Fig. 24D).

Stage 11

Definitive dorsal closure is almost complete, and the head capsule acquires its definitive form (Figs. 4K, 5K, 25A, B). A transparent embryonic cuticle is secreted, and a sclerotized, conical-shaped egg tooth forms on the frons (Figs. 25C, D, 26). The compound eyes appear (Fig. 5K). The thoracic appendages further elongate and develop.

Stage 12

The larval cuticle, on the surface of which the setation is observed, is secreted, and the embryo acquires the configuration of the first instar larva (Figs. 4L, 5L, 27A–C). The thoracic legs further elongate, and the bifurcated claws on their tips are distinct (Fig. 27A, B). The full-grown embryo tears the chorion and serosal cuticle using the egg tooth and hatches out.

The formation of the pleura was examined under the low-vacuum SEM of non-coated specimens. Lateral region of subcoxa was observed to differentiate into pleural sclerites between coxa and terga (Fig. 27B). The anterior episternum and posterior epimeron are defined by the pleural suture (Fig. 27B).

First instar

The body length is approximately 1.2 mm. The antenna is composed of nine antennomeres (Fig. 28A). The head is prognathous and is trapezoidal, being wider toward the posterior (Fig. 28A, B). The maxillary coxopodites are divided into a distal cardo and proximal stipes (Fig. 28C). The maxillary palp and the endites of maxilla, mesal lacinia and lateral galea, are well developed (Fig. 28C). The distal and proximal parts of coxopodites of the labial appendages of both sides have been in close contact with and fused with each other to form the prementum and postmentum, respectively (Fig. 28C). The labial palp is well developed. The glossa is still rudimentary (Fig. 28C). The thoracic appendage consists of coxa, trochanter, femur, tibia, tarsus with three tarsomeres and pretarsus with unguis (Fig. 28D). Thoracic sternal and pleural sclerites are well sclerotized and clearly distinguished (Fig. 29A, B). Sternal apophysis can be seen between the basisternum and spinasternum (Fig. 29A). In the end of 10th abdominal segment supraanal lobe and subanal lobe are visible (Fig. 28E). Three-segmented cerci are bamboo-shoot-like in shape (Fig. 28E).

1.2 *Obipteryx* sp. (Taeniopterygidae)

1.2.1 Egg

Eggs are spheroidal with long and short diameters approximately 230 μm and 170 μm, respectively (Fig. 30A). The chorion is thin and transparent. A pair of micropylar areas is on both lateral sides at the level of equator, each of which has three to four micropyles ca. 2 μm in diameter with a hood which is the chorionic extension overhanging the micropyle (Fig. 30B).

1.2.2 Embryonic Development

The egg period is approximately 125 days, including the diapause period of two months, at 12°C.

The embryonic development of *Obipteryx* sp. closely resembles that in *Scopura montana* in general aspects, but in *Obipteryx* sp. the germ disc approximately 20 µm in diameter is much smaller than that of *S. montana*, even when considering its smaller egg size (Stage 1, Fig. 31A). Soon after the amnioserosal folds fuse with each other at the onset of anatrepsis, development enters diapause of approximately 60 days (Stage 2, Fig. 31B). During diapause period, the thickened serosa is formed beneath the embryo (Fig. 32A): the same as in the size of embryo, the thickened serosa is remarkably small compared to *S. montana*. When diapause terminates, the embryo elongates along the posterior egg surface (Stage 3, Fig. 31C). The embryo elongates posterior with its caudal end ahead, attaining more than one-third of the egg circumference (Stage 4, Fig. 31D). In this stage, the serosal cuticle becomes a little thickened beneath the embryo as the thickened serosa (Fig. 32B). The anterior abdomen (Stage 5, Fig. 31E), followed by the thoracic region, sinks into the yolk with the cephalic region and posterior abdomen remaining on the egg surface, and the embryo assumes an S-shape (Stages 6–8, Fig. 31F–H). The embryo orientation is opposite that of the egg. Katatrepsis (Stage 9, Fig. 31I) and development in post-katatrepsis stages (Stages 10–12, Fig. 31J–L) of *Obipteryx* sp. are similar to those in *S. montana*, and the embryo reaches hatching with its orientation contrary to that of the egg.

1.3 *Paraleuctra cercia* (Leuctridae)

1.3.1 Egg

Eggs are spheroidal with long and short diameters approximately 140 μm and 120 μm, respectively (Fig. 33). The chorion is thin and transparent. No data were obtained on micropyles.

1.3.2 Embryonic Development

The egg period is 45–55 days at 12°C.

The embryonic development of *Paraleuctra cercia* basically resembles those of the stoneflies described above. The embryo formed (Stages 1, 2, Fig. 34A, B) posteriorly elongates with its caudal end ahead, attaining approximately 40% of the egg circumference (Stages 3, 4, Fig. 34C, D). The thickened serosa is formed beneath the embryo, of which cells show a radial arrangement (Fig. 35A). The following elongation of the embryo and its positioning in the yolk are similar to those shown in the stoneflies described above (Stages 5–8, Fig. 34E–H). The egg and embryo are orientated opposite of each other. During embryogenesis the serosal cuticle beneath the thickened serosa becomes bloated, and the thickened serosal cuticle is formed (Fig. 35B). Katatrepsis (Stage 9, Fig. 34I) and development in post-katatrepsis stages (Stages 10–12, Fig. 34J–L) are similar to those of the two species described above, and the embryo reaches hatching with its orientation contrary to that of egg.

1.4 *Apteroperla tikumana* (Capniidae)

1.4.1 Egg

Eggs are spheroidal with long and short diameters approximately 170 μm and 135 μm, respectively (Fig. 36). The chorion is thin and transparent. No data were obtained on micropyles.

1.4.2 Embryonic Development

The egg period is approximately 55 days at 4°C.

Prior to katatrepsis, embryonic development of *Apteroperla tikumana* resembles the species shown above (Stages 1–8, Fig. 37A–H), with few minor differences regarding the positioning of the embryo. The early embryo grows also anteriorly (Stages 3, 4, Fig. 37C, D), and the cephalic end of the embryo attains approximately the middle of the ventral side of the egg (Stages 6–8, Fig. 37F–H). The thickened serosa and thickened serosal cuticle are formed beneath the embryo (Fig. 38). The immersion of the embryo into the yolk in Stage 5 is restricted to the caudal region of the abdomen (Fig. 37E). In katatrepsis, differently from the three above-mentioned stoneflies, the embryo appeared on the egg surface moves along the egg surface with its head ahead, passing the posterior pole of the egg, then on the egg's ventral side toward the anterior pole. Consequently, the anteroposterior and dorsoventral axes of the embryo, which had been in an opposite orientation to those of the egg during intertrepsis (e.g., Stage 8, Fig. 37H), are reversed and now correspond to those of the egg. The serosa is condensed dorsoposterior to the head, and the secondary dorsal organ is formed on the dorsal side of the egg (Stage 9, Fig. 37I). The embryo maintains its orientation in accord with the egg, and the embryo continues developing and reaches hatching (Stages 10–12, Fig. 37J–L).

1.5 *Protonemura towadensis* (Nemouridae)

1.5.1 Egg

Eggs are spheroidal, with long and short diameters approximately 150 μm and 130 μm, respectively (Fig. 39A). The chorion is thin and transparent. In the egg, two micropyles approximately 2 μm in diameter are located on the equator (Fig. 39B).

1.5.2 Embryonic Development

The egg period is approximately 45 days at 8°C.

The embryonic development of *Protonemura towadensis* (Fig. 40A–L) resembles that of *Apteroperla tikumana* in general aspects (Fig. 37A–L), with minor differences regarding the positioning of the embryo. In *Pr*. *towadensis*, the embryo extends less anteriorly (Fig. 40E–H), and the immersion of the embryo in Stage 5 is more extensive relative to *A*. *tikumana* (Fig. 37E). The thickened serosa is formed beneath the embryo, of which cells show a radial arrangement (Fig. 41A), and beneath it the serosal cuticle is thickened as the thickened serosa (Fig. 41B). Katatrepsis occurs in Stage 9 (Fig. 40I), and as in *A*. *tikumana*, the anteroposterior and dorsoventral axes of the embryo become to correspond to those of the egg (Stages 9–12, Figs. 40I–L, 54D–F).

2. Eggs and embryonic development of Systellognatha

Due to the thick, tough chorion of Systellognatha eggs, the chorion was removed prior to observing embryonic development. However, it is very difficult to remove the chorion from Stage 1 eggs because the serosal cuticle is yet to be secreted. Therefore, with the exception of *Yoraperla uenoi* (Peltoperlidae), which has an anteroposteriorly flattened egg, I could not observe Stage 1 in the remaining Systellognatha.

2.1 *Calineuria stigmatica* (Perlidae)

2.1.1 Egg

The eggs are spheroidal with long and short diameters approximately 550 μm and 400 μm, respectively (Fig. 42A). The chorion is smooth and fuscous in color. At the posterior pole of the egg, the chorion is modified into a collar-shaped protrusion (Fig. 42A, C), which is covered with an adhesive attachment apparatus, known as the anchor plate (anchor, anchor base, or basal plate) (Fig. 42B). At one third from the anterior pole of the egg, 10–15 micropyles about 5 μm in diameter are arranged in a circle (Fig. 42A, D, E).

2.1.2 Embryonic Development

The egg period is 200–250 days, including the diapause period of three months, at 12°C.

Embryonic development basically resembles those of the stoneflies described above, especially those stoneflies whose embryos' axes reversed during katatrepsis. When the embryo is about 90 μm in diameter, it forms at the ventral side near the posterior pole (Stage 2, Fig. 43A), and the embryos soon enter diapause for approximately 90 days. During this period, the thickened serosa and thickened serosal cuticle are formed beneath the embryo (Fig. 44). When diapause terminates, the embryo starts to elongate (Stage 3, Fig. 43B) with the protocephalon and protocorm differentiated, and the embryo continues to elongate along the egg surface until it extends to approximately 200 μm and covers more than one-third of the egg circumference (Stage 4, Fig. 43C). The anterior abdomen sinks into the yolk in Stage 4, and gnathal and thoracic regions follow in Stages 5–6 (Fig. 43D, E). The embryo develops and acquires an S-shape, with the head and posterior

abdomen remaining on the egg surface (Stages 7, 8, Fig. 43F, G). Katatrepsis occurs in Stage 9. The embryo reverses its anteroposterior and dorsoventral axes, and the orientation of the embryo corresponds to that of the egg (Fig. 43H). Keeping its orientation according with that of the egg, the embryo continues to develop and then hatches (Stages 10–12, Fig. 43I–K).

2.2 *Sweltsa* sp. (Chloroperlidae)

2.2.1 Egg

The eggs are spheroidal with long and short diameters approximately 400 μm and 250 μm, respectively (Fig. 45A). The chorion is smooth and light yellow in color. The specialized structures, including the collar and anchor plate, are lacking. On a third of the anterior part of the egg, six to nine micropyles about 5 μm in diameter are arranged in a circle (Fig. 45B, C).

2.2.2 Embryonic Development

The egg period is 50–65 days at 12°C.

The embryonic development resembles those of the stoneflies described above, especially those stoneflies whose embryos' axes are reversed in katatrepsis. An embryo of approximately 100 μm in diameter forms at the posterior pole of the egg, which looks thick because of a large curvature around the posterior egg pole (Stage 2, Fig. 46A). The embryo elongates along the egg surface in Stages 3 to 4 (Fig. 46B, C), and the anterior abdomen sinks into the yolk with the cephalic and thoracic regions and posterior abdomen remaining on the egg surface in Stage 5 (Fig. 46D). The thickened serosa and thickened serosal cuticle are formed beneath the embryo (Fig. 47). Development

continues through Stages 6–8, with the embryo retaining this posture (Fig. 46E–G). As a result of katatrepsis occurred in Stage 9, the embryo reverses its anteroposterior and dorsoventral axes, and the orientation of the embryo corresponds to that of the egg (Fig. 46H). Maintaining this orientation, the embryo continues to develop and reaches hatching using the egg tooth formed on the frons (Stages 10–12, Fig. 46I–K).

2.3 *Ostrovus* sp. (Perlodidae)

2.3.1 Egg

The eggs are light yellow in color and unique in shape (Fig. 48A–F). Newly laid eggs are limpet-like in shape and are flattened laterally, i.e., from side to side, their left side being less convex (Fig. 48A–C). As development proceeds, the left side of the egg swells (Fig. 48D). The posterior refers to the direction where the collar and anchor plate exist, and the anterior is opposite: the anchor plate is on the posterior end of the left side (Fig. 48A) and the collar is on the right side (Fig. 48B). When observing the egg from its right side as shown in Fig. 48A, the ventral side is to the right hand and the dorsal side to the left. The length (anteroposterior length) of the egg is ca. 400 μm, the width (dorsoventral length) is ca. 320 μm (Fig. 48A, B), and the thickness is ca. 150 μm just after oviposition (Fig. 48C), and ca. 220 μm just before hatching (Fig. 48D). The chorion shows a weak polygonal pattern on its left side and toward the posterior (Fig. 48E, F). Along the equator of the left side of the egg, five to eight longitudinal micropyles are arranged, each with a width of 3 μm (Fig. 48B, E, F).

2.3.2 Embryonic Development

The egg period is approximately 80 days at 12°C.

In the representations of embryogenesis in the above descriptions, the ventral side is to the left (Figs. 4, 31, 34, 37, 40, 43, 46). However, it is difficult to place the eggs with their convex dorsal side down in this species. Therefore, embryogenesis is presented in Figure 49 with the ventral side of the egg to the right.

The embryo ca. 50 μm in diameter forms around the posterior pole (Stage 2, Fig. 49A). However, due to the unique shape of the egg, the newly formed embryo is positioned a little biased to the right side of the egg, as shown in Figure 49A. The embryo elongates partially twisted (Fig. 49B–F), and the embryos, which have not largely grown within the egg, are seen as if they are sunk in the yolk (Fig. 49B–G). Therefore, while it is difficult to precisely compare embryonic development of *Ostrovus* sp. with the other species, it is clear that it resembles other plecopterans, especially those whose embryonic axes are reversed during katatrepsis. Namely, the formed embryo elongates along the dorsal surface of the egg with its caudal end ahead, and the embryo's anteroposterior and dorsoventral axes become opposed to those of the egg (Fig. 49B–G). The thickened serosa and thickened serosal cuticle are formed beneath the embryo (Fig. 50A, B). Katatrepsis then occurs in Stage 9 (Fig. 49H). The embryo reverses its anteroposterior and dorsoventral axes, and the orientation of the embryo eventually corresponds to that of the egg (Fig. 49H). The embryo grows further and hatches out from the egg, tearing the egg membrane around the anterior third of the right side of the egg using the egg tooth formed on the frons (Fig. 49I–K).

2.4 *Yoraperla uenoi* (Peltoperlidae)

2.4.1 Egg

The eggs are reddish-brown. Initially the eggs are strongly flattened anteroposteriorly, with a diameter and thickness of approximately 400 μm and 150 μm, respectively (Fig. 51A–D), but as development progresses, they expand to about 240 μm. A transparent anchor plate is on the posterior side of egg, but the collar is inconspicuous (Fig. 51B, C). The anterior side of the egg has a honeycomb pattern (Fig. 51A–C). On the anterior side of the egg five to eight micropylar protuberances of several microns in diameter are roughly arranged in a circle, and a micropyle approximately 1.5 μm in diameter opens at the center of each protuberance (Fig. 51A, D).

2.4.2 Embryonic Development

The egg period is approximately 40 days at 12°C.

Due to difficultly observing the extremely flattened eggs from the lateral side, I represent embryogenesis in *Yoraperla uenoi* using photos from the posterior side (Fig. 52), which differs from the other species (Figs. 4, 31, 34, 37, 40, 43, 46, 49).
The germ disc forms at the posterior pole (Stage 1, Fig. 52A). In Stage 2, anatrepsis begins and the amnioserosal folds fuse with each other (Fig. 52B). The serosa converged beneath the embryo to form the thickened serosa, being attached to the posterior end of embryo (Fig. 53A). The embryo begins to elongate in an inverted-triangular shape, with the protocephalon and protocorm differentiated (Stage 3, Fig. 52C), and then forms into a slug-like shape (Stage 4, Fig. 52D). Segmentation and appendage formation commence, and the anterior abdomen sinks into the yolk with the cephalic and thoracic regions and posterior abdomen remaining on the egg surface (Stage 5, Fig. 52E). The thickened serosa is formed beneath the embryo, of which cells show a radial arrangement; the caudal end of the embryo remains attached to the

thickened serosa (Fig. 53B, C). The embryo then acquires an S-shape (Stages 5–8, Figs. 52E–H, 53B, D). The serosal cuticle becomes bloated beneath the thickened serosa as the thickened serosal cuticle (Fig. 53C, E). Katatrepsis occurs, the embryo slips out of the yolk (Stage 9, Fig. 52I), and is put down sideways with its right side down, changing its posture from warped to ventrally bent (Stage 10, Fig. 52J). Keeping this condition, the embryo further develops (Stage 11, Fig. 52K) and hatches from the egg, tearing the egg membrane at its lateral side (Stage 12, Fig. 52L).

DISCUSSION

1. Egg

Zwick (1973, 2000) suggested that: 1) the sclerotized hard chorion is a groundplan character of Plecoptera, being universally present in Antarctoperlaria and systellognathan Arctoperlaria; 2) the soft chorion is likely apomorphic to euhologнathan Arctoperlaria; whereas 3) systellognathan Arctoperlaria retain the hard chorion, which differentiates into a collar surrounding the adhesive attachment apparatus (anchor plate) at the posterior pole of the egg. The collar and anchor plate represent the apomorphic groundplan of Systellognatha, because as Hinton (1981) pointed out, these features are not found in other plecopterans, i.e., Antarctoperlaria and Euhologнatha, nor in other Neoptera.

Examining the egg structures of nine Japanese arctoperlarians, i.e., five species for Euhologнatha – *Scopura montana* (Scopuridae), *Obipteryx* sp. (Taeniopterygidae), *Paraleuctra cercia* (Leuctridae), *Apteroperla tikumana* (Capniidae), and *Protonemura towadensis* (Nemouridae) – and four species for Systellognatha – *Calineuria stigmatica* (Perlidae), *Sweltsa* sp. (Chloroperlidae), *Ostrovus* sp. (Perlodidae), and *Yoraperla uenoi* (Peltoperlidae) , the present study corroborates Zwick's (1973, 2000) understanding of arctoperlarian eggs. I characterize the eggs of Euhologнatha and Systellognatha as follows, referring to previous studies as necessary. The eggs of Euhologнatha are: 1) spherical or ellipsoid in shape (Figs. 2A, 30A, 33, 36, 39A); 2) without specialized structures such as a collar or anchor plate (Figs. 2A, 30A, 33, 36, 39A); and 3) covered by a thin, transparent chorion, which is smooth and without a conspicuous superficial

pattern (Figs. 30A, B, 33, 36, 39A, B), although the exochorion of the anterior third of the egg wears a weak, polygonal network in *S. montana* (Fig. 2B–D).

The scopurid egg structure has been previously described with "*Scopura longa* Uéno, 1929" by Kawai and Isobe (1984), but it is likely that the materials examined at the time were in fact *S. montana*, as the scopurids from this sampling site in Mt. Hachibuse, Nagano Prefecture, were more recently identified as *S. montana* (see Uchida and Maruyama, 1987). Later Kishimoto (1997b) preliminarily reported the external morphology of *S. montana*. However, no TEM information on the ultrastructure of the egg membranes has been reported. Therefore, in the present study, for the first time, I report the fine structures of the Scopuridae egg membranes using *S. montana* as a representative species. The fine structures of the *S. montana* egg membranes were characterized by the following features: 1) a chorion composed of an exochorion, an endochorion, and a vitelline membrane (Fig. 3A, B), 2) a thick exochorion of low electron density (Fig. 3A), 3) an endochorion composed of two sublayers of differing electron density (Fig. 3B), 4) the endochorionic surface ornamented with rod-like materials and numerous small hemispherical protuberances (Figs. 2B, 3A, B), and 5) a fairly thin vitelline membrane of high electron density (Fig. 3A, B). In Euholognatha, to which Scopuridae belongs, several TEM studies exist on the egg membranes: *Brachyptera risi* of Taeniopterygidae (Michalik et al., 2015), *Leuctra autumnalis* of Leuctridae (Poprawa et al., 2002), and *Protonemura intricata* of Nemouridae (Rościszewska, 1996). Features 1)–3), mentioned above, are shared with these euholognathan stoneflies, and they are possibly the groundplan of the egg membranes in Euholognatha.

The eggs of the other arctoperlarian infraorder Systellognatha may be characterized as: 1) spherical or ellipsoidal (Figs. 42A, 45A), but they sometimes take a specific shape characteristic of each group (Figs. 48A–F, 51A–D); 2) equipped with a collar and anchor plate on their posterior pole (Figs. 42A–C, 48A–E, 51B, C); and 3) covered by a thick and hard, colored chorion occasionally containing conspicuous superficial patterns or sculptures (Figs. 48A–F, 51A–C) (see also Knight et al., 1965a,b). The eggs of the chloroperlid species, *Sweltsa* sp., lack the collar and anchor plate. However, because these structures are found predominantly in Systellognatha, and chloroperlid genera are known to include species with and without these structures (Stark et al., 2015), the absence of these structures in *Sweltsa* sp. may be due to a secondary modification (Fig. 45A).

In the present study, I observed the micropyles of three euholognathan stoneflies: *S. montana*, *Obipteryx* sp., and *Pr. towadensis* (Figs. 2C, D, 30B, 39B). In *S. montana*, several micropyles are distributed in a circle in a rosette pattern around the anterior pole of the egg (Fig. 2C, D). In *Obipteryx* sp., micropylar areas with three to four micropyles are located on the equator on both lateral sides of the egg (Fig. 30B), as reported for another taeniopterygid *Brachyptera trifasciata* (Pictet, 1832) (Degrange, 1957), and this micropylar arrangement may be characteristic of the Taeniopterygidae. Two micropyles are located on the equator in *Pr. towadensis* (Fig. 39B), while several micropyles were distributed along the equator and in the posterior half of the egg in another *Protonemura*, *Pr. praecox* (Morton, 1894) (Degrange, 1957). Although I failed to detect micropyles in *A. tikumana*, Kishimoto (1997a; personal comm.) reported two micropyles located on the lateral side of the egg.

With the exception of *Ostrovus* sp., the micropyles of Systellognatha were arranged in a circle (Figs. 42A, D, 45B, 51A). A similar pattern of micropyle distribution has been found in *Pteronarcys proteus*, in the Pteronarcyidae (Miller, 1939), as well as in other systellognathan representatives (Stark and Stewart, 1981; Isobe, 1988), with the circular arrangement being a part of the groundplan of Systellognatha. In *Ostrovus* sp., eggs have a laterally-flattened shape and a unique arrangement of micropyles, with several micropyles arranged in a straight line on the left side of the egg (Fig. 48B, E, F). This unusual micropylar arrangement in this species may be due to a secondary modification related to its unique egg shape.

Additional studies in other species, especially the Antarctoperlaria, are required to reconstruct the groundplan of micropylar distributions in the Plecoptera and Arctoperlaria. However, the circular arrangement of micropyles is quite likely a part of the groundplan of Systellognatha. Moreover, given that one of the euholognathan families Scopuridae and that a brief description of some antarctoperlarian egg structure (Hynes, 1974) also show a circular arrangement of micropyles, this feature may be regarded as a potential groundplan of Plecoptera (Fig. 55). Potential explanations for the absence of a circular arrangement of micropyles in the remaining euholognathan species include a partial interruption of the micropylar arrangement or a reduction of the micropyles, i.e., the micropyles may have been lost in *Obipteryx* sp. on the dorsal and ventral sides of the egg, and most of those may have been reduced in *Pr*. *towadensis* and *A*. *tikumana*. However, explaining the extraordinary arrangement of micropyles reported for *Pr*. *praecox* will require a reexamination of micropylar arrangement in this and other related species.

2. Embryonic development

2.1 Formation of the embryo

Mashimo et al. (2014) compared embryogenesis in Hemimetabola, and proposed two embryological autapomorphies of Polyneoptera. One involves elongation of the embryo, as I discuss below in the section "2.4.1. Anatrepsis and elongation of the embryo," and the other is on the manner of the embryo's formation. In Polyneoptera, the embryo is formed by the fusion of paired blastoderm regions with higher cellular density: Dermaptera (Shimizu, 2013), Embioptera (Jintsu, 2010), Phasmatodea (Bedford, 1970), Orthoptera (Miyawaki et al., 2004), Zoraptera (Mashimo et al., 2014), Grylloblattodea (Uchifune and Machida, 2005), and Blattodea (Fujita and Machida, 2017). However, in the Palaeoptera and Acercaria (e.g., Ephemeroptera: Tojo and Machida, 1997; Odonata: Ando, 1962; Psocodea: Goss, 1952; Thysanoptera: Heming, 1979), blastoderm cells around the posterior pole concentrate in one area and proliferate to form the embryo. This type of germ disc formation is also known for the apterygote Ectognatha, i.e., Archaeognatha (Machida et al., 1990) and Zygentoma (Masumoto and Machida, 2006), clearly suggesting that this is a plesiomorphic condition to Pterygota. Consequently, the formation of the embryo or germ disc by the fusion of paired blastoderm areas with higher cellular density, may be regarded as an apomorphic groundplan of Polyneoptera.

Information on the formation of embryo in Plecoptera is fragmentary. Only two embryological analyses exist for Systellognatha, including Miller (1939) for *Pteronarcys proteus* (Pteronarcyidae) and Kishimoto (1986) for *Kamimuria tibialis* (Perlidae). In *Pt. proteus*, a small germ disc is formed by the direct migration of a cell group appeared in the yolk on to the blastoderm. In *K. tibialis*, a small germ disc is formed by the simple

migration of blastoderm cells. These imply that the embryos form in Plecoptera without involving the fusion of paired blastoderm areas with higher cellular density, which is different from other groups of Polyneoptera. Thus, in the present study, I examined embryo formation in five euholognathan and four systellognathan arctoperlarians, employing DAPI staining, with special reference to the euholognathan *Scopura montana*. I demonstrated that the embryo is formed by the concentration and proliferation of blastoderm cells around the posterior pole (Fig. 6), as Kishimoto (1986) observed for the systellognathan, *K. tibialis*. Specifically, in Plecoptera the embryo is formed not in the manner involving the fusion of paired blastoderm areas with higher cellular density, which Mashimo et al. (2014) proposed as an apomorphic groundplan feature of Polyneoptera, but in a simple concentration and proliferation of blastoderm cells, as shown in apterygote Ectognatha, Palaeoptera and Acercaria, that may be taken to be plesiomorphic to Pterygota. As described in "INTRODUCTION," the phylogenetic position of Plecoptera has been debated, but recent comparative morphologies and phylogenomics (e.g., Beutel et al. 2014; Misof et al. 2014) have often bestowed basal positions to Plecoptera within Polyneoptera. The manner of embryo formation in Plecoptera, which seems unique in Polyneoptera, is expected to be critically discussed with respect to phylogenetic reconstruction of Polyneoptera (Fig. 55).

In addition, embryo formation in *Pt. proteus* occurs as a compact cellular aggregation beginning early in development. However, according to Miller (1939), the streaming of a cellular group from inside to the periphery of the egg is involved in embryo formation. Such a convergent migration of a mass of presumptive embryonic cells is a singular example reported in insects, and critical reexamination is needed.

2.2 Germ band type

In insects, the elongation and segmentation patterns of the embryo are categorized as either the short or long germ band types (Krause, 1939; Sander, 1984; Ando and Kobayashi, 1996). The long germ band type only occurs in derived insects such as Holometabola, and the short germ band type is generally found in ancestral insects such as apterygote ectognathans (Archaeognatha and Zygentoma) and Palaeoptera. In the long germ band type, almost all segments simultaneously develop in the germ band directly formed from the blastoderm. In contrast, the short germ band type is characterized by sequential development of most segments from anterior to posterior as the germ band elongates (Nakagaki et al., 2015).

Reviewing the embryos of insects in light of the germ band type, we know that the germ band type cannot be critically distinguished into these two typical ones (Ando and Kobayashi, 1996), and the germ band type in which not all but more segments develop simultaneously are called the semi-long germ band or intermediate type (Krause, 1939; Sander, 1984). In the present study I use the “short germ band type” because there is no fundamental difference between the short and semi-long germ band types.

In Polyneoptera, the embryogenesis of short germ band type is generally performed: Dermaptera (Shimizu, 2013), Embioptera (Jintsu, 2010), Phasmatodea (Bedfold, 1970), Orthoptera (Krause, 1939), Zoraptera (Mashimo et al., 2014), Grylloblattodea (Uchifune and Machida, 2005), Mantophasmatodea (Machida et al., 2004), Mantodea (Fukui et al., 2018), “Blattaria” (Fujita and Machida, 2017), and Isoptera (Knower, 1900). The present study revealed that in Plecoptera the embryogenesis of a typical short germ band type: first a small germ disc or embryo with

no sign of segmentation, then with the sequential formation of segments from the anterior to posterior, the embryo elongates (Figs. 5–7) in the same way as that has been reported previously for plecopterans (Miller, 1939; Kishimoto and Ando, 1985). Since the short germ band type is predominant in more ancestral insects including apterygote ectognathans, i.e., Archaeognatha (Machida et al., 1994a) and Zygentoma (Masumoto and Machida, 2006), and Palaeoptera, i.e., Ephemeroptera (Tojo and Machida, 1997) and Odonata (Ando, 1962), the sharing of this type of germ band in Polyneoptera can be regarded as symplesiomorphy of polyneopteran orders, and the embryogenesis of the short germ band type can be regarded as a plesiomorphic groundplan of Polyneoptera (Fig. 55).

2.3 Thickened serosa and serosal cuticle beneath the embryo

It has been previously reported that the serosa is thickened beneath the embryo in some stoneflies, such as *Pteronarcys proteus* by Miller (1939, 1940) and *Kamimuria tibialis* by Kishimoto and Ando (1985). In addition, as Miller described in *Pt. proteus*, the thickened serosa secretes a thickened serosal cuticle, the former and latter of which were respectively named the grumulus and grumorium. The present study, which dealt with the embryogeneses of five euholognathan and four systellognathan arctoperlarian stoneflies focusing on the euholognathan *Scopura montana*, is the first detailed and comprehensive investigation of the development and fine structure of the thickened serosa and serosal cuticle formed beneath the plecopteran embryos. The thickened serosa and thickened serosal cuticles of the nine Japanese plecopterans examined in the present study closely resemble the grumulus in *Pt. proteus* (Miller, 1939, 1940) as well as to the columnar serosal cells in *K. tibialis* (Kishimoto and Ando, 1985) and the

grumorium in *Pt. proteus* (Miller, 1939, 1940). Therefore, the thickening serosa, and possibly also the thickened serosal cuticle, represent the groundplan features of Plecoptera.

The thickened serosa and serosal cuticle formed beneath the plecopteran embryos can be summarized as follows: 1) the thickened serosa is formed by the convergence of serosa beneath the embryo and is closely related to the formation of the amnioserosal fold (Figs. 8A–C, 9A, C, 10A, C); the thickened serosal cells show a radial arrangement with the apical surface converged to the posterior pole of the egg (Figs. 11A–C, 32A, 35A, 38, 41A, 44, 47, 50A, B, 53A–C); 2) the four layers of the serosal cuticle differing in their fine structure and electron density are secreted, thus forming a remarkably thick serosal cuticular structure (i.e., the thickened serosal cuticle; Figs. 16A, B, 32B, 35B, 38, 41B, 44, 47, 50A, B, 53D, E); and 3) after accomplishing the secretion of the thickened serosal cuticle beneath the embryo, the thickened serosa then disintegrates in the final stage of intertrepsis (Figs. 18A, B, 19A–F). Liberated serosal cells from the disintegrated thickened serosa float for a short period in the peripheral region of the egg (Fig. 22A, B). The thickened serosa, then, is responsible for segregating the thickened serosal cuticle beneath the embryo, which Miller (1940) named as grumulus that functions to secrete grumorium. In addition, the radial cell arrangement in the thickened serosa, where the apical surfaces of its constituents converge to a restricted area, is favorable for producing the thickened cuticular structure.

In some polyneopteran insects, a specialized serosa and/or serosal cuticle, similar to the plecopteran thickened serosa and serosal cuticle have been reported for Embioptera (Jintsu and Machida, 2009), Phasmatodea (Jintsu et al., 2010), Orthoptera

(Slifer, 1938; Matthée, 1951; Slifer and Sekhon, 1963), and Grylloblattodea (Uchifune and Machida, 2005). Slifer (1938) and Slifer and Sekhon (1963) previously conducted experimental embryological studies, combined with TEM, using the grasshopper *Melanoplus differentialis*. They revealed that the serosal cuticle beneath the embryo is specialized for the water absorption. They named this serosal cuticle the hydropyle(s), whereas the thickened serosa cells that secrete the hydropyle(s) were named hydropylar cells. The hydropyle(s) and/or hydropylar cells have also been described in many hemipterans (Cobben, 1968; Mori, 1970; Hinton, 1981) and some ancestral lepidopterans (Kobayashi and Ando, 1982, 1987; Kobayashi, 1998), and their water absorption ability was previously suggested.

Plecopteran eggs are exclusively aquatic, and Miller (1940) associated the grumulus and grumorium of *Pt. proteus* with the hydropylar cells and hydropyle(s) of *M. differentialis*. In addition, Zwick (1999) correlated the egg swelling that often occurs during plecopteran embryogenesis with water absorption. Although I could not directly associate the thickened serosa and serosal cuticle with water uptake in the present developmental study of *S. montana*, it is noteworthy that serosal cuticles 2 and 3 are vertically striated, whereas serosal cuticle 4-I is fibrous, in the thickened serosal cuticle (Figs. 13, 16B). Miller (1940) also depicted vertical striations in the outer part of the grumorium. Therefore, if the correlation of the fine structural features of serosal cuticles 2, 3, and 4-I with water transportation is valid, the dense-lamellar construction of serosal cuticle 4-II (Fig. 16B) may be related to the cessation of water transportation. Detailed embryological and physiological studies, including the use of radioactive tracers, may provide further insight into this process.

In the peltoperlid systellognathan *Yoraperla uenoi*, the caudal end of the embryo is attached to the thickened serosa during embryogenesis (Fig. 53A–C), the same as described by Miller (1939, 1940) for the pteronarcyid *Pt. proteus*. This embryo's posture has not been reported ever in other plecopterans, and it may reflect a phylogenetic affinity of these two families.

2.4 Blastokinesis

According to Fujita and Machida (2017), I define terms related to blastokinesis as follows. Embryos of Insecta s. str. (Ectognatha: Archaeognatha, Zygentoma, and Pterygota), immerse in the yolk in the early stage of development due to the formation of amnioserosal folds. The embryos then elongate and take their final position in the pre-katatrepsis period. The entire descending process of the embryo from commencement of the amnioserosal fold formation up to this point, is the "anatrepsis." After anatrepsis, the embryos develop until katatrepsis occurs, maintaining this positioning, this phase being the "intertrepsis." The rupture and withdrawal of the amnioserosal folds then occur, which leads to the embryo's reappearance on the egg surface, this ascending process being the "katatrepsis." These processes related to developmental phase are collectively the "blastokinesis." In the present study, I examined blastokinesis in five euholognathan and four systellognathan arctoperlarians, focusing on the euholognathan *Scopura montana*.

2.4.1 Anatrepsis and formation of the embryo

As soon as the germ disc or embryo forms at the posterior pole of the egg, the marginal region begins to extend over the embryo, forming the amnioserosal folds, and

anatrepsis starts (Figs. 7A–C, 8A, B, 9A, B). The amnioserosal folds soon fuse with each other (Figs. 7D, 8C, 9C, D), and the amniotic pore is completely closed. Thus, in the earliest stage of development, fusion of amnioserosal folds occurs and a compact, ball-shaped "embryo-amnion composite" forms, of which the dorsal and ventral constituents are represented by the embryo proper and amnion, respectively. This process is the same as that reported previously in *Pteronarcys proteus* (Miller, 1939) and *Kamimuria tibialis* (Kishimoto and Ando, 1985; Kishimoto, 1986). The fusion of amnioserosal folds in the earliest stage of development, which leads to the formation of a ball-shaped embryo-amnion composite, is unique to Plecoptera within the Polyneoptera and could be a potential autapomorphy of this group.

The formed embryos elongate along the dorsal side of the egg with their posterior end ahead. After this elongation on the egg surface, the middle part of the embryos curve and sink into the yolk, with their cephalic and caudal ends remaining on the egg periphery (Figs. 4C–E, 5C–E, 31C–E, 34C–E, 37C–E, 40C–E, 43B–D, 46B–D, 49B–D, 52C–E), as described in previous embryological studies on Plecoptera (Miller, 1939, 1940; Kishimoto and Ando, 1985; Kishimoto, 1997a). Thus, in Plecoptera, as in the other polyneopteran orders, including Dermaptera (Heymons, 1895; Shimizu, 2013), Embioptera (e.g., Kershaw, 1914), Phasmatodea (e.g., Bedford, 1970), Orthoptera (e.g., Roonwal, 1937), Zoraptera (Mashimo et al., 2014), Grylloblattodea (Uchifune and Machida, 2005), Mantophasmatodea (Machida et al., 2004), Mantodea (Hagan, 1917; Fukui et al., 2018), "Blattaria" (Heymons, 1895; Fujita and Machida, 2017), and Isoptera (e.g., Knower, 1900), the formation of amnioserosal folds ends at an earlier stage of development and the elongation of the embryo occurring on the egg surface. Mashimo et al. (2014) suggested this feature as another embryological autapomorphy of

Polyneoptera, taking it into considerations that in Palaeoptera and Acercaria, the embryo elongates, keeping step with its immersion into the yolk and with the formation of the amnioserosal folds: i.e., Ephemeroptera (Tojo and Machida, 1997), Odonata (Ando, 1962), Psocoptera (Goss, 1952), Phthiraptera (Schölzel, 1937), Thysanoptera (Heming, 1979), and Hemiptera (Cobben, 1968; Heming and Huebner, 1994). The present study demonstrates that embryos of Plecoptera elongate in a manner regarded as autapomorphic to Polyneoptera, and the placement of Plecoptera among the Polyneoptera is strongly corroborated. In contrast, there is little support for the phylogenetic hypotheses that places Plecoptera outside of Polyneoptera, i.e., those proposing the sister group relationship of Plecoptera with Neoptera or with "Paraneoptera + Holometabola."

2.4.2 Intertrepsis

In most Plecoptera, as a result of anatrepsis (e.g., Fig. 4C–G), the anteroposterior and dorsoventral axes of the embryo become opposed to those of the egg. The exceptions to this pattern are in *Yoraperla uenoi* (Figs. 52, 53B, D) and *Pteronarcys proteus* (Miller, 1939), in which free movement of the embryos during blastokinesis may be limited due to their flattened egg shape (cf. "2.4.3. Katatrepsis").

As described above, the plecopteran embryos descend into the yolk with their cephalic and caudal ends remaining on the egg periphery, and they keep this posture during intertrepsis (Figs. 4E–G, 31E–G, 34E–G, 37E–G, 40E–G, 43D–F, 46D–F, 49D–F). Such a posture of embryos in intertrepsis may be unique to the Plecoptera within Polyneoptera (see the literature cited in the previous section 2.4.1) and may be regarded as a part of the groundplan of Plecoptera.

2.4.3 Katatrepsis

In the present study, I examined katatrepsis of nine families of the arctoperlarian Plecoptera, and distinguished three katatrepsis types.

Type 1 – Katatrepsis begins, and the embryo appears on the egg surface. The embryo moves along the egg surface with its head ahead, via the posterior pole of the egg. It then moves to the ventral side of the egg, toward the anterior pole of the egg, and katatrepsis completes. The anteroposterior and dorsoventral axes are reversed to those in intertrepsis. Among the plecopterans examined, the euholognathan Capniidae and Nemouridae, and the systellognathan Perlidae, Chloroperlidae, and Perlodidae fall into this category (Figs. 37I, 40I, 43H, 46H, 49H, 54D–F). Another representative of the Perlidae, *Kamimuria tibialis* also shows Type 1 katatrepsis (Kishimoto and Ando, 1985).

Type 2 – Different from Type 1 katatrepsis, the embryo does not change its orientation throughout the course of katatrepsis, and its anteroposterior and dorsoventral axes remain opposed to those of the egg. Among the plecopterans examined, three euholognathan families Scopuridae, Taeniopterygidae, and Leuctridae, are categorized in this type (Figs. 4I, 5I, 22A, B, 31I, 34I, 54A–C). In the study on diapause in the taeniopterygid euholognathan *Brachyptera risi* (Morton, 1896), Khoo (1968b) provided figures showing that this species performs Type 2 katatrepsis.

Type 3 – In the peltoperlid systellognathan *Yoraperla uenoi*, of which eggs are strongly flattened anteroposteriorly (Fig. 51A–C), the embryo forms at the center of the broad bottom of the egg (Figs. 52A, B, 53A), and it grows and elongates there (Figs. 52C–H, 53B, D). Katatrepsis occurs subsequently (Fig. 52I), and the embryo rotates around its anteroposterior axis by 90 degrees, lying sideways on the bottom side of the egg (Fig. 52J). Katatrepsis of this type is also found in the pteronarcyid systellognathan

Pteronarcys proteus, which has eggs with anterodorsally flattened shape, as in *Y. uenoi* (Miller, 1939, 1940).

Katatrepsis involving a reversion of the embryo's axes like Type 1 is predominant in non-holometabolan Pterygota: i.e., in Palaeoptera: Ephemeroptera (Tojo and Machida, 1997), and Odonata (Ando, 1962); Polyneoptera: Dermaptera (Heymons 1895; Shimizu, 2013), Embioptera (e.g., Kershaw, 1914), Phasmatodea (e.g., Bedford, 1970), Orthoptera (e.g., Roonwal, 1937), Zoraptera (Mashimo et al., 2014), Grylloblattodea (Uchifune and Machida, 2005), Mantophasmatodea (Machida et al., 2004), "Blattaria" (Heymons, 1895; Fujita and Machida, 2017), and Isoptera (e.g., Knower, 1900); Acercaria: Psocoptera (Goss, 1952), Phthiraptera (Schölzel, 1937), Thysanoptera (Heming, 1979), and Hemiptera (Cobben, 1968). On the other hand, the apterygote Ectognatha, such as the Archaeognatha (Machida et al., 1994a) and Zygentoma (Masumoto and Machida, 2006), do not follow one of these established types of katatrepsis involving the reversion of the embryo's axes. Therefore, I conclude that this type of katatrepsis is an apomorphic groundplan of Pterygota, and the sharing of Type 1 katatrepsis by some plecopteran lineages, such as the euholognathan Capniidae and Nemouridae, and the systellognathan Perlidae, Chloroperlidae, and Perlodidae, can be referred to as symplesiomorphic.

In contrast, the Type 2 and Type 3 forms of katatrepsis are apparently derived features in Plecoptera. Interfamily relationships in Euholognatha are not well understood, especially the monophyly of Nemouroidea, which consists of five families, i.e., Taeniopterygidae, Leuctridae, Capniidae, Nemouridae and Notonemouridae has been debated over for a long time (e.g., Ricker, 1950; Illies, 1965; Thomas et al., 2000; Zwick, 2000; Terry, 2004; Kjer et al., 2006), but the affinity of the euholognathan Scopuridae,

Taeniopterygidae, and Leuctridae is suggested, taking Type 2 katatrepsis for a synapomorphy of them. In Systellognatha, the monophyly of Peltoperlidae, Pteronarcyidae and Styloperlidae is well supported (e.g., Zwick, 2000). The sharing of both Type 3 katatrepsis and a flattened egg shape phenotype by the former two families may reflect their phylogenetic affinity.

Figure 55 depicts the distribution of the different katatrepsis types on the phylogeny of the 10 plecopteran families for which katatrepsis type is known.

2.5 Egg tooth

The egg tooth is a derivative structure of embryonic cuticle, formed usually on the head capsule, and functions as a hatching device. They are distributed in apterygote Zygentoma (Konopová and Zrzavý, 2005) and Pterygota (e.g., Sikes and Wigglesworth, 1931; Ando and Kobayashi, 1996): as for Polyneoptera, the egg teeth have been reported for some orders including Dermaptera (Shimizu, 2013), Embioptera (Jintsu, 2010), Zoraptera (Mashimo et al., 2014), Grylloblattodea (Uchifune and Machida, 2005), and “Blattaria” (Fujita and Machida, 2017).

In Plecoptera, the egg tooth formed as a small pointed projection on the frons has been described in systellognathan *Pteronarcys proteus* of Pteronarcyidae (Miller 1939, 1940) and *Kamimuria tibialis* of Perlidae (Kishimoto and Ando, 1985). The present study revealed that the egg teeth are formed as a sclerotized, conical-shaped projection on the frons in euholognathan *Scopura montana* of Scopuridae, systellognathan *Sweltsa* sp. of Chloroperlidae, and *Ostrovus* sp. of Perlodidae (Figs. 25C, D, 26, 27B, 46K, 49K). Thus, sharing of the egg tooth may be regarded as a groundplan of Plecoptera, although its understanding in the light of evolution is almost

impossible because of its sporadic distribution and morphological variation in insects (Ando and Kobayashi, 1996; Mashimo et al., 2014, Fig. 55).

3. Concluding remarks

The present study has been conducted, aiming: 1) to describe the egg structure and embryonic development of Plecoptera, 2) to compare the results with previous works to reconstruct the groundplan of Plecoptera and Polyneoptera, 3) to discuss the interfamily relationships in Arctoperlaria, and 4) to provide a new, sound basis contributing to solving the phylogenetic issues concerning Plecoptera and Polyneoptera.

I examined and described the egg structure and embryonic development of the nine plecopterans from all the nine Japanese arctoperlarian families. The embryonic development of Plecoptera was summarized as: 1) formation of the embryo by the simple concentration and proliferation of blastoderm cells, 2) fusion of amnioserosal folds in the earliest stage of development, which leads to the formation of a ball-shaped embryo-amnion composite, 3) intertrepsis in which the embryo immerses in the egg inside with its cephalic and caudal ends left on the egg periphery, 4) formation of the thickened serosa and serosal cuticle beneath the embryo, and 5) conical-shaped egg tooth formed on the frons (Fig. 55).

Three types were distinguished in katatrepsis of arctoperlarian plecopterans. 1) The type 1, in which the embryo's anteroposterior and dorsoventral axes change in reverse during katatrepsis, is found in Capniidae, Nemouridae, Perlidae, Chloroperlidae, and Perlodidae; 2) the type 2, in which the embryo's axes are not changed during katatrepsis, is found in Scopuridae, Taeniopterygidae, and Leuctridae; and 3) the type 3, in which the embryo rotates around its anteroposterior axis by 90° during katatrepsis as

hitherto known for Pteronarcyidae, is found also in Peltoperlidae. The type 1 is symplesiomorphic to Capniidae, Nemouridae, Perlidae, Chloroperlidae, and Perlodidae, and the type 2 and 3 are synapomorphies of three euholognathan Scopuridae, Taeniopterygidae, and Leuctridae and two systellognathan Peltoperlidae and Pteronarcyidae, respectively. Peltoperlid and pteronarcyid embryos share a feature that their caudal end attaches to the thickened serosa during embryogenesis, and this may reflect a close affinity of these two families. The manner of blastokinesis proposed a phylogenetic reconstruction of Arctoperlaria formulated as: Euholognatha [= (Scopuridae + Taeniopterygidae + Leuctridae) + Capniidae + Nemouridae] + Systellognatha [= Perlidae + Chloroperlidae + Perlodidae + (Peltoperlidae + Pteronarcyidae)], with the current phylogenetic understanding (e.g., Zwick, 2000), i.e., each of Arctoperlaria, Euholognatha, and Systellognatha is monophyletic, also incorporated (Fig. 55).

As for the egg structure, euholognathan and systellognathan eggs were characterized by “thin, soft chorion of euholognathan egg,” and “collar and anchor plate at the posterior pole of the systellognathan egg.” These features may represent the apomorphic groundplan of Euholognatha and Systellognatha, respectively (Fig. 55). The circular arrangement of micropyles, and sclerotized hard chorion of Antarctoperlaria and Systellognatha may be represented as a groundplan feature of Plecoptera (Fig. 55).

For better embryological understandings of Plecoptera, further information from more lineages of Plecoptera, especially the Antarctoperlaria, is strongly desired.

The present, detailed comparative embryological study on Plecoptera provided the polyneopteran comparative embryology with a new spectrum of information. Hence, the embryological groundplan of Polyneoptera was collaborated and reconstructed by:

1) embryogenesis of the short germ band type, and 2) the elongation of the embryo on the egg surface. The former is a plesiomorphic groundplan, whereas the latter is an apomorphic groundplan of Polyneoptera, which strongly support the monophyly of the group, as suggested by Mashimo et al. (2014).

ACKNOWLEDGMENTS

I wish to express my hearty thanks to Prof. Dr. Ryuichiro Machida of the Sugadaira Research Station, Mountain Science Center, University of Tsukuba (SRS) for his constant guidance as well as invaluable suggestions and advices given to me throughout the present study and critical reading of the manuscript.

For the valuable advice and critical reading of the manuscript, I wish to express my sincerest thanks to Prof. Dr. Hiroshi Wada, Prof. Dr. Ken-ichiro Ishida, and Assis. Prof. Dr. Ryusuke Niwa of the University of Tsukuba. I am also grateful to Dr. Makiko Fukui of Ehime University, Prof. Dr. Peter Zwick of Max Plank Institute, Prof. Dr. Tadaaki Tsutsumi of Fukushima University, Prof. Dr. Toru Kishimoto of Tsukuba International University, Prof. Dr. Rolf G. Beutel of Friedrich-Schiller-Universität Jena, and Dr. Alexander Blanke of Universität zu Köln for their valuable discussion and advices.

I deeply thank Dr. Shigekazu Tomizuka, Dr. Yuta Mashimo, Dr. Mari Fujita, Mr. Kazuki Kojima, Mr. Takayuki Yamamoto, Dr. Kensuke Seto, late Mr. Muneki Yamada, Mr. Hiroshi Masumoto, and the staff of SRS for their kind help and hospitality.

Finally, I would like to express my sincere appreciation of my parents and Mitsuki Yamauchi for their understanding support and continuous encouragements.

The present study was partly supported by the Sasakawa Scientific Research Grant (28-515) from The Japan Science Society and by the Japan Society for the Promotion of Science (JSPS) Research Fellowship for Young Scientists (JP18J10360).

LETERATURE CITED

Anderson, D.T. (1972) The development of hemimetabolous insects. *In*: S.J. Counce and C.H. Waddington (eds.), *Developmental Systems: Insects, Vol. 1*, pp. 95–163. Academic Press, New York.

Ando, H. (1962) *The Comparative Embryology of Odonata with Special Reference to a Relic Dragonfly* Epiophlebia superstes *Selys*. The Japan Society for the Promotion of Science, Tokyo.

Ando, H. and Y. Kobayashi (1996) Outline of embryogenesis. *In*: H. Ando and Y. Kobayashi (eds.), *Insect Embryology, Vol. 1*, pp. 48–98. Baifukan, Tokyo. (in Japanese).

Bedfold, G.O. (1970) The development of the egg of *Didymuria violescens* (Phasmatodea: Phasmatidae: Podacanthinae)–embryology and determination of the stage at which first diapause occurs. *Australian Journal of Zoology*, **18**, 155–169.

Beutel, R.G. and S.N. Gorb (2006) A revised interpretation of the evolution of attachment structures in Hexapoda with special emphasis on Mantophasmatodea. *Arthropod Systematics and Phylogeny*, **64**, 3–25.

Beutel, R.G. and D. Weide (2005) Cephalic anatomy of *Zorotypus hubbardi* (Hexapoda: Zoraptera): new evidence for a relationship with Acercaria. *Zoomorphology*, **124**, 121–136.

Beutel, R.G., B. Wipfler, M. Gottardo and R. Dallai (2013) Polyneoptera or “lower Neoptera” – new light on old and difficult phylogenetic problems. *Atti Accademia Nazionale Italiana di Entomologia*, **61**, 133–142.

Beutel, R.G., F. Friedrich, S.-Q. Ge and X.-K. Yang (2014) *Insect Morphology and Phylogeny*. Walter de Gruyter, Berlin.

Beutel, R.G., M.I. Yavorskaya, Y. Mashimo, M. Fukui and K. Meusemann (2017) The phylogeny of Hexapoda (Arthropoda) and the evolution of megadiversity. *Proceedings of the Arthropodan Embryological Society of Japan*, **51**, 1–15.

Blanke, A. and R. Machida (2016) The homology of cephalic muscles and endoskeletal elements between Diplura and Ectognatha (Insecta). *Organisms Diversity and Evolution*, **16**, 241–257.

Blanke, A., B. Wipfler, H. Letsch, M. Koch, F. Beckmann, R.G. Beutel and B. Misof (2012) Revival of Palaeoptera–head characters support a monophyletic origin of Odonata and Ephemeroptera (Insecta). *Cladistics*, **28**, 560–581.

Blumer, M.J.F., P. Gahleitner, T. Narzt, C. Handl and B. Ruthensteiner (2002) Ribbons of semithin sections: an advanced method with a new type of diamond knife. *Journal of Neuroscience Methods*, **120**, 11–16.

Boudreaux, H.B. (1979) *Arthropod Phylogeny with Special Reference to Insects*. John Wiley & Sons, New York.

Cobben, R.H. (1968) *Evolutionary Trends in Heteroptera. Part I Eggs, Architecture of the Shell, Gross Embryology and Eclosion*. Centre for Agricultural Publishing and Documentation, Wageningen.

Degrange, C. (1957) L'œuf et le mode d'éclosion de quelques Plécoptères. *Travaux du Laboratoire d'Hydrobiologie et de Pisciculture de l'Université de Grenoble*, **48/49**, 37–49.

DeWalt, R.E., B.C. Kondratieff and J.B. Sandberg (2015) Order Plecoptera. *In*: J. Thorp and D.C. Rogers (eds.), *Ecology and General Biology: Thorp and Covich's Freshwater Invertebrates, Vol. 1*, pp. 933–949. Academic Press, Cambridge.

DeWalt, R.E., M.D. Maehr, U. Neu-Becker and G. Stueber (2019) *Plecoptera Species File Online*. Version 5.0/5.0. http://Plecoptera.SpeciesFile.org. (date of access: 22. i. 2019).

Faull, K.J. and C.R. Williams (2016) Differentiation of *Aedes aegypti* and *Aedes notoscriptus* (Diptera: Culicidae) eggs using scanning electron microscopy. *Arthropod Structure and Development*, **45**, 273–280.

Fausto, A.M., M. Belardinelli, R. Fochetti and M. Mazzini (2001) Comparative spermatology in Plecoptera (Insecta): an ultrastructural investigation on four species. *Arthropod Structure and Development*, **30**, 55–62.

Fochetti, R. and J.M. Tierno de Figueroa (2008) Global diversity of stoneflies (Plecoptera; Insecta) in freshwater. *Hydrobiologia*, **595**, 365–377.

Fujita, M. and R. Machida (2017) Embryonic development of *Eucorydia yasumatsui* Asahina, with special reference to external morphology (Insecta: Blattodea, Corydiidae). *Journal of Morphology*, **278**, 1469–1489.

Fujita, M., A. Blanke, S. Nomura and R. Machida (2016) Simple, artifact-free SEM observations of insect embryos: application of the nano-suit method to insect embryology. *Proceedings of the Arthropodan Embryological Society of Japan*, **50**, 7–10.

Fukui, M. and R. Machida (2006) Embryonic development of *Baculentulus densus* (Imadaté): an outline (Hexapoda: Protura, Acerentomidae). *Proceedings of Arthropodan Embryological Society of Japan*, **41**, 21–28.

Fukui, M. and R. Machida (2009) Formation of the entognathy in *Baculentulus densus* (Imadaté) (Hexapoda: Protura, Acerentomidae). *Proceedings of the Arthropodan Embryological Society of Japan*, **44**, 25–27.

Fukui, M., M. Fujita, S. Tomizuka, Y. Mashimo, S. Shimizu, C.-Y. Lee, Y. Murakami and R. Machida (2018) Egg structure and outline of embryonic development of the basal mantodean, *Metallyticus splendidus* Westwood, 1835 (Insecta, Mantodea, Metallyticidae). *Arthropod Structure and Development*, **47**, 64–73.

Goss, R.J. (1952) The early embryology of the book louse, *Liposcelis divergens* Badonnel (Psocoptera; Liposcelidae). *Journal of Morphology*, **91**, 135–167.

Grimaldi, D. and M.S. Engel (2005) *Evolution of the Insects*. Cambridge University Press, New York.

Hagan, H.R. (1917) Observations on the embryonic development of the mantid *Paratenodera sinensis*. *Journal of Morphology*, **30**, 223–243.

Hamilton, K.G.A. (1972) The insect wing, part IV. Venational trends and the phylogeny of the winged orders. *Journal of the Kansas Entomological Society*, **45**, 295–308.

Heming, B.S. (1979) Origin and fate of germ cells in male and female embryos of *Haplothrips verbasci* (Osborn) (Insecta, Thysanoptera, Phlaeothripidae). *Journal of Morphology*, **160**, 323–344.

Heming, B.S. and E. Huebner (1994) Development of the germ cells and reproductive primordia in male and female embryos of *Rhodnius prolixus* Stål (Hemiptera: Reduviidae). *Canadian Journal of Zoology*, **72**, 1100–1119.

Hennig, W. (1981) *Insect Phylogeny*. John Wiley & Sons, New York.

Heymons, R. (1895) *Die Embryonalentwickelung von Dermapteren und Orthopteren unter Besonderer Berücksichtigung der Keimblätterbildung*. Gustav Fischer, Jena.

Hinton, H.E. (1981) *Biology of Insect Eggs*. Pergamon Press, Oxford.

Hynes, H.B.N. (1974) Observations on the adults and eggs of Australian Plecoptera. *Australian Journal of Zoology*, **29**, 37–52.

Ikeda, Y. and R. Machida (1998) Embryogenesis of the dipluran *Lepidocampa weberi* Oudemans (Hexapoda, Diplura, Campodeidae): external morphology. *Journal of Morphology*, **237**, 101–115.

Ikeda, Y. and R. Machida (2001) Embryogenesis of the dipluran *Lepidocampa weberi* Oudemans (Hexapoda: Diplura, Campodeidae): formation of dorsal organ and related phenomena. *Journal of Morphology*, **249**, 242–251.

Illies, J. (1965) Phylogeny and zoogeography of the Plecoptera. *Annual Review of Entomology*, **10**, 117–140.

Inaga, S., T. Katsumoto, K. Tanaka, T. Kameie, H. Nakane and T. Naguro (2007) Platinum blue as an alternative to uranyl acetate for staining in transmission electron microscopy. *Archives of Histology and Cytology*, **70**, 43–49.

Ishiwata, K., G. Sasaki, J. Ogawa, T. Miyata and Z.-H. Su (2011) Phylogenetic relationships among insect orders based on three nuclear protein-coding gene sequences. *Molecular Phylogenetics and Evolution*, **58**, 169–180.

Isobe, Y. (1988) Eggs of Plecoptera from Japan. *Biology of Inland Waters*, **4**, 27–39.

Jintsu, Y. (2010) *Embryological Studies on* Aposthonia japonica *(Okajima) (Insecta: Embioptera)*. Doctoral dissertation. University of Tsukuba, Tsukuba.

Jintsu, Y. and R. Machida (2009) TEM observations of the egg membranes of a webspinner, *Aposthonia japonica* (Okajima) (Insecta: Embioptera). *Proceedings of the Arthropodan Embryological Society of Japan*, **44**, 19–24.

Jintsu, Y., T. Uchifune and R. Machida (2010) Structural features of eggs of the basal phasmatodean *Timema monikensis* Vickery & Sandoval, 1998 (Insecta: Phasmatodea: Timematidae). *Arthropod Systematics and Phylogeny*, **68**, 71–78.

Kawai, T. (1967) *Fauna Japonica Plecoptera (Insecta)*. Tokyo Electrical Engineering College Press, Tokyo.

Kawai, T. and Y. Isobe (1984) Notes on the egg of *Scopura longa* Uéno (Plecoptera). *Annales de Limnologie*, **20**, 57–58.

Kershaw, J.C. (1914) Development of an embiid. *Journal of the Royal Microscopical Society*, **34**, 24–27.

Khoo, S.G. (1968a) Experimental studies on diapause in stoneflies. II. Eggs of *Diura bicaudata* (L.). *Proceedings of the Royal Entomological Society of London, Series A, General Entomology*, **43**, 49–56.

Khoo, S.G. (1968b) Experimental studies on diapause in stoneflies III. Eggs of *Brachyptera risi* (Morton). *Proceedings of the Royal Entomological Society of London, Series A, General Entomology*, **43**, 141–146.

Kishimoto, T. (1986) *Embryological Studies on the Stonefly* Kamimuria tibialis *(Pictet) (Insecta, Plecoptera, Perlidae)*. Doctoral dissertation. University of Tsukuba, Tsukuba.

Kishimoto, T. (1987) Embryonic development of the ventral nervous system of the stonefly, *Kamimuria tibialis* (Pictét) (Plecoptera, Perlidae). *In*: H. Ando and Cz. Jura (eds.), *Recent Advances in Insect Embryology in Japan and Poland*, pp. 215–223. Isebu, Tsukuba.

Kishimoto, T. (1997a) Comparison of embryonic development among some arctoperlarian species (Plecoptera). *In*: P. Landolt and M. Sartori (eds.), *Ephemeroptera*

& Plecoptera: Biology-Ecology-Systematics, pp. 21–25. Mauron + Tinguely & Lachat SA., Fribourg.

Kishimoto, T. (1997b) Egg envelopes of a stonefly *Scopura montana* Maruyama (Plecoptera: Scopuridae). *Proceedings of Arthropodan Embryological Society of Japan*, **32**, 35–37. (in Japanese with English figure legend).

Kishimoto, T. and H. Ando (1985) External features of the developing embryo of the stonefly, *Kamimuria tibialis* (Pictet) (Plecoptera, Perlidae). *Journal of Morphology*, **183**, 311–326.

Kishimoto, T. and H. Ando (1986) Alimentary canal formation in the stonefly, *Kamimuria tibialis* (Pictet) (Plecoptera: Perlidae). *International Journal of Insect Morphology and Embryology*, **15**, 97–105.

Kjer, K.M., F.L. Carle, J. Litman and J. Ware (2006) A molecular phylogeny of Hexapoda. *Arthropod Systematics and Phylogeny*, **64**, 35–44.

Kjer, K.M., C. Simon, M. Yavorskaya and R.G. Beutel (2016) Progress, pitfalls and parallel universes: a history of insect phylogenetics. *Journal of the Royal Society Interface*, **13**, 20160363.

Klass, K.-D. (2003) The female genitalic region in basal earwigs (Insecta: Dermaptera: Pygidicranidae s.l.). *Entomologische Abhandlungen*, **61**, 173–225.

Klass, K.-D. (2009) A critical review of current data and hypotheses on hexapod phylogeny. *Proceedings of the Arthropodan Embryological Society of Japan*, **43**, 3–22.

Klug, R. and K.-D. Klass (2007) The potential value of the mid-abdominal musculature and nervous system in the reconstruction of interordinal relationships in lower Neoptera. *Arthropod Systematics and Phylogeny*, **65**, 73–100.

Knight, A.W., A.V. Nebeker, and A.R. Gaufin (1965a) Description of the eggs of common Plecoptera of Western United States. *Entomological News*, **76**, 105–111.

Knight, A.W., A.V. Nebeker, and A.R. Gaufin (1965b) Further descriptions of the eggs of Plecoptera of Western United States. *Entomological News*, **76**, 233–239.

Knower, H.M. (1900) The embryology of a termite, *Eutermes* (*Rippertii?*). *Journal of Morphology*, **16**, 505–568.

Kobayashi, Y. (1998) Embryogenesis of the fairy moth, *Nemophora albiantennella* Issiki (Lepidoptera, Adelidae), with special emphasis on its phylogenetic implications. *International Journal of Insect Morphology and Embryology*, **27**, 157–166.

Kobayashi, Y. and H. Ando (1982) The early embryonic development of the primitive moth, *Neomicropteryx nipponensis* Issiki (Lepidoptera, Micropterygidae). *Journal of Morphology*, **172**, 259–269.

Kobayashi, Y. and H. Ando (1987) Early embryonic development and external features of developing embryos in the primitive moth, *Eriocrania* sp. (Lepidoptera, Eriocraniidae). *In*: H. Ando and Cz. Jura (eds.), *Recent Advances in Insect Embryology in Japan and Poland*, pp. 159–180. Isebu, Tsukuba.

Kômoto, N., K. Yukuhiro and S. Tomita (2012) Novel gene rearrangements in the mitochondrial genome of a webspinner, *Aposthonia japonica* (Insecta: Embioptera). *Genome*, **55**, 222–233.

Konopová, B. and J. Zrzavý (2005) Ultrastructure, development, and homology of insect embryonic cuticles. *Journal of Morphology*, **264**, 339–362.

Krause, G. (1939) Die Eitypen der Insekten. *Biologisches Zentralblatt*, **59**, 495–536.

Kristensen, N.P. (1975) The phylogeny of hexapod “orders”. A critical review of recent accounts. *Journal of Zoological Systematics and Evolutionary Research*, **13**, 1–44.

Kristensen, N.P. (1991) Phylogeny of extant hexapods. *In*: CSIRO (ed.), *The Insects of Australia, Vol. 1*, pp. 125–140. Melbourne University Press, Carlton.

Kukalová-Peck, J. (2008) Phylogeny of higher taxa in Insecta: finding synapomorphies in the extant fauna and separating them from homoplasies. *Evolutionary Biology*, **35**, 4–51.

Luan, Y., J.M. Mallatt, R. Xie, Y. Yang and W. Yin (2005) The phylogenetic positions of three basal-hexapod groups (Protura, Diplura, and Collembola) based on ribosomal RNA gene sequences. *Molecular Biology and Evolution*, **22**, 1579–1592.

Machida, R. (2000) Usefulness of low-vacuum scanning electron microscopy in descriptive insect embryology. *Proceedings of Arthropodan Embryological Society of Japan*, **35**, 17–19.

Machida, R. (2006) Evidence from embryology for reconstructing the relationships of hexapod basal clades. *Arthropod Systematics and Phylogeny*, **64**, 95–104.

Machida, R. (2009) Reconstruction of hexapod basal clades from embryological evidence. *Proceedings of the Arthropodan Embryological Society of Japan*, **43**, 39–42.

Machida, R. and H. Ando (1998) Evolutionary changes in developmental potentials of the embryo proper and embryonic membranes along with the derivative structures in Atelocerata, with special reference to Hexapoda (Arthropoda). *Proceedings of Arthropodan Embryological Society of Japan*, **33**, 1–13.

Machida, R. and I. Takahashi (2003) Embryonic development of a proturan *Baculentulus densus* (Imadaté): reference to some developmental stages (Hexapoda: Protura, Acerentomidae). *Proceedings of Arthropodan Embryological Society of Japan*, **38**, 13–17.

Machida, R., T. Nagashima and H. Ando (1990) The early embryonic development of the jumping bristletail *Pedetontus unimaculatus* Machida (Hexapoda: Microcoryphia, Machilidae). *Journal of Morphology*, **206**, 181–195.

Machida, R., T. Nagashima and H. Ando (1994a) Embryonic development of the jumping bristletail *Pedetontus unimaculatus* Machida, with special reference to embryonic membranes (Hexapoda: Microcoryphia, Machilidae). *Journal of Morphology*, **220**, 147–165.

Machida, R., T. Nagashima and T. Yokoyama (1994b) Mesoderm segregation of a jumping bristletail, *Pedetontus unimaculatus* Machida (Hexapoda, Microcoryphia), with a note on an automatic vacuum infiltrator. *Proceedings of Arthropodan Embryological Society of Japan*, **29**, 23–24. (in Japanese with English figure legend).

Machida, R., Y. Ikeda and K. Tojo (2002) Evolutionary changes in developmental potentials of the embryo proper and embryonic membranes in Hexapoda: a synthesis revised. *Proceedings of Arthropodan Embryological Society of Japan*, **37**, 1–11.

Machida, R., K. Tojo, T. Tsutsumi, T. Uchifune, K.-D. Klass, M.D. Picker and L. Pretorius (2004) Embryonic development of heel-walkers: reference to some prerevolutionary stages (Insecta: Mantophasmatodea). *Proceedings of Arthropodan Embryological Society of Japan*, **39**, 31–39.

Mashimo, Y. and R. Machida (2017) Embryological evidence substantiates the subcoxal theory on the origin of pleuron in insects. *Scientific Reports*, **7**, 12597.

Mashimo, Y., R.G. Beutel, R. Dallai, C.-Y. Lee and R. Machida (2014) Embryonic development of Zoraptera with special reference to external morphology, and its phylogenetic implications (Insecta). *Journal of Morphology*, **275**, 295–312.

Masumoto, M. and R. Machida (2006) Development of embryonic membranes in the silverfish *Lepisma saccharina* Linnaeus (Insecta: Zygentoma, Lepismatidae). *Tissue and Cell*, **38**, 159–169.

Matsumura, Y., B. Wipfler, H. Pohl, R. Dallai, R. Machida, Y. Mashimo, J.T. Câmara, J.A. Rafael and R.G. Beutel (2015) Cephalic anatomy of *Zorotypus weidneri* New, 1978: new evidence for a placement of Zoraptera. *Arthropod Systematics and Phylogeny*, **73**, 85–105.

Matthée, J.J. (1951) The structure and physiology of the egg of *Locustana pardalina* (Walk). *Science Bulletin, Union of South Africa*, **316**, 1–83.

McCulloch, G.A., G.P. Wallis and J.M. Waters (2016) A time-calibrated phylogeny of southern hemisphere stoneflies: testing for Gondwanan origins. *Molecular Phylogenetics and Evolution*, **96**, 150–160.

Michalik, A., E. Rościszewska and M. Miliša (2015) The structure and ultrastructure of the egg capsule of *Brachyptera risi* (Plecoptera, Nemouroidea, Taeniopterygidae) with some remarks concerning choriogenesis. *Microscopy Research and Technique*, **78**, 180–186.

Miller, A. (1939) The egg and early development of the stonefly, *Pteronarcys proteus* Newman (Plecoptera). *Journal of Morphology*, **64**, 555–609.

Miller, A. (1940) Embryonic membranes, yolk cells, and morphogenesis of the stonefly *Pteronarcys proteus* Newman (Plecoptera: Pteronarcidae). *Annals of the Entomological Society of America*, **33**, 437–477.

Misof, B., S. Liu, K. Meusemann, R.S. Peters, A. Donath, C. Mayer, P.B. Frandsen, J. Ware, T. Flouri, R.G. Beutel, O. Niehuis, M. Petersen, F. Izquierdo-Carrasco, T. Wappler, J. Rust, A.J. Aberer, U. Aspöck, H. Aspöck, D. Bartel, A. Blanke, S. Berger,

A. Böhm, T.R. Buckley, B. Calcott, J. Chen, F. Friedrich, M. Fukui, M. Fujita, C. Greve, P. Grobe, S. Gu, Y. Huang, L.S. Jermiin, A.Y. Kawahara, L. Krogmann, M. Kubiak, R. Lanfear, H. Letsch, Y. Li, Z. Li, J. Li, H. Lu, R. Machida, Y. Mashimo, P. Kapli, D.D. McKenna, G. Meng, Y. Nakagaki, J.L. Navarrete-Heredia, M. Ott, Y. Ou, G. Pass, L. Podsiadlowski, H. Pohl, B.M. von Reumont, K. Schütte, K. Sekiya, S. Shimizu, A. Slipinski, A. Stamatakis, W. Song, X. Su, N.U. Szucsich, M. Tan, X. Tan, M. Tang, J. Tang, G. Timelthaler, S. Tomizuka, M. Trautwein, X. Tong, T. Uchifune, M.G. Walzl, B.M. Wiegmann, J. Wilbrandt, B. Wipfler, T.K.F. Wong, Q. Wu, G. Wu, Y. Xie, S. Yang, Q. Yang, D.K. Yeates, K. Yoshizawa, Q. Zhang, R. Zhang, W. Zhang, Y. Zhang, J. Zhao, C. Zhou, L. Zhou, T. Ziesmann, S. Zou, Y. Li, X. Xu, Y. Zhang, H. Yang, J. Wang, J. Wang, K.M. Kjer and X. Zhou (2014) Phylogenomics resolves timing and pattern of insect evolution. *Science*, **346**, 763–767.

Miyawaki, K., T. Mito, I. Sarashina, H.J. Zhang, Y. Shinmyo, H. Ohuchi and S. Noji (2004) Involvement of Wingless/Armadillo signaling in the posterior sequential segmentation in the cricket, *Gryllus bimaculatus* (Orthoptera), as revealed by RNAi analysis. *Mechanisms of Development*, **121**, 119–130.

Mori, H. (1970) The distribution of the columnar serosa of eggs among the families of Heteroptera, in relation to phylogeny and systematics. *Japanese Journal of Zoology*, **16**, 89–98.

Nakagaki, Y., M. Sakuma and R. Machida (2015) Expression of engrailed-family genes in the jumping bristletail and discussion on the primitive pattern of insect segmentation. *Development Genes and Evolution*, **225**, 313–318.

Poprawa, I., A. Baran and E. Rościszewska (2002) Structure of ovaries and formation of egg envelopes in the stonefly, *Leuctra autumnalis* Aubert, 1948 (Plecoptera: Leuctridae). Ultrastructural studies. *Folia Biologica (Kraków)*, **50**, 29–38.

Ricker, W.E. (1950) Some evolutionary trends in Plecoptera. *Proceedings of the Indiana Academy of Science*, **59**, 197–209.

Roonwal, M.L. (1937) Studies on the embryology of the African migratory locust, *Locusta migratoria migratorioides* Reiche and Frm. (Orthoptera, Acrididae). II. Organogeny. *Philosophical Transactions of the Royal Society of London, Series B, Biological Sciences*, **227**, 175–244.

Ross, H.H. (1955) The evolution of the insect orders. *Entomological News*, **66**, 197–208.

Ross-Gillespie, V., M.D. Picker, H.F. Dallas and J.A. Day (2018) The role of temperature in egg development of three aquatic insects *Lestagella penicillata* (Ephemeroptera), *Aphanicercella scutata* (Plecoptera), *Chimarra ambulans* (Trichoptera) from South Africa. *Journal of Thermal Biology*, **71**, 158–170.

Rościszewska, E. (1996) Egg capsule structure of the stonefly *Protonemura intricata* (Ris 1902) (Plecoptera: Nemouridae). *Acta Biologica Cracoviensia Series Zoologia*, **38**, 41–48.

Sander, K. (1984) Extrakaryotic determinants, a link between oogenesis and embryonic pattern formation in insects. *Proceedings of Arthropodan Embryological Society of Japan*, **19**, 1–12.

Schölzel, G. (1937) Die Embryologie der Anopluren und Mallophagen. *Zeitschrift für Parasitenkunde*, **9**, 730–770.

Sekiya, K. and R. Machida (2009) Embryonic development of *Occasjapyx japonicus* (Enderlein): notable features (Hexapoda: Diplura, Dicellurata). *Proceedings of the Arthropodan Embryological Society of Japan*, **44**, 13–18.

Sekiya, K. and R. Machida (2011) Formation of the entognathy of Dicellurata, *Occasjapyx japonicus* (Enderlein, 1907) (Hexapoda: Diplura, Dicellurata). *Soil Organisms*, **83**, 399–404.

Shimizu, S. (2013) *Comparative Embryology of Dermaptera (Insecta)*. Doctoral dissertation. University of Tsukuba, Tsukuba.

Shimizu, T., K. Inada and S. Uchida (2005) Plecoptera. *In*: T. Kawai and K. Tanida (eds.), *Aquatic Insects of Japan: Manual with Keys and Illustrations*, pp. 237–290. Tokai University Press, Hadano. (in Japanese).

Sikes, E.K. and V.B. Wigglesworth (1931) The hatching of insects from the egg, and the appearance of air in the tracheal system. *Quarterly Journal of Microscopical Science*, **74**, 165–192.

Slifer, E.H. (1938) The formation and structure of a special water-absorbing area in the membranes covering the grasshopper egg. *Quarterly Journal of Microscopical Science*, **80**, 437–457.

Slifer, E.H. and S.S. Sekhon (1963) The fine structure of the membranes which cover the egg of the grasshopper, *Melanoplus differentialis*, with special reference to the hydropyle. *Quarterly Journal of Microscopical Science*, **104**, 321–334.

Song, N., H. Li, F. Song and W. Cai (2016) Molecular phylogeny of Polyneoptera (Insecta) inferred from expanded mitogenomic data. *Scientific Reports*, **6**, 36175.

Stark, B.P. and K.W. Stewart (1981) The Nearctic genera of Peltoperlidae (Plecoptera). *Journal of the Kansas Entomological Society*, **54**, 285–311.

Stark, B.P., B.C. Kondratieff and C.J. Verdone (2015) *Kathroperla siskiyou*, a new stonefly species from California and Oregon, U.S.A. (Plecoptera: Chloroperlidae). *Illiesia*, **11**, 92–103.

Takaku, Y., H. Suzuki, I. Ohta, D. Ishii, Y. Muranaka, M. Shimomura and T. Hariyama (2013) A thin polymer membrane, nano-suit, enhancing survival across the continuum between air and high vacuum. *Proceedings of the National Academy of Science of the United States of America*, **110**, 7631–7635.

Terry, M.D. (2004) *Phylogeny of the Polyneopterous Insects with Emphasis on Plecoptera: Molecular and Morphological Evidence*. Doctoral dissertation. Brigham Young University, Provo.

Terry, M.D. and M.F. Whiting (2005) Mantophasmatodea and phylogeny of the lower neopterous insects. *Cladistics*, **21**, 240–257.

Thomas, M.A., K.A. Walsh, M.R. Wolf, B.A. McPheron and J.H. Marden (2000) Molecular phylogenetic analysis of evolutionary trends in stonefly wing structure and locomotor behavior. *Proceedings of the National Academy of Science of the United States of America*, **97**, 13178–13183.

Tojo, K. and R. Machida (1997) Embryogenesis of the mayfly *Ephemera japonica* McLachlan (Insecta: Ephemeroptera, Ephemeridae), with special reference to abdominal formation. *Journal of Morphology*, **234**, 97–107.

Tomizuka, S. and R. Machida (2015). Embryonic development of a collembolan, *Tomocerus cuspidatus* Börner, 1909: with special reference to the development and developmental potential of serosa (Hexapoda: Collembola, Tomoceridae). *Arthropod Structure and Development*, **44**, 157–172.

Tomizuka, S. and R. Machida (2017) Tentorial invaginations of the collembolan *Tomocerus cuspidatus* Börner, 1909 (Hexapoda: Collembola, Tomoceridae). *Proceedings of the Arthropodan Embryological Society of Japan*, **48**, 43–45.

Tsutsumi, K. and R. Machida (2006) Embryonic development of a snakefly, *Inocellia japonica* Okamoto: an outline (Insecta: Neuroptera, Raphidiodea). *Proceedings of Arthropodan Embryological Society of Japan*, **41**, 37–45.

Uchida, S. and H. Maruyama (1987) What is *Scopura longa* Uéno, 1929 (Insecta, Plecoptera)? A revision of the genus. *Zoological Science*, **4**, 699–709.

Uchifune, T. and R. Machida (2005) Embryonic development of *Galloisiana yuasai* Asahina, with special reference to external morphology (Insecta: Grylloblattodea). *Journal of Morphology*, **266**, 182–207.

Venable, J.H. and R. Coggeshall (1965) A simplified lead citrate stain for use in electron microscopy. *Journal of Cell Biology*, **25**, 407–408.

Wheeler, W.M. (1893) A contribution to insect embryology. *Journal of Morphology*, **8**, 1–160.

Wipfler, B., R. Klug, S.-Q. Ge, M. Bai, J. Göbbels, X.-K. Yang and T. Hörnschemeyer (2015) The thorax of Mantophasmatodea, the morphology of flightlessness, and the evolution of the neopteran insects. *Cladistics*, **31**, 50–70.

Wipfler, B., H. Letsch, P.B. Frandsen, P. Kapli, C. Mayer, D. Bartel, T.R. Buckley, A. Donath, J.S. Edgerly-Rooks, M. Fujita, S. Liu, R. Machida, Y. Mashimo, B. Misof, O. Niehuis, R.S. Peters, M. Petersen, L. Podsiadlowski, K. Schütte, S. Shimizu, T. Uchifune, J. Wilbrandt, E. Yan, X. Zhou and S. Simon (2019) Evolutionary history of Polyneoptera and its implications for our understanding of early winged insects.

Proceedings of the National Academy of Science of the United States of America, in press.

Yoshizawa, K. (2011) Monophyletic Polyneoptera recovered by wing base structure. *Systematic Entomology*, **36**, 377–394.

Zwick, P. (1973) Insecta: Plecoptera. Phylogenetisches System und Katalog. *Das Tierreich*, **94**, i–xxxii, 1–465. De Gruyter, Berlin, New York.

Zwick, P. (1999) Egg diapause, egg swelling and mother-child size relationships in Plecoptera (Insecta). *Advances in Limnology*, **54**, 373–386.

Zwick, P. (2000) Phylogenetic system and zoogeography of the Plecoptera. *Annual Review of Entomology*, **45**, 709–746.

Zwick, P. (2009) The Plecoptera – who are they? The problematic placement of stoneflies in the phylogenetic system of insects. *Aquatic Insects*, **31**, 181–194.

TABLES

Table 1. Nine Japanese arctoperlarian stoneflies of which egg structure and embryonic development were examined in present study.

Materials	**Month of oviposition**	**Temperature for incubation of adults and eggs**
Euholognatha		
Scopuridae: *Scopura montana* Maruyama, 1987	October–December	8°C
Taeniopterygidae: *Obipteryx* Okamoto, 1922 sp.	June	12°C
Leuctridae: *Paraleuctra cercia* (Okamoto, 1922)	May–June	12°C
Capniidae: *Apteroperla tikumana* (Uéno, 1938)	February–April	4°C
Nemouridae: *Protonemura towadensis* (Kawai, 1954)	November–December	8°C
Systellognatha		
Perlidae: *Calineuria stigmatica* (Klapálek, 1907)	September–October	12°C
Chloroperlidae: *Sweltsa* Ricker, 1943 sp.	May–June	12°C
Perlodidae: *Ostrovus* Ricker, 1952 sp.	June– July	12°C
Peltoperlidae: *Yoraperla uenoi* (Kohno, 1946)	June– July	12°C

FIGURES

Fig. 1. Proposed phylogeny of insects s. str./pterygotes. A: Phylogeny by Beutel and Gorb (2006) based on 120 morphological characters. B: Phylogeny by Wipfler et al. (2015) based on 119 morphological characters. C: Phylogeny by Ross (1955) based on comparative morphology.

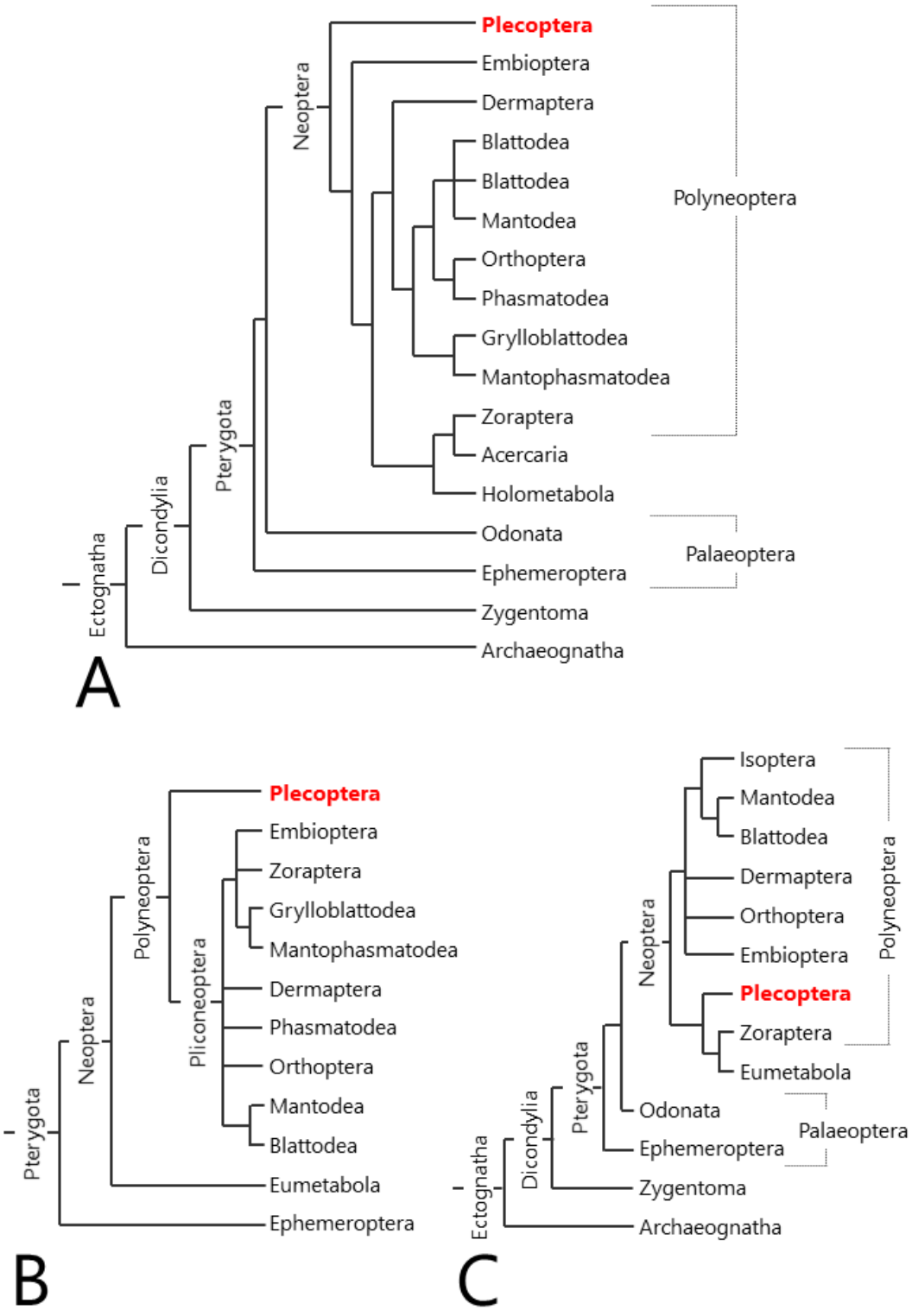
Plecoptera
Embioptera
Dermaptera
Blattodea
Blattodea
Mantodea
Orthoptera
Phasmatodea
Grylloblattodea
Mantophasmatodea
Zoraptera
Acercaria
Holometabola
Odonata
Ephemeroptera
Zygentoma
Archaeognatha
Neoptera
Pterygota
Dicondylia
Ectognatha
Polyneoptera
Palaeoptera
A
Plecoptera
Embioptera
Zoraptera
Grylloblattodea
Mantophasmatodea
Dermaptera
Phasmatodea
Orthoptera
Mantodea
Blattodea
Eumetabola
Ephemeroptera
Polyneoptera
Pliconeoptera
Neoptera
Pterygota
B
Isoptera
Mantodea
Blattodea
Dermaptera
Orthoptera
Embioptera
Plecoptera
Zoraptera
Eumetabola
Odonata
Ephemeroptera
Zygentoma
Archaeognatha
Polyneoptera
Palaeoptera
Neoptera
Pterygota
Dicondylia
Ectognatha
C

Fig. 1. Continued. D: Phylogeny by Ishiwata et al. (2011) based on protein-coded genes (*DPD1*, *RPB1*, *RPB2*). E: Phylogeny by Misof et al. (2014) based on transcriptomes of 1,478 genes.

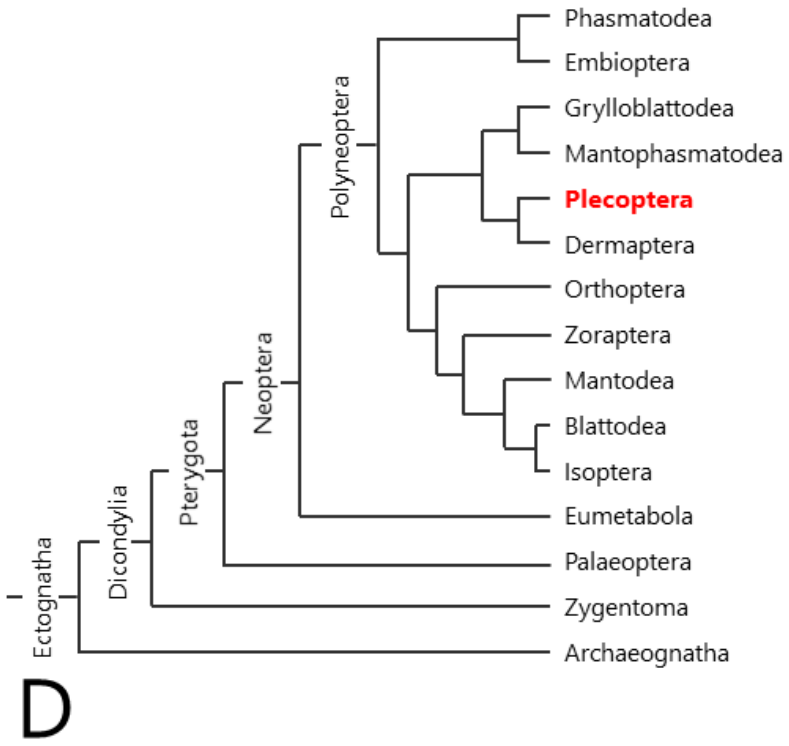
Phasmatodea
Embioptera
Grylloblattodea
Mantophasmatodea
Plecoptera
Dermaptera
Orthoptera
Zoraptera
Mantodea
Blattodea
Isoptera
Eumetabola
Palaeoptera
Zygentoma
Archaeognatha
Polyneoptera
Neoptera
Pterygota
Dicondylia
Ectognatha
D

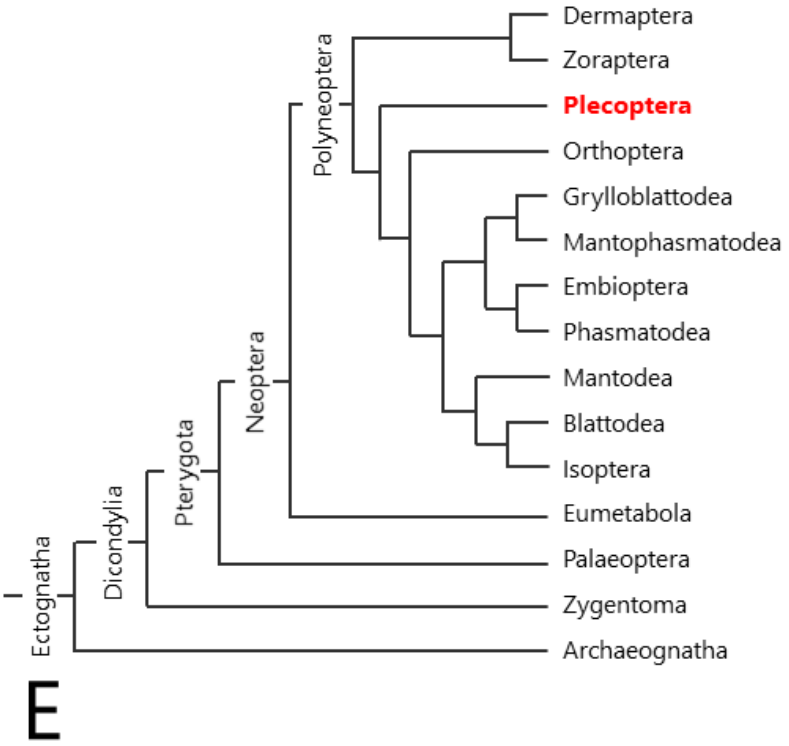
Dermaptera
Zoraptera
Plecoptera
Orthoptera
Grylloblattodea
Mantophasmatodea
Embioptera
Phasmatodea
Mantodea
Blattodea
Isoptera
Eumetabola
Palaeoptera
Zygentoma
Archaeognatha
Polyneoptera
Neoptera
Pterygota
Dicondylia
Ectognatha
E

Fig. 2. Eggs of *Scopura montana*, SEM. A: Egg, lateral view, anterior to the top. B: Enlargement of the egg surface near the anterior pole. Endochorion can be seen through a tear of the exochorion. C, D: Egg surface of the anterior pole (C) and its enlargement (D). Arrowheads indicate micropyles.

Ench, endochorion; Exch, exochorion.

Scale bars = A, 100 μm; B, D, 10 μm; C, 50 μm.

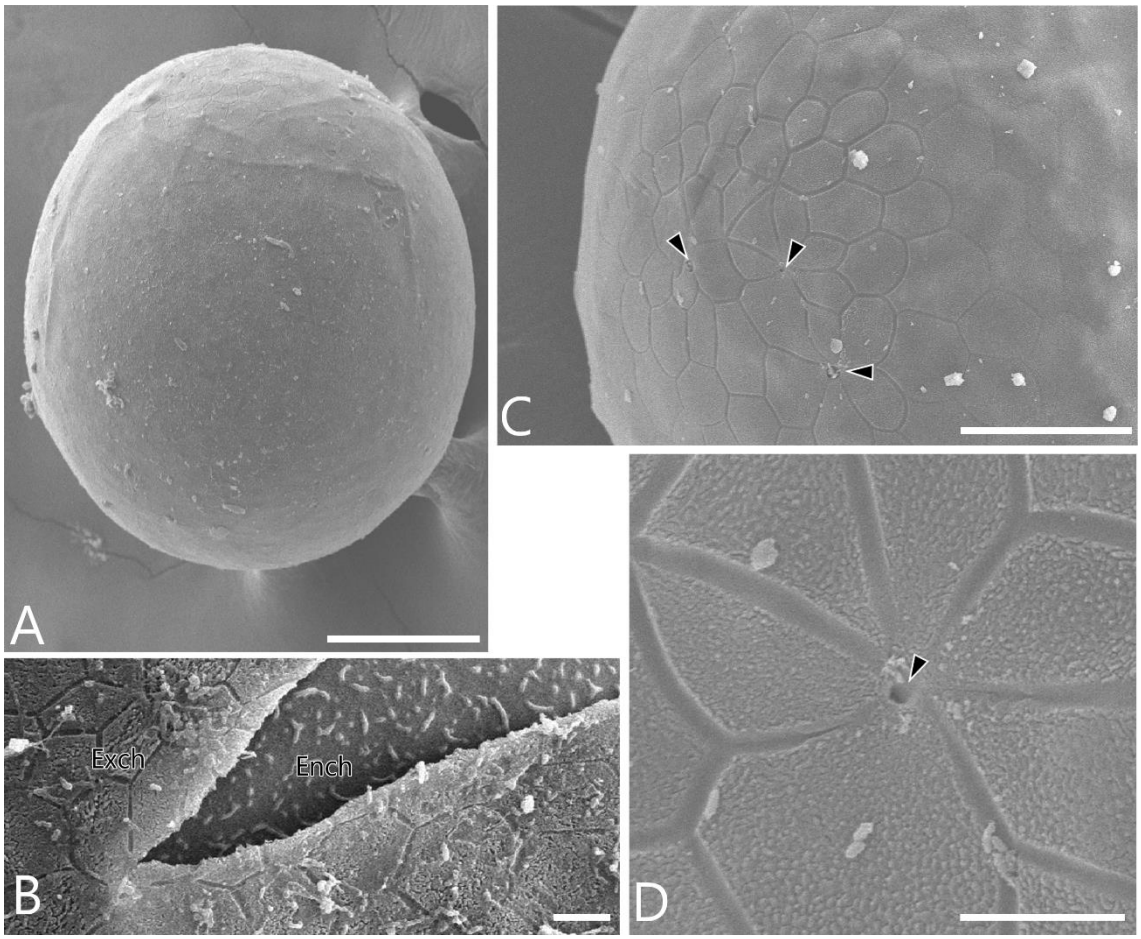
A
B
Exch
Ench
C
D

Fig. 3. Egg membrane of a newly laid egg of *Scopura montana*, TEM. A, B: The egg membrane, including a rod-like material (A) and enlargement of the egg membrane, showing details of the endochorion and the vitelline membrane (B). The stars show small hemispherical protuberances on the surface of the endochorion.

Ench, endochorion; Ench1, endochorion 1; Ench1-I, sublayer I of endochorion 1; Ench1-II, sublayer II of endochorion 1; Ench2, endochorion 2; Ench2-I, sublayer I of endochorion 2; Ench2-II, sublayer II of endochorion 2; Exch, exochorion; Pe, periplasm; RLM, rod-like material; VM, vitelline membrane; Y, yolk.

Scale bars = A, 1 μm; B, 200 nm.

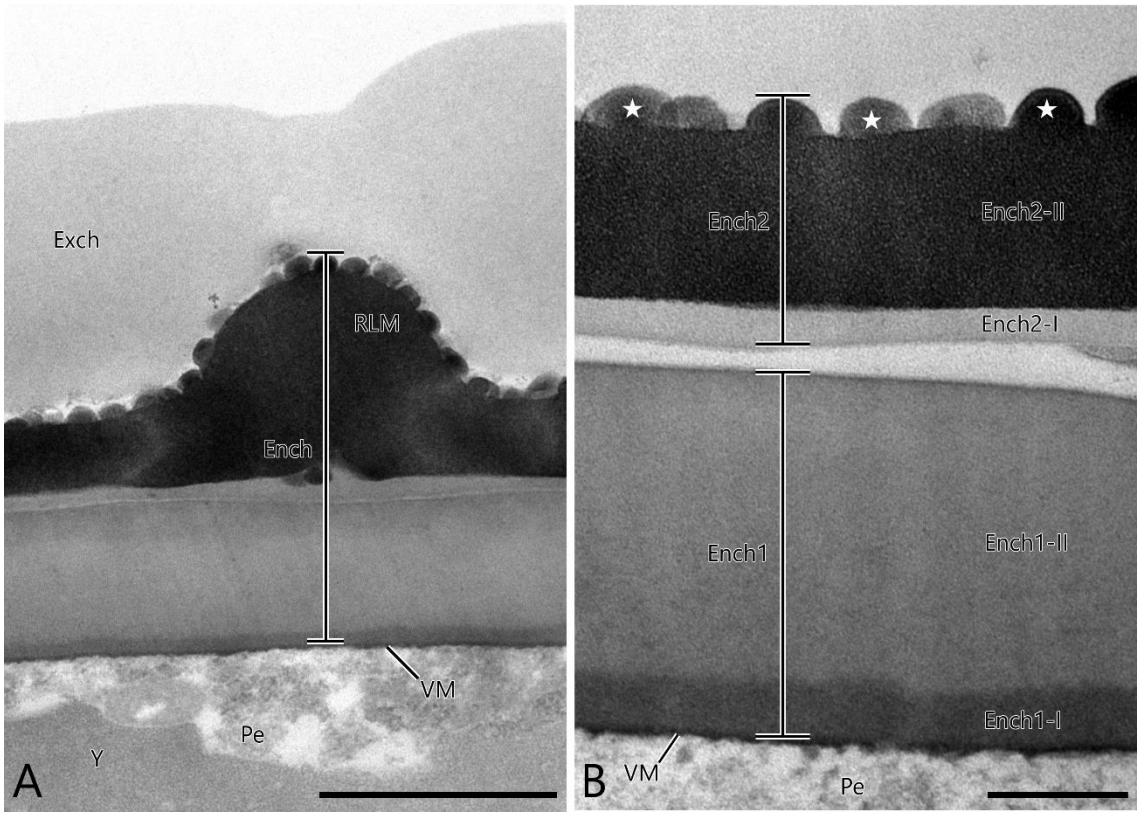
Exch
RLM
Ench
VM
Pe
Y
A
Ench2
Ench2-II
Ench2-I
Ench1
Ench1-II
Ench1-I
VM
Pe
B

Fig. 4. Embryonic development of *Scopura montana*, fluorescence microscopy with DAPI staining, lateral view, anterior of the egg to the top, ventral of the egg to the left. A: Stage 1. B: Stage 2. C: Stage 3. D: Stage 4. E: Stage 5. F: Stage 6. G: Stage 7. H: Stage 8. I: Stage 9. J: Stage 10. K: Stage 11. L: Stage 12.

Am, amnion; An, antenna; Ce, cercus; CE, compound eye; Cllr, clypeolabrum; Em, embryo; Ga, galea; GD, germ disc; HC, head capsule; HL, head lobe; La, lacinia; Md, mandible; MxCp, maxillary coxopodite; MxP, maxillary palp; Pce, protocephalon; Pco, protocorm; SDO, secondary dorsal organ; Se, serosa; Th1L, prothoracic leg.

Scale bars = 100 µm.

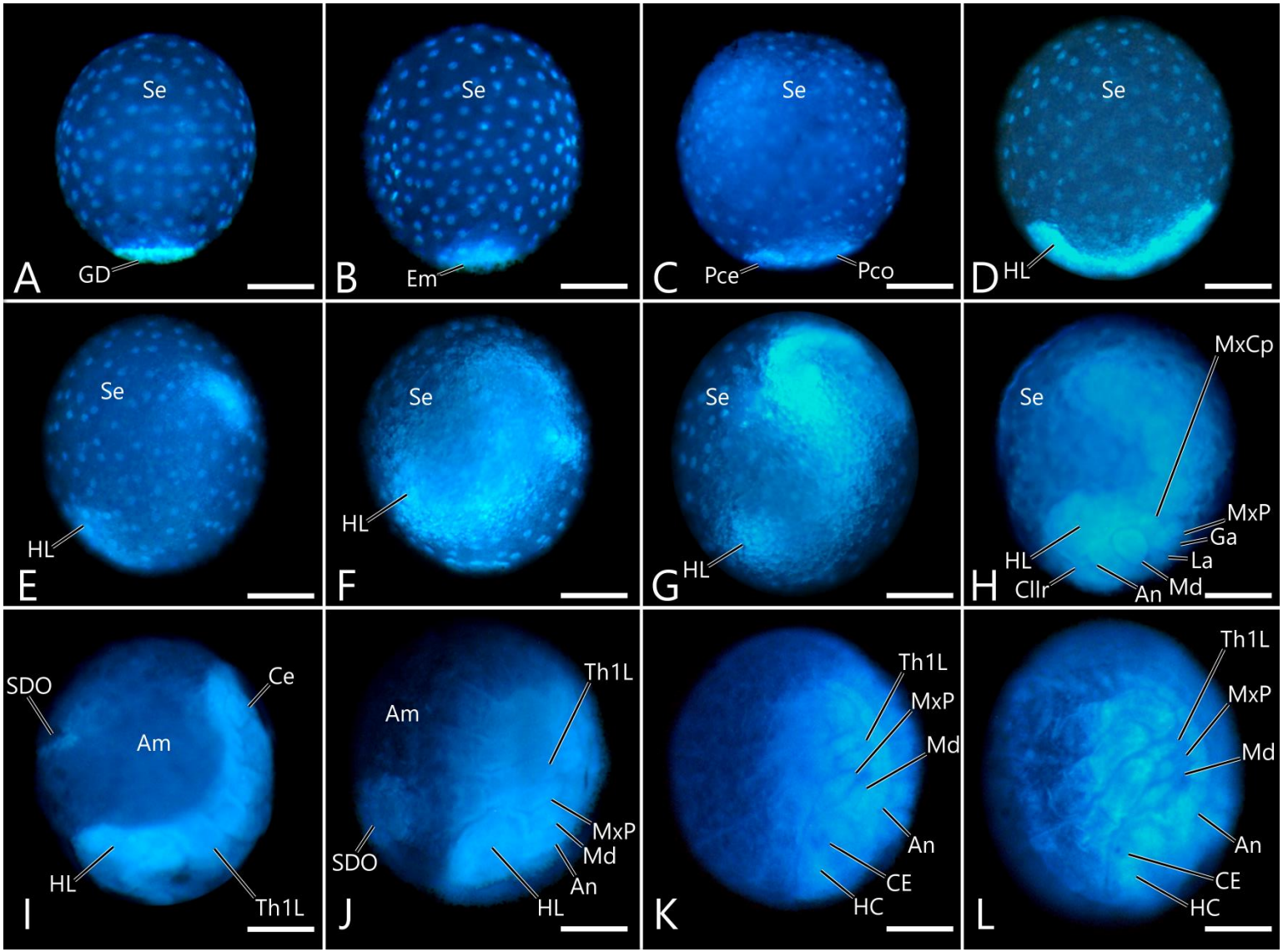
A
Se
GD
B
Se
Em
C
Se
Pce
Pco
D
Se
HL
E
Se
HL
F
Se
HL
G
Se
HL
H
Se
MxCp
MxP
Ga
La
HL
Cllr
An
Md
I
SDO
Ce
Am
HL
Th1L
J
Am
Th1L
MxP
Md
SDO
An
HL
K
Th1L
MxP
Md
An
CE
HC
L
Th1L
MxP
Md
An
CE
HC

Fig. 5. Embryonic development of *Scopura montana*, fluorescence microscopy with DAPI staining, posterior view, ventral of the egg at the top. A: Stage 1. B: Stage 2. C: Stage 3. D: Stage 4. E: Stage 5. F: Stage 6. G: Stage 7. H: Stage 8. I: Stage 9. J: Stage 10. K: Stage 11. L: Stage 12.

An, antenna; CE, compound eye; Cl, clypeus; Cllr, clypeolabrum; Em, embryo; ET, egg tooth; Fr, frons; Ga, galea; GD, germ disc; HC, head capsule; HL, head lobe; La, lacinia; LbP, labial palp; Lr, labrum; Md, mandible; MxCp, maxillary coxopodite; MxP, maxillary palp; Pce, protocephalon; Pco, protocorm; Pgl, paraglossa; Sd, stomodaeum; SDO, secondary dorsal organ; Se, serosa; Th1, prothoracic segment.

Scale bars = 100 μm.

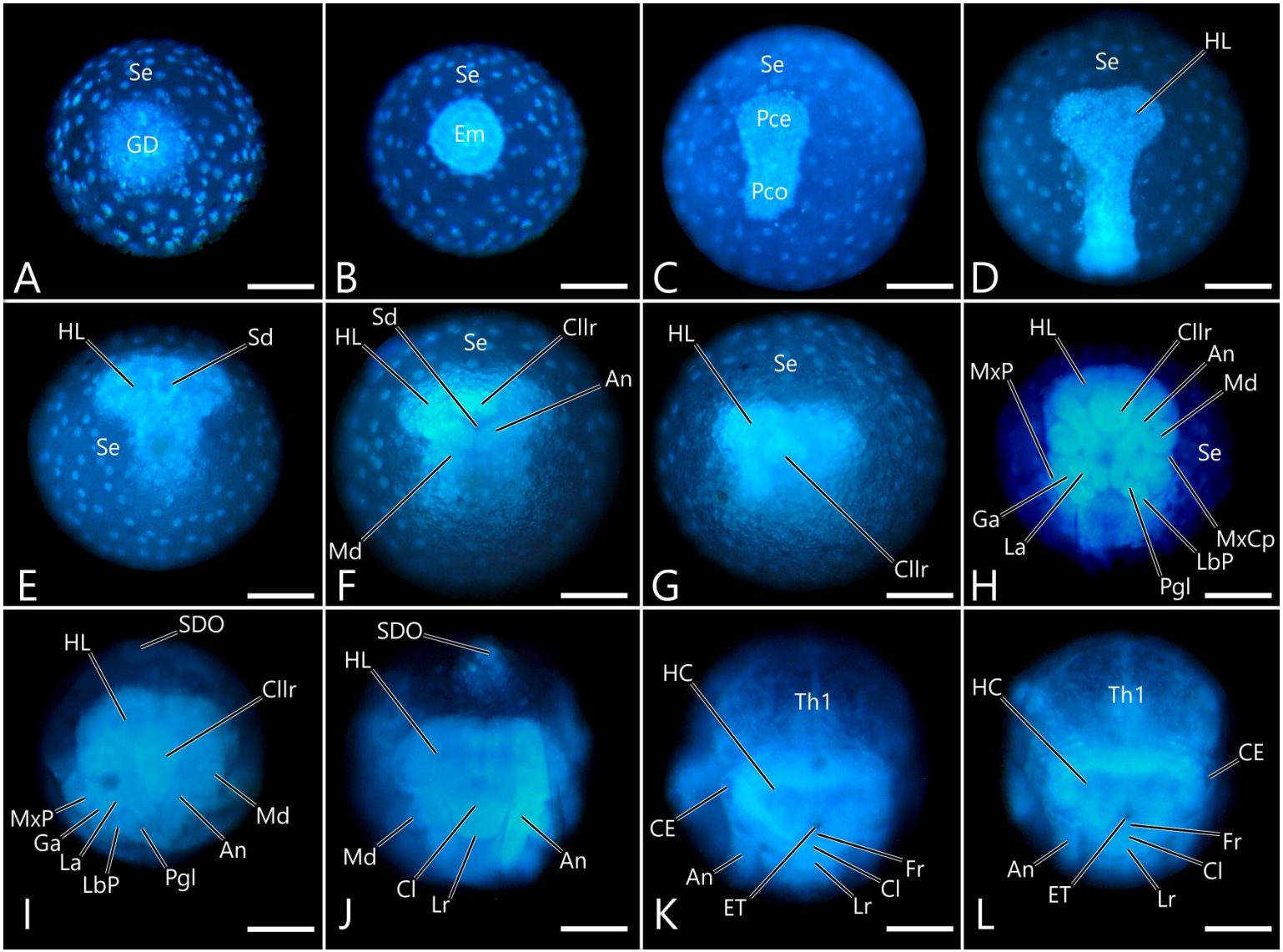
A
Se
GD
B
Se
Em
C
Se
Pce
Pco
D
Se
HL
E
HL
Sd
Se
F
Sd
HL
Se
CIIr
An
Md
G
HL
Se
CIIr
H
HL
CIIr
An
MxP
Md
Se
Ga
La
MxCp
LbP
Pgl
I
SDO
HL
CIIr
MxP
Md
Ga
An
La
LbP
Pgl
J
SDO
HL
Md
An
Cl
Lr
K
HC
Th1
CE
Fr
An
Cl
ET
Lr
L
HC
Th1
CE
Fr
An
Cl
ET
Lr

Fig. 6. Embryonic development of *Scopura montana*, Stage 1, fluorescence microscopy with DAPI staining, A–F. lateral view, anterior of the egg to the top, G–L. posterior view. A, G: Cleavage, late stage. B, H: Blastoderm. C–E, I–K: Differentiation of embryonic and extraembryonic areas, beginning (C, I), middle (D, J), and late (E, K) stages. F, L: Newly formed germ disc.

Bd, blastoderm; BdC, blastoderm cell; CN, cleavage nucleus; EA, embryonic area; EeA, extraembryonic area; GD, germ disc; Se, serosa; SeC, serosal cell.

Scale bars = 100 μm.

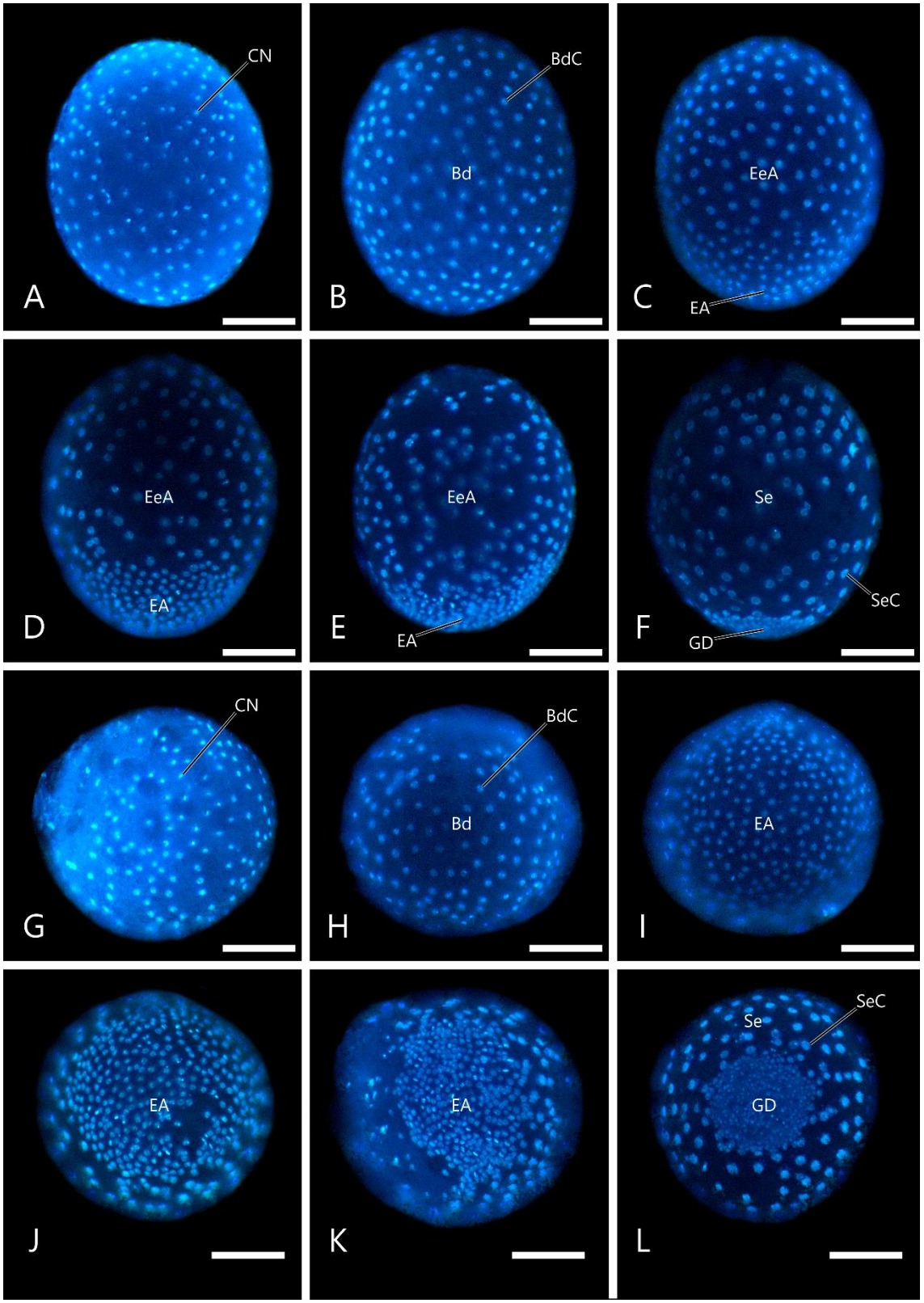
A
CN
B
BdC
Bd
C
EeA
EA
D
EeA
EA
E
EeA
EA
F
Se
SeC
GD
G
CN
H
BdC
Bd
I
EA
J
EA
K
EA
L
SeC
Se
GD

Fig. 7. Embryonic development of *Scopura montana*, Stage 2, fluorescence microscopy with DAPI staining, posterior view, anterior of the embryo to the top. A–D: Formation of amnioserosal fold, successive stages (A) to (D).

AmC, amniotic cell; AmP, amniotic pore; ASF, amnioserosal fold; Em, embryo; Se, serosa; SeC, serosal cell.

Scale bars = 100 μm.

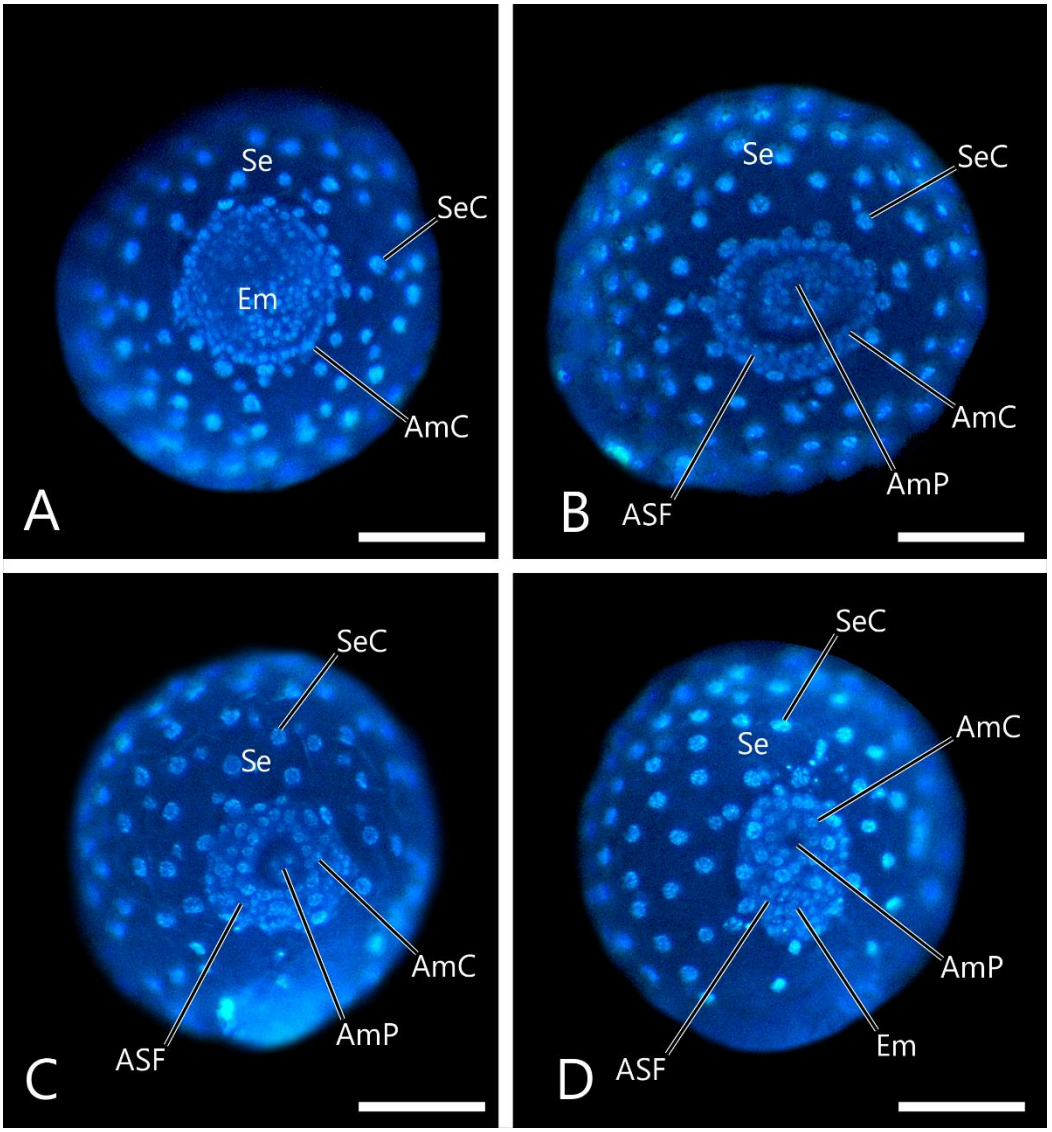
Se
SeC
Em
AmC
A
Se
SeC
AmC
AmP
ASF
B
SeC
Se
AmC
AmP
ASF
C
SeC
Se
AmC
AmP
Em
ASF
D

Fig. 8. Sections of *Scopura montana* embryo undergoing the formation of amnioserosal folds, Stage 2, anterior of the egg to the top (exochorion removed). A: A sagittal section of an embryo in the early phase of amnioserosal fold formation. Anterior of the embryo to the left. B, C: Vertical sections of an embryo with amnioserosal folds just before fusion. (B) and (C) show serial sections at a distance of approximately 3 μm. Arrowheads show the boundaries between the amnion and serosa.

Am, amnion; ASF, amnioserosal fold; Em, embryo; Ench, endochorion; Se, serosa; Y, yolk.

Scale bars = 20 μm.

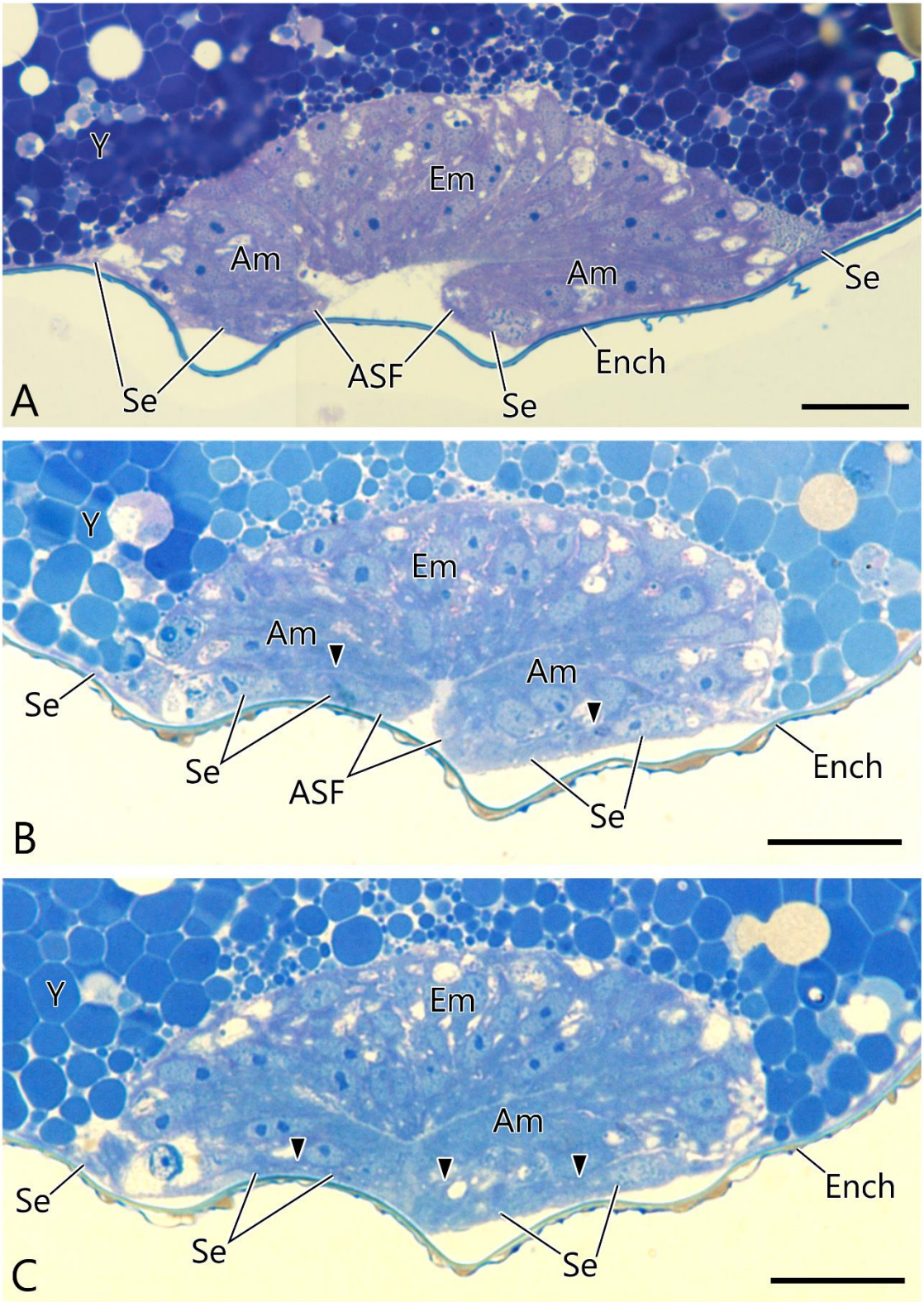
Y
Em
Am
Am
Se
Se
ASF
Se
Ench
A
Y
Em
Am
Am
Se
Se
ASF
Se
Ench
B
Y
Em
Am
Se
Se
Ench
C

Fig. 9. Embryos in the formation of the amnioserosal fold of *Scopura montana*, early (A, B) and middle (C, D) Stage 2, TEM, anterior of the egg to the top. A, B: An embryo forming the amnioserosal fold (A) and its enlargement revealing the detail of the amnioserosal fold (B). C, D: The amnioserosal folds just contacted with each other (C) and its enlargement (D). Arrowheads show the contiguous point of the amnioserosal folds.

Am, amnion; AmCv, amniotic cavity; AmP, amniotic pore; ASF, amnioserosal fold; Em, embryo; Mt, mitochondria; Mv, microvilli; Se, serosa; Y, yolk.

Scale bars = A, 20 μm; B, 5 μm; C, 10 μm; D, 1 μm.

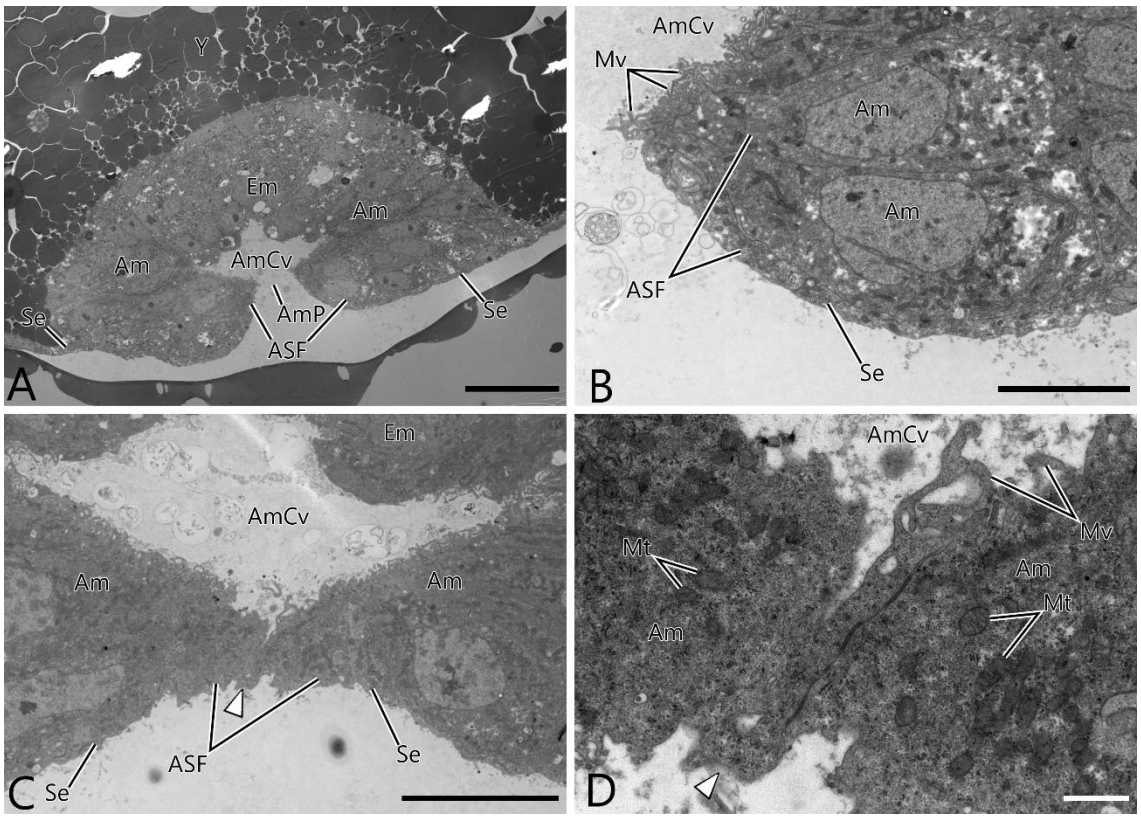
A
Y
Em
Am
Am
AmCv
AmP
ASF
Se
Se
B
AmCv
Mv
Am
Am
ASF
Se
C
Em
AmCv
Am
Am
ASF
Se
Se
D
AmCv
Mv
Mt
Am
Am
Mt

Fig. 10. Embryos of *Scopura montana*, with the thickened serosa beneath the embryo, late Stage 2. (A) and (B), and (C) and (D) are from the same eggs. A, C: Sections of an embryo with the newly formed thickened serosa (A), and that with a little developed one (C), anterior of the egg to the top (exochorion removed). B, D: TEM showing the secretion of serosal cuticle 1, being discontinuously secreted at first (B), but soon becoming a continuous layer (D).

Am, amnion; Em, embryo; Ench, endochorion; Ench1, endochorion 1; Mv, microvilli; Se, serosa; SeCt1, serosal cuticle 1; TSe, thickened serosa; VM, vitelline membrane, Y, yolk.

Scale bars = A, C, 20 μm; B, D, 1μm.

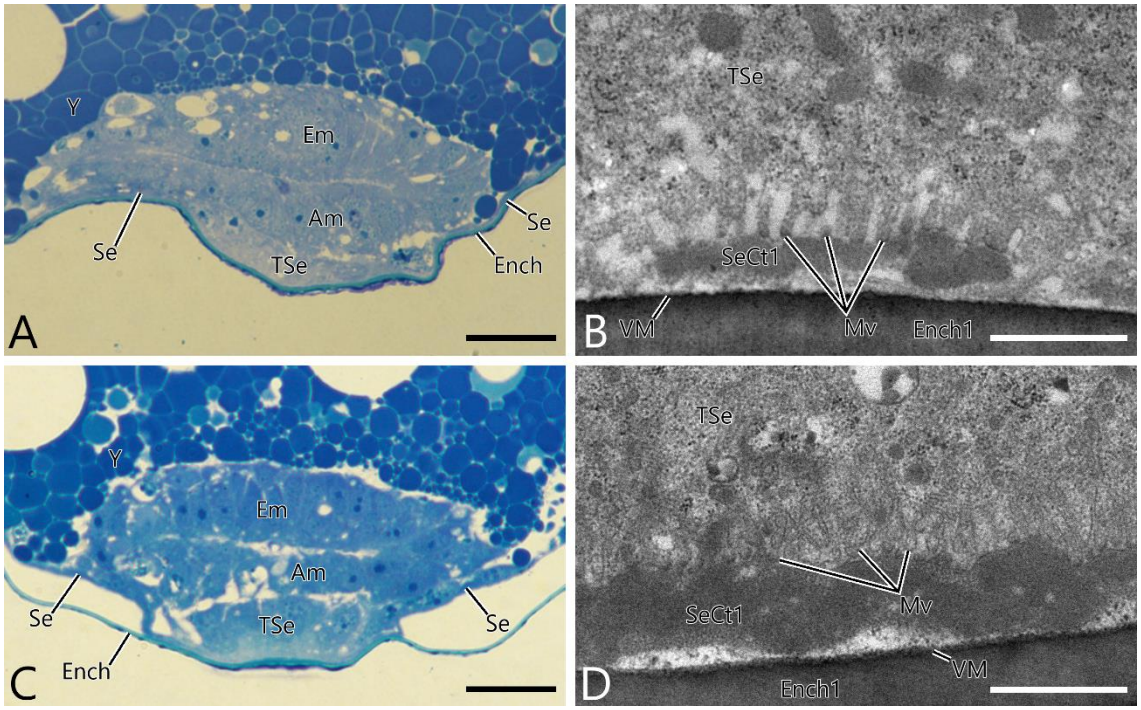
Y
Em
Am
Se
Se
TSe
Ench
A
TSe
SeCt1
VM
Mv
Ench1
B
Y
Em
Am
Se
Se
TSe
Ench
C
TSe
Mv
SeCt1
VM
Ench1
D

Fig. 11. Thickened serosa beneath the embryo of *Scopura montana*, Stage 3, anterior of the embryo to the left (exochorion removed). A: A sagittal section of an embryo. B, C: SEM of an embryo, which was dissected out of a fixed egg, with the thickened serosa left on its ventral side (B) and the enlargement of the thickened serosa (C).

Am, amnion; AmCv, amniotic cavity; Em, embryo; Ench, endochorion; Me, mesoderm; Se, serosa; SeCt, serosal cuticle; TSe, thickened serosa; TSeC, thickened serosal cell; Y, yolk.

Scale bars = A, 20 μm; B, 50 μm; C, 10 μm.

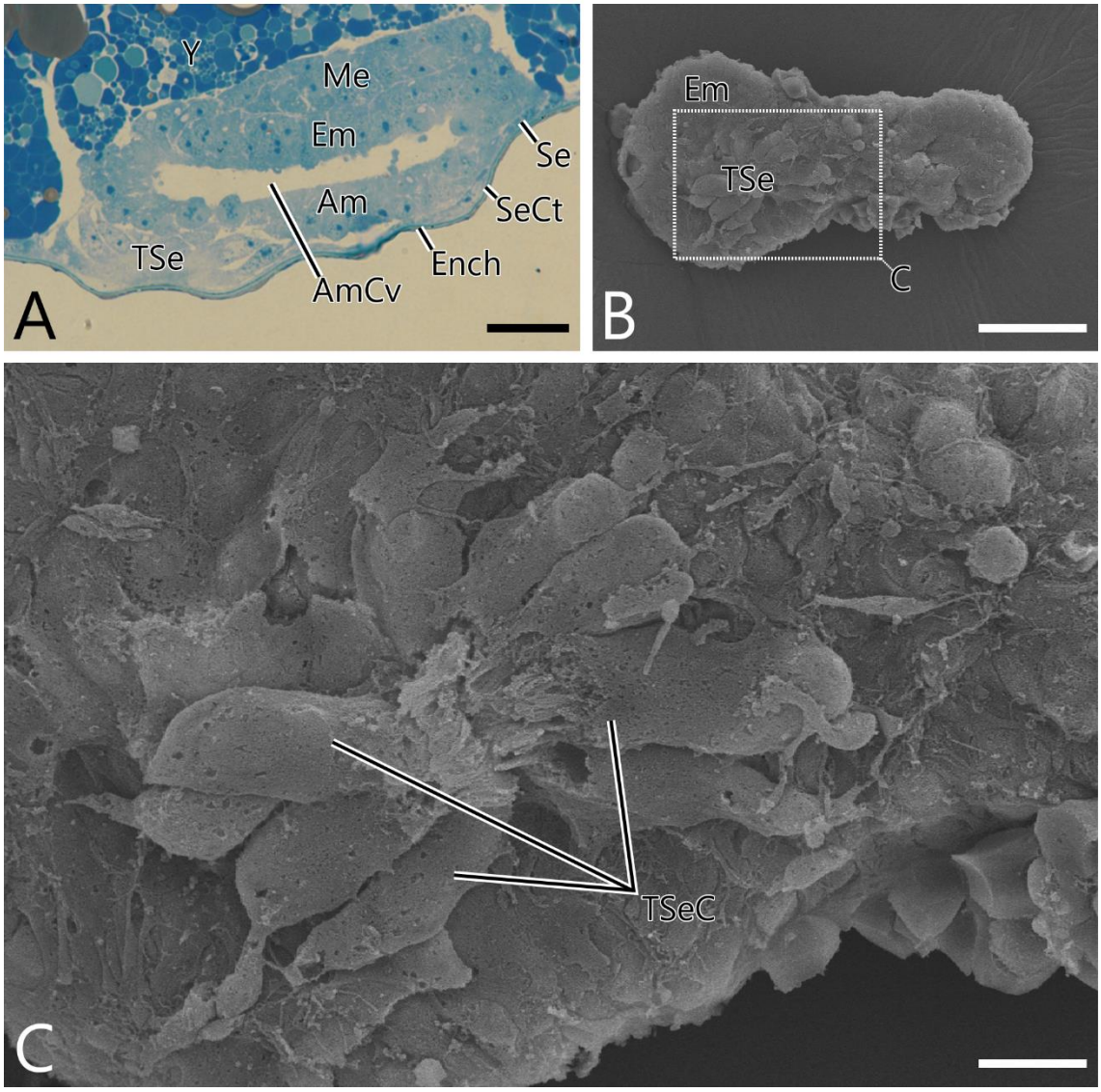
Y
Me
Em
Se
Am
SeCt
TSe
Ench
AmCv
A
Em
TSe
C
B
TSeC
C

Fig. 12. Apical part of the thickened serosa beneath the embryo of *Scopura montana*, Stage 3, TEM, anterior of the egg to the top. A, B: The apical area of the thickened serosa of different embryos. Secretion with a similar electron density (stars in B) to that of the granules found at the apical area of the thickened serosa (arrowheads in A) is observed in the interspace between the microvilli. A new cuticular layer, termed the "serosal cuticle 2," of a similar electron density is deposited beneath the serosal cuticle 1.

De, desmosome; Ench1, endochorion 1; Mv, microvilli; SeCt1, serosal cuticle 1; SeCt2, serosal cuticle 2; TSe, thickened serosa.

Scale bars = A, 500 nm; B, 1 μm.

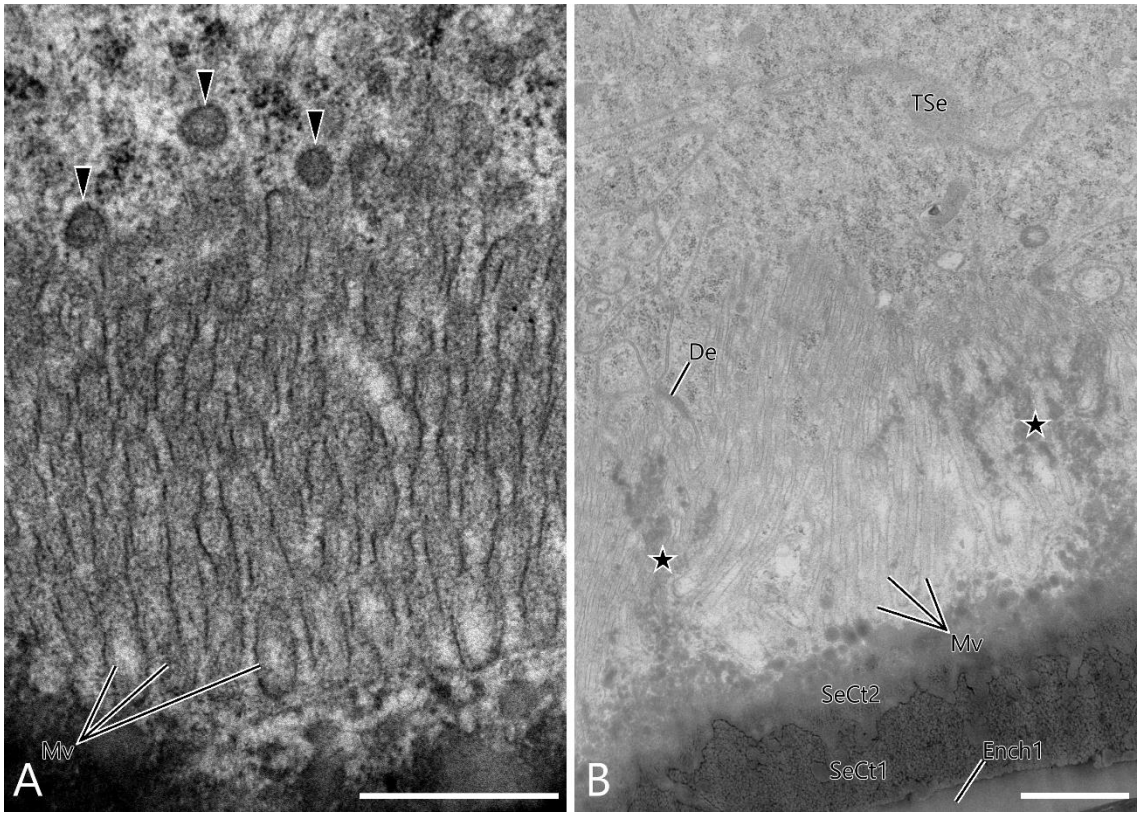
A
Mv
B
TSe
De
Mv
SeCt2
SeCt1
Ench1

Fig. 13. The thickened serosa beneath the embryo of *Scopura montana*, Stage 4, TEM, anterior of the egg to the top. A TEM of the thickened serosa under the secretion of serosal cuticle 3. Asterisks show the vertical striations in the serosal cuticles.

Ench1, endochorion 1; Mv, microvilli; SeCt1, serosal cuticle 1; SeCt2, serosal cuticle 2; SeCt3, serosal cuticle 3; TSe, thickened serosa.

Scale bar = 1 μm.

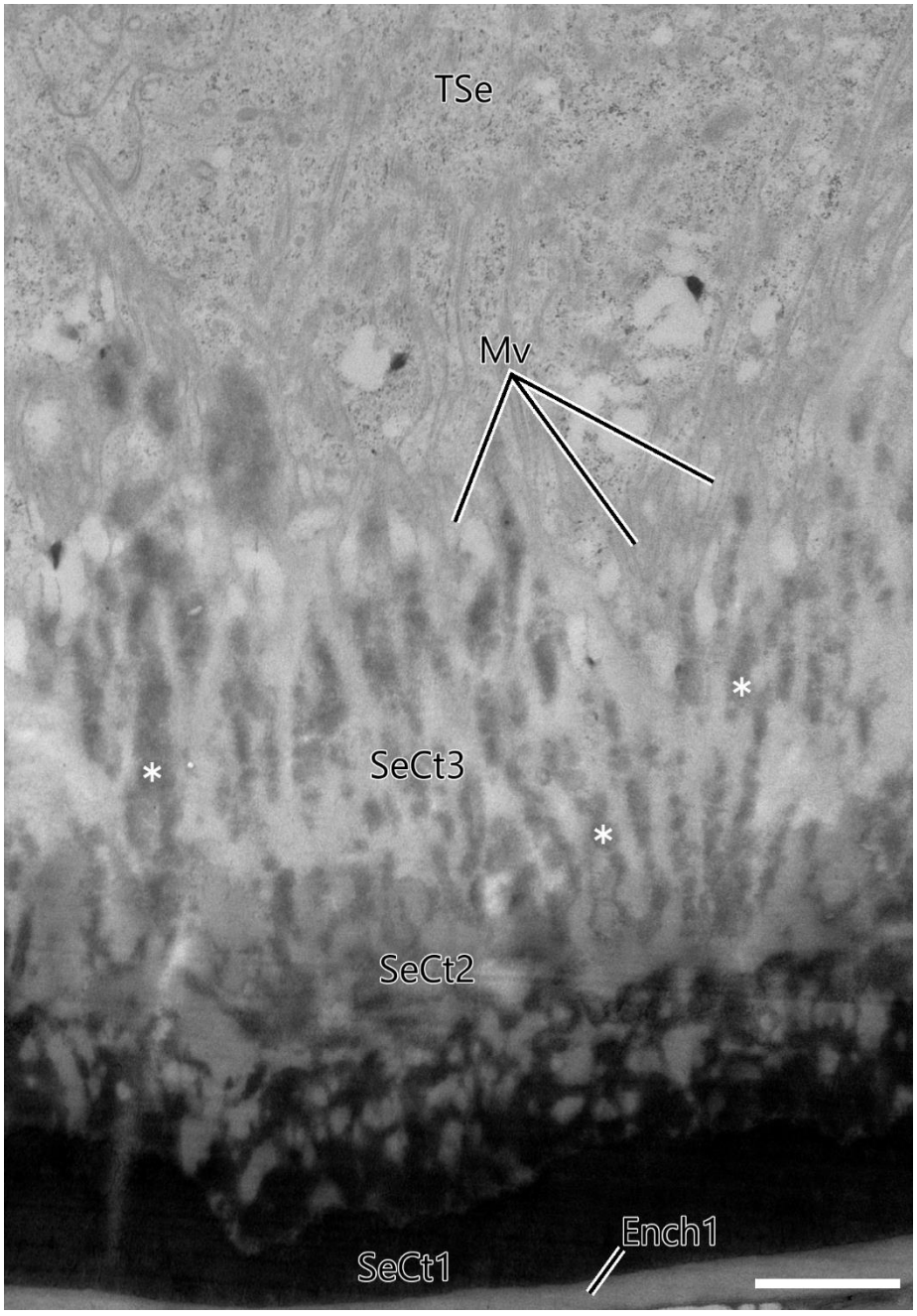
TSe
Mv
SeCt3
SeCt2
SeCt1
Ench1

Fig. 14. An embryo of *Scopura montana*, Stage 5, SEM, ventral view.

An, antenna; HL, head lobe; InS, intercalary segment; Lb, labium; Md, mandible; Mx, maxilla; NG, neural groove; Sd, stomodaeum; Th1-3L, pro-, meso- and metathoracic legs.

Scale bar = 50 μm.

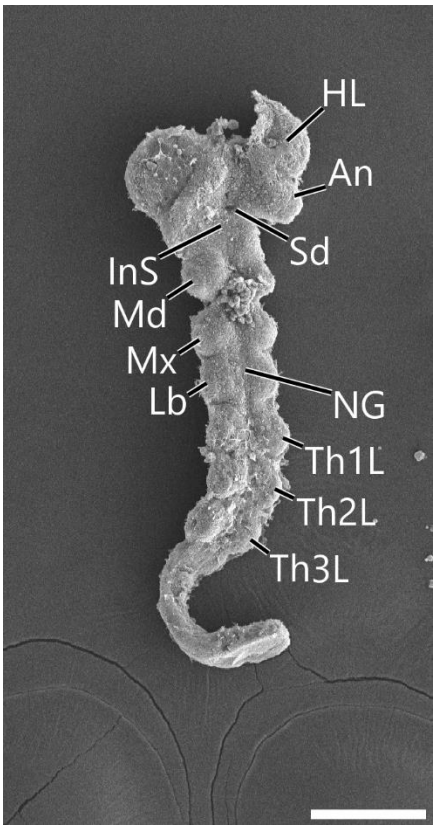
HL
An
Sd
InS
Md
Mx
Lb
NG
Th1L
Th2L
Th3L

Fig. 15. An embryo of *Scopura montana*, Stage 6, SEM. A: Lateral view of embryo. B, C: Ventral views of cephalic (B) and gnathal-thoracic (C) regions of embryo.

An, antenna; Cllr, clypeolabrum; HL, head lobe; InS, intercalary segment; Lb, labium; Md, mandible; Mx, maxilla; NG, neural groove; Pd, proctodaeum; Sd, stomodaeum; Th1-3L, pro-, meso- and metathoracic legs.

Scale bars = 50 μm.

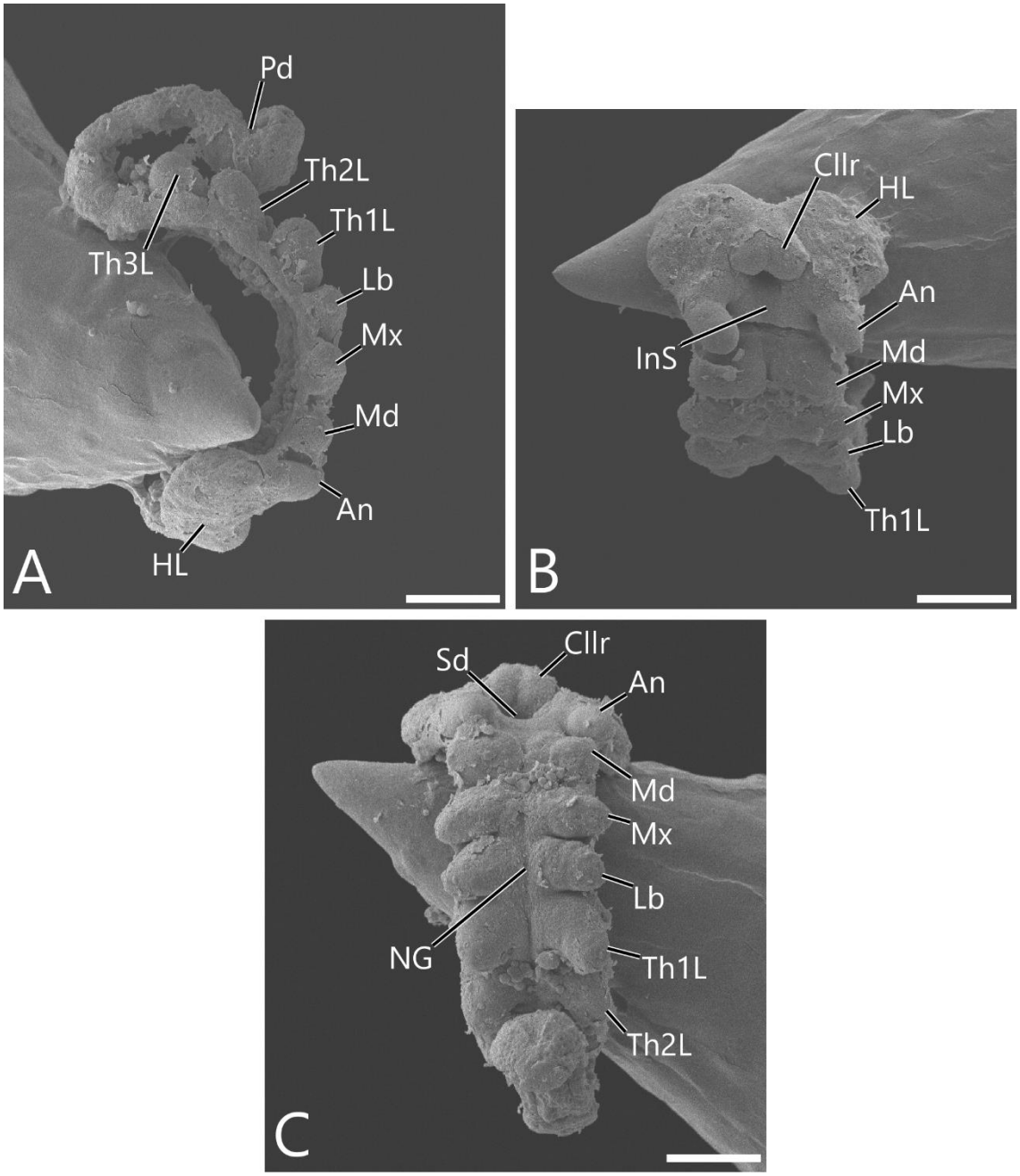
Pd
Th2L
Th1L
Th3L
Lb
Mx
Md
An
HL
A
CIIr
HL
An
InS
Md
Mx
Lb
Th1L
B
Sd
CIIr
An
Md
Mx
Lb
NG
Th1L
Th2L
C

Fig. 16. Completed serosal cuticles of *Scopura montana*, Stage 6, TEM, anterior of the egg to the top (exochorion removed). A–C: The thickened serosa and serosal cuticle beneath the embryo (A), their enlargement (B), and the serosal cuticles secreted in other regions than the thickened serosa (C).

Ench1, endochorion 1; Mv, microvilli; Se, serosa; SeCt1, serosal cuticle 1; SeCt2, serosal cuticle 2; SeCt3, serosal cuticle 3; SeCt4, serosal cuticle 4; SeCt4-I, sublayer I of serosal cuticle 4; SeCt4-II, sublayer II of serosal cuticle 4; TSe, thickened serosa; TSeCt, thickened serosal cuticle; Y, yolk.

Scale bars = A, 20 μm; B, 2 μm; C, 1 μm.

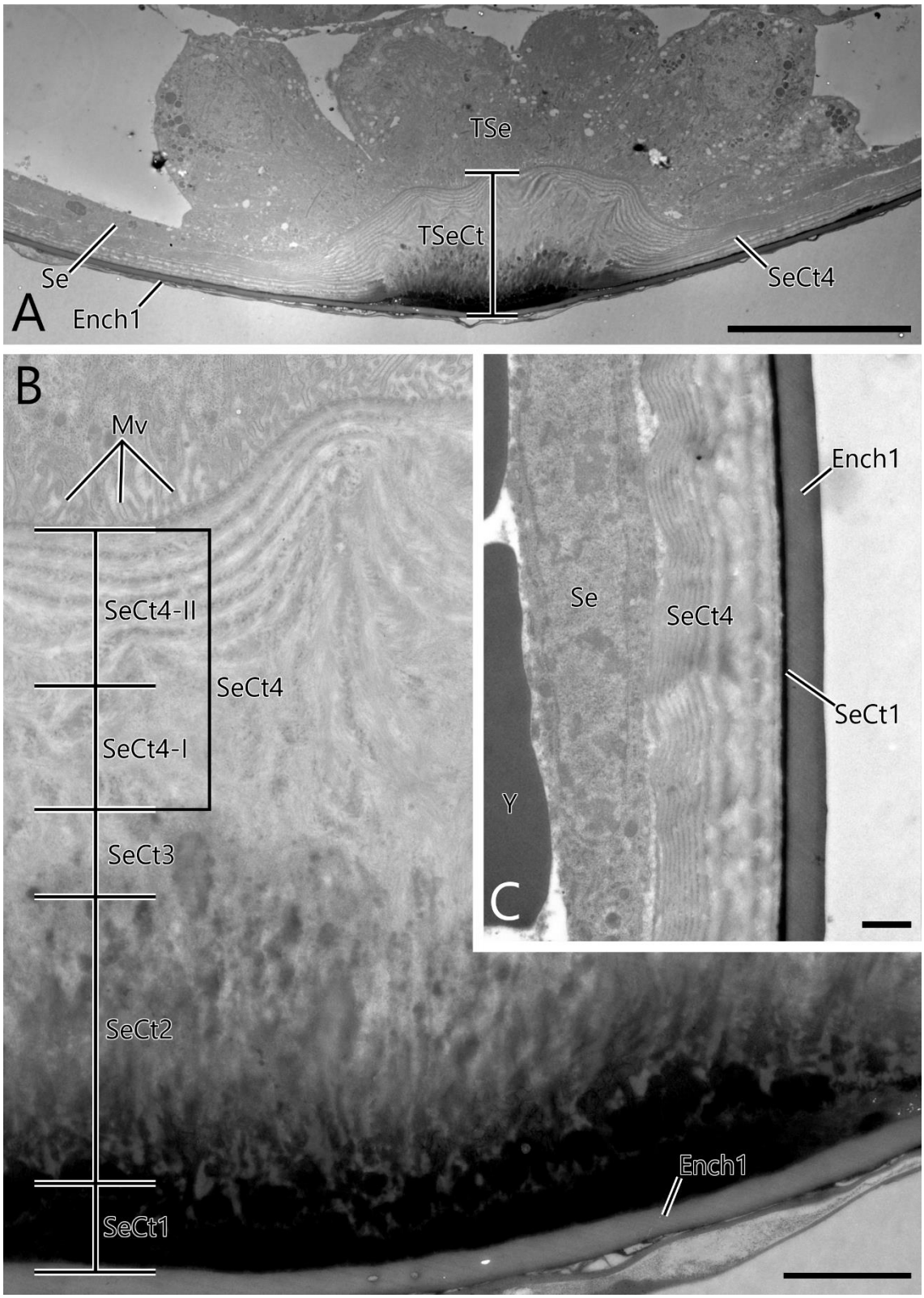
TSe
TSeCt
Se
Ench1
SeCt4
A
B
Mv
SeCt4-II
SeCt4
SeCt4-I
SeCt3
SeCt2
SeCt1
Ench1
Se
SeCt4
SeCt1
Y
C

Fig. 17. An embryo of *Scopura montana*, Stage 7, SEM. A, B: Lateral view of embryo (A) and the enlargement (B). C: Frontal view of embryo. D: Ventral view of embryo.

An, antenna; Cllr, clypeolabrum; Cp, coxopodite; Ga, galea; HL, head lobe; La, lacinia; Lb, labium; LbCp, labial coxopodite; LbP, labial palp; Md, mandible; Mx, maxilla; MxCp, maxillary coxopodite; MxP, maxillary palp; Pd, proctodaeum; Th1-3L, pro-, meso- and metathoracic legs; Tp, telopodite.

Scale bars = 50 μm.

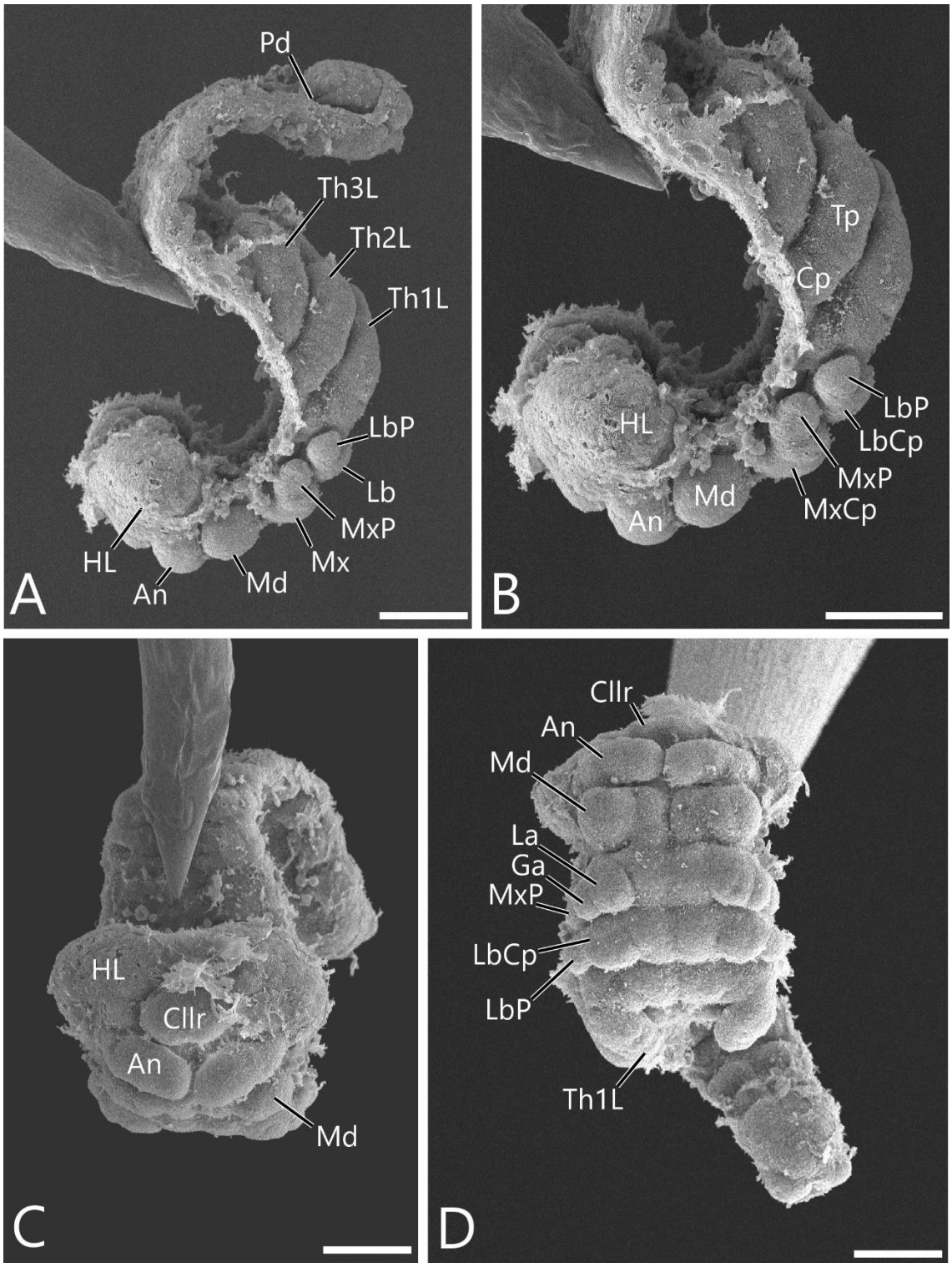
Pd
Th3L
Th2L
Th1L
LbP
Lb
MxP
Mx
HL
An
Md
A
Tp
Cp
LbP
LbCp
MxP
MxCp
HL
Md
An
B
HL
Cllr
An
Md
C
Cllr
An
Md
La
Ga
MxP
LbCp
LbP
Th1L
D

Fig. 18. Thickened serosa beneath the embryo of *Scopura montana*, at the beginning of degeneration, early Stage 7, TEM. A: The apical part of the thickened serosa. Asterisks show the interspace between the microvilli. B: TEM showing the contact of the serosa with the thickened serosa (arrow).

Mt, mitochondria; Mv, microvilli; Se, serosa; SeCt, serosal cuticle; TSe, thickened serosa.

Scale bars = 1 μm.

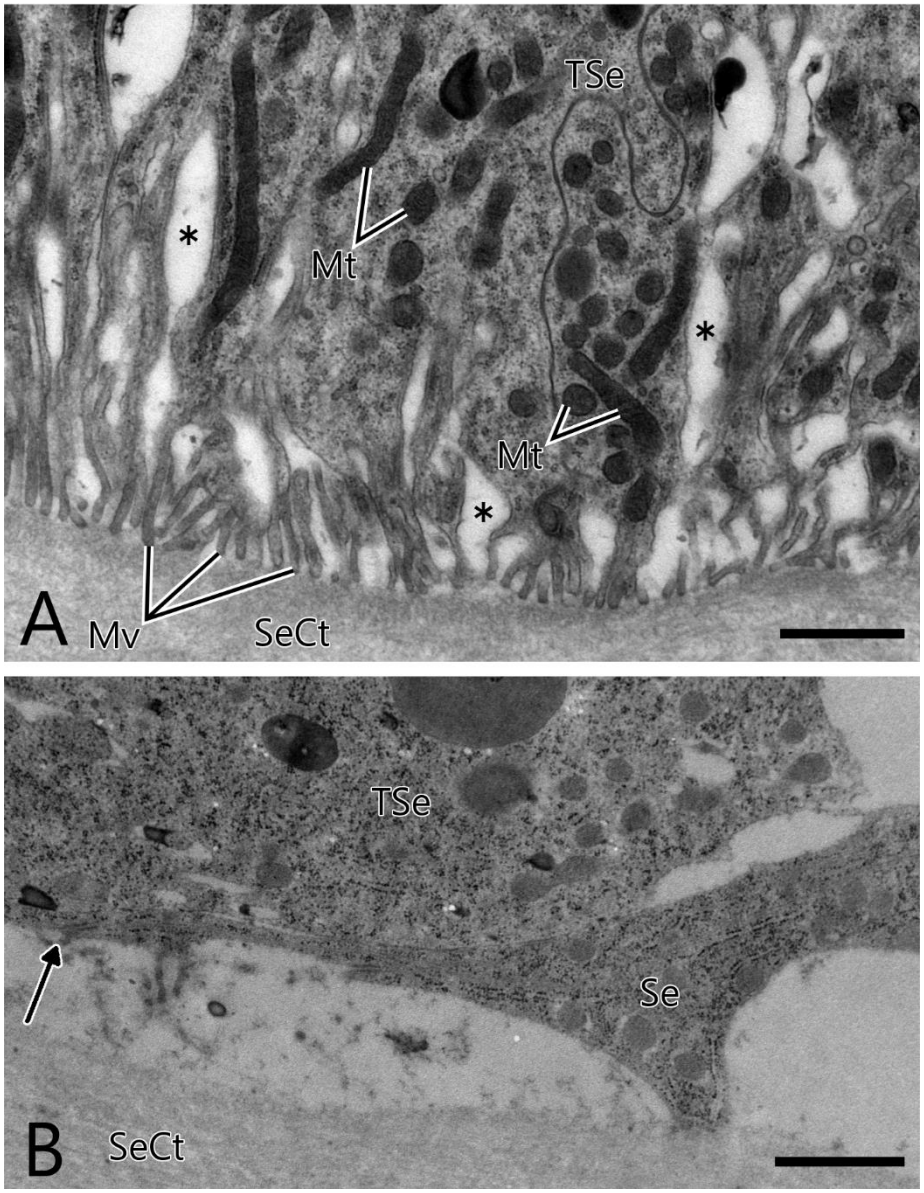
TSe
Mt
Mt
A
Mv
SeCt
TSe
Se
B
SeCt

Fig. 19. Sagittal sections of thickened serosa beneath the embryo of *Scopura montana*, heading for disintegration, early (A, B) and late (C, D) Stage 7, and early Stage 8 (E, F), anterior of the embryo to the left (exochorion removed). (B, D, F) are the enlargements of (A, C, E), respectively. (A) and (B) are the same egg of Fig. 15B. Arrows show the contact point of the serosa and the thickened serosa.

Am, amnion; AmCv, amniotic cavity; An, antenna; ASF, amnioserosal fold; Cllr, clypeolabrum; Em, embryo; Ench, endochorion; Sd, stomodaeum; Se, serosa; SeCt, serosal cuticle; SeCt3, serosal cuticle 3; TSe, thickened serosa; TSeCt, thickened serosal cuticle; Y, yolk.

Scale bars = A, C, E, 50 μm; B, D, F, 20 μm.

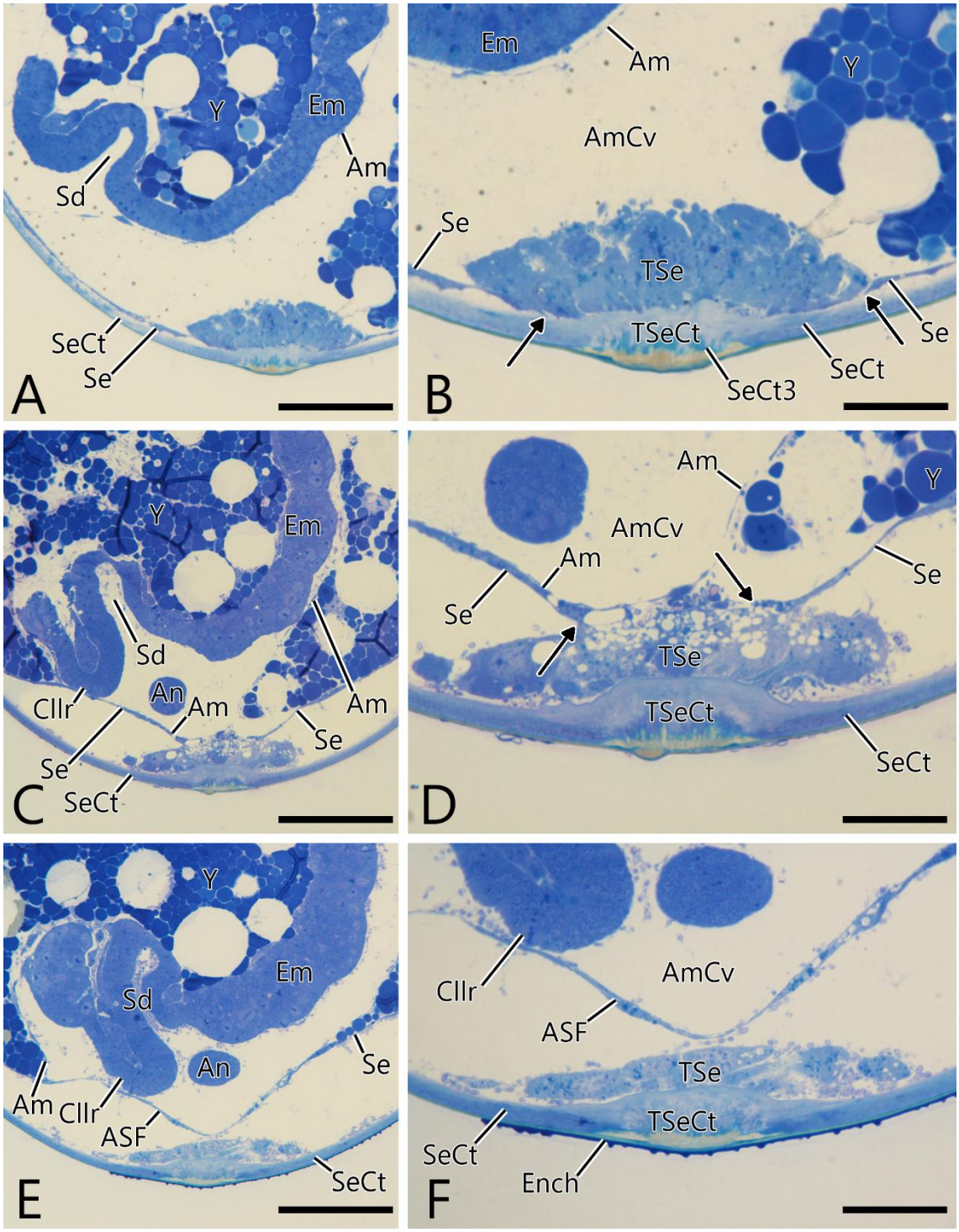
A
Y
Em
Am
Sd
SeCt
Se
B
Em
Am
Y
AmCv
Se
TSe
TSeCt
Se
SeCt
SeCt3
C
Y
Em
Sd
An
Am
Cllr
Am
Se
Se
SeCt
D
Am
Y
AmCv
Am
Se
Se
TSe
TSeCt
SeCt
E
Y
Em
Sd
An
Se
Am
Cllr
ASF
SeCt
F
Cllr
AmCv
ASF
TSe
TSeCt
SeCt
Ench

Fig. 20. An embryo of *Scopura montana*, Stage 8, SEM. A, B: Lateral view of embryo (A) and the enlargement (B). C: Frontal view of embryo. D: Ventral view of embryo.

Ab1, 5, 10, first, fifth and 10th abdominal segments; An, antenna; Ce, cercus; Cllr, clypeolabrum; Cp, coxopodite; Cx, coxa; Fe, femur; Ga, galea, Gl, glossa; HL, head lobe; La, lacinia; LbP, labial palp; Md, mandible; MxCp, maxillary coxopodite; MxP, maxillary palp; Pgl, paraglossa; Pp, pleuropodium; Pta, pretarsus; Scx, subcoxa; Ta, tarsus; Th1-3L, pro-, meso- and metathoracic legs; Th1-3T, pro-, meso- and metathoracic terga; Ti, tibia; Tp, telopodite; Tr, trochanter.

Scale bars = 50 μm.

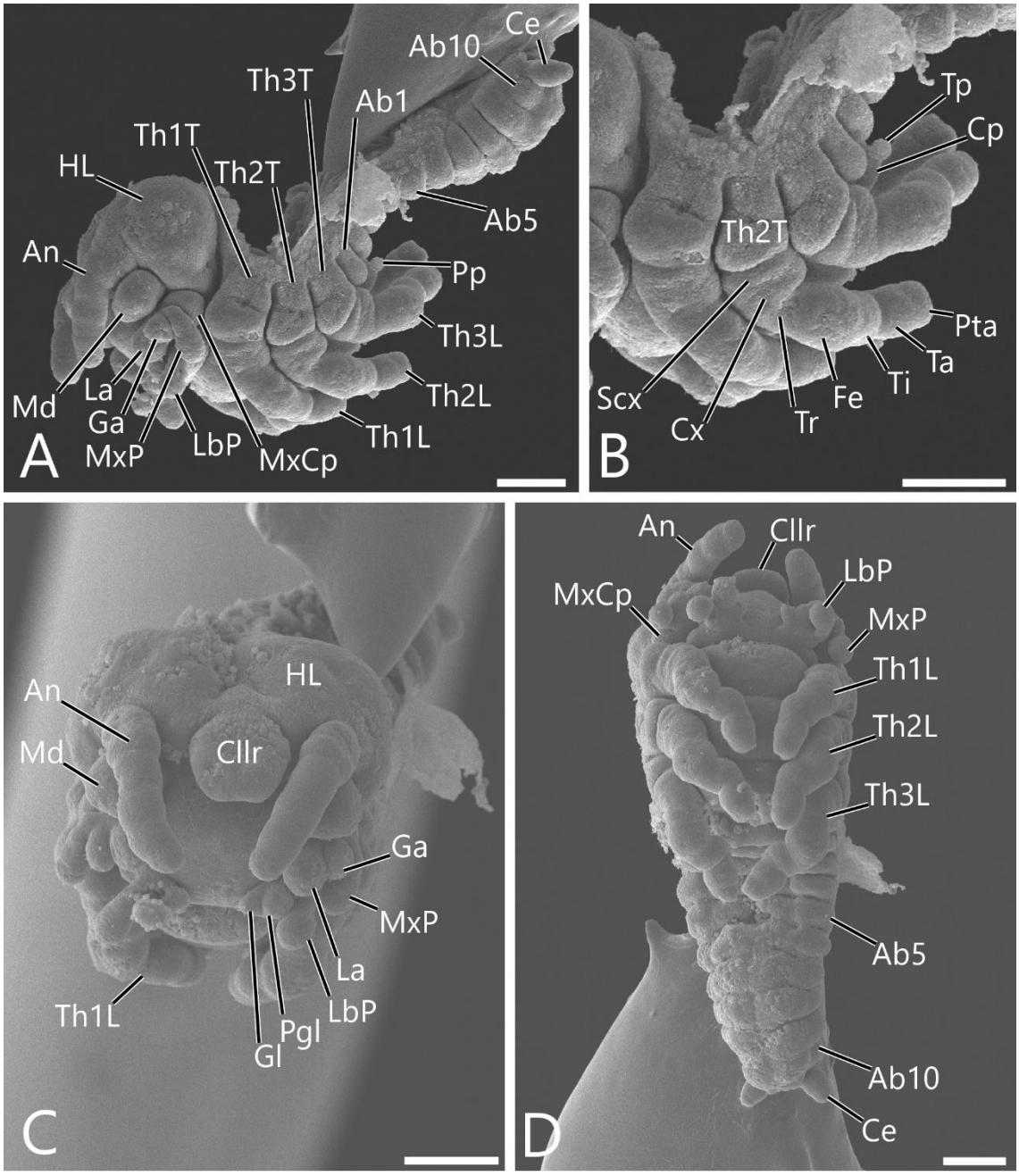
Ce
Ab10
Th3T
Ab1
Th1T
HL
Th2T
Ab5
An
Pp
Th3L
Md
La
Th2L
Ga
Th1L
MxP
LbP
MxCp
A
Tp
Cp
Th2T
Pta
Ta
Ti
Scx
Fe
Cx
Tr
B
An
Cllr
LbP
MxCp
MxP
Th1L
Th2L
Th3L
Ab5
Ab10
Ce
D
HL
An
Md
Cllr
Ga
MxP
La
LbP
Th1L
PgI
Gl
C

Fig. 21. A sagittal section of pleuropodium of *Scopura montana*, Stage 8.

Cp, coxopodite; Tp, telopodite.

Scale bar = 20 μm.

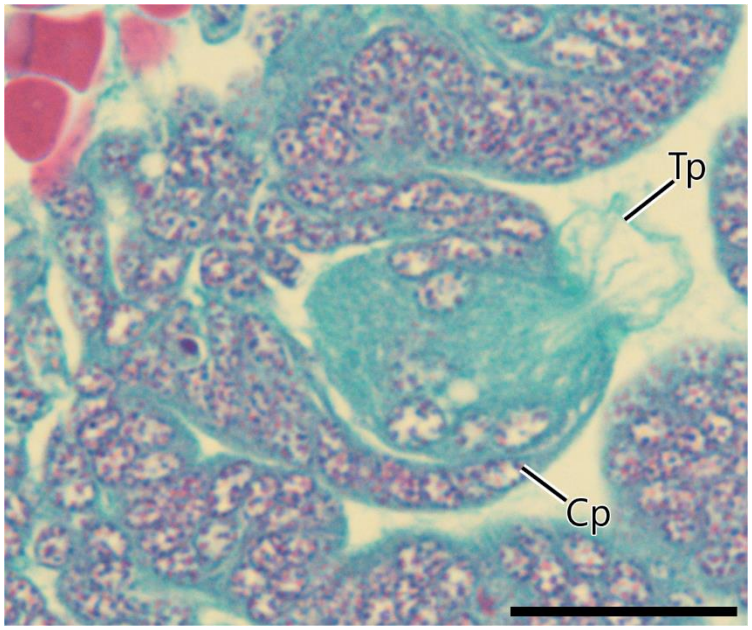
Tp
Cp

Fig. 22. Sagittal sections of embryos of *Scopura montana*, late Stage 8 (A) and Stage 9 (B), anterior of the embryo to the left (exochorion removed). Arrows show serosal cells liberated from the disintegrated thickened serosa.

Am, amnion; AmCv, amniotic cavity; An, antenna; ASF, amnioserosal fold; Br, brain; Cllr, clypeolabrum; Sd, stomodaeum; Se, serosa; SeCt, serosal cuticle; Th1, prothoracic segment; Th1L, prothoracic leg; TSeCt, thickened serosal cuticle; Y, yolk.

Scale bars = 20 μm.

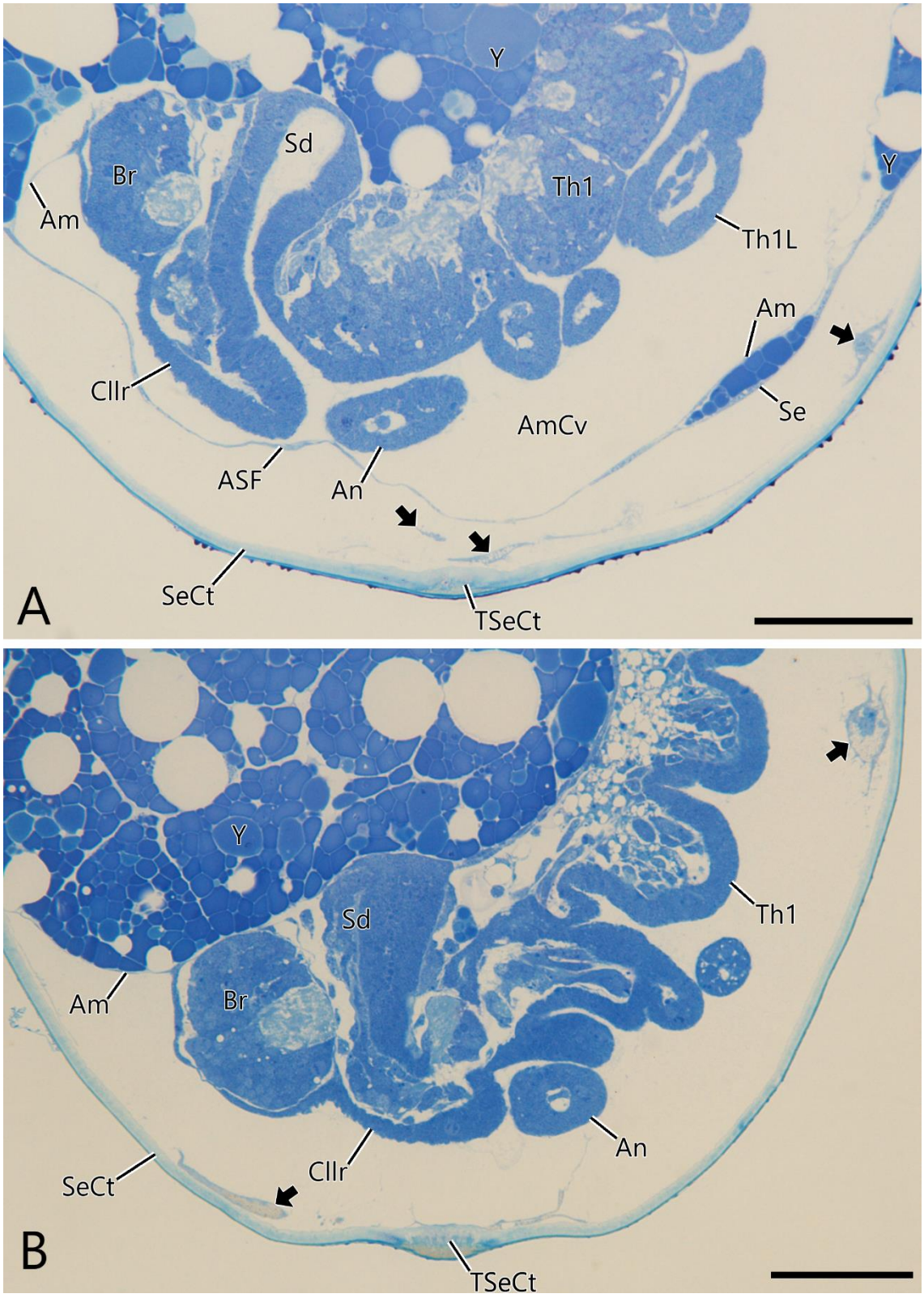
Y
Sd
Br
Th1
Y
Am
Th1L
Am
Cllr
Se
AmCv
ASF
An
SeCt
TSeCt
A
Y
Th1
Sd
Am
Br
An
SeCt
Cllr
TSeCt
B

Fig. 23. An embryo of *Scopura montana*, Stage 9, SEM, nano-suit method. A, B: Lateral view of embryo (A) and the enlargement (B). C, D: Ventral view of embryo (C) and the enlargement (D).

Ab10, 10th abdominal segment; An, antenna; Ce, cercus; Cllr, clypeolabrum; Cx, coxa; Fe, femur; Ga, galea, HL, head lobe; La, lacinia; LbP, labial palp; Md, mandible; MxCp, maxillary coxopodite; MxP, maxillary palp; Pgl, paraglossa; Pta, pretarsus; Sba, subanal lobe; Scx, subcoxa; Spa, supraanal lobe; Ta, tarsus; Th1-3L, pro-, meso- and metathoracic legs; Th1-3T, pro-, meso- and metathoracic terga; Ti, tibia; Tr, trochanter.

Scale bars = A, C, 50 μm; B, D, 20 μm.

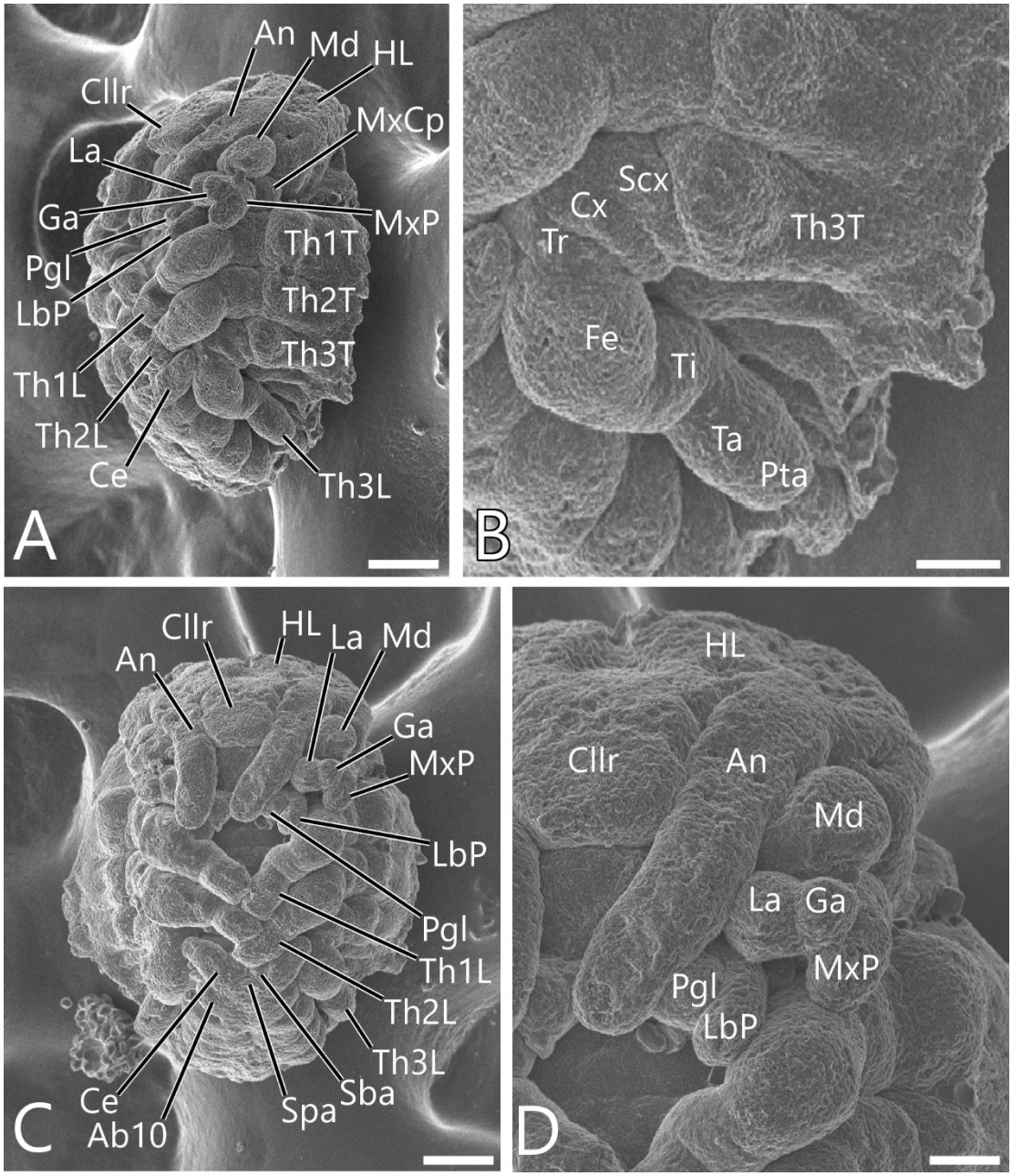
An
Md
HL
Cllr
MxCp
La
Ga
MxP
Th1T
Pgl
Th2T
LbP
Th3T
Th1L
Th2L
Ce
Th3L
A
Scx
Cx
Tr
Th3T
Fe
Ti
Ta
Pta
B
Cllr
HL
La
Md
An
Ga
MxP
LbP
Pgl
Th1L
Th2L
Th3L
Sba
Spa
Ce
Ab10
C
HL
Cllr
An
Md
La
Ga
MxP
Pgl
LbP
D

Fig. 24. An embryo of *Scopura montana*, Stage 10, SEM, nano-suit method. A, B: Lateral view of embryo (A) and the enlargement (B). C, D: Ventral view of embryo (C) and the enlargement (D).

Ab10, 10th abdominal segment; An, antenna; Ce, cercus; Cl, clypeus; Cx, coxa; Fe, femur; Fr, frons; HL, head lobe; Md, mandible; MxCp, maxillary coxopodite; MxP, maxillary palp; Lr, labrum; Pta, pretarsus; Scx, subcoxa; Ta, tarsus; Th1-3L, pro-, meso- and metathoracic legs; Th1-3T, pro-, meso- and metathoracic terga; Ti, tibia; Tr, trochanter.

Scale bars = A, C, D 50 μm; B, 20 μm.

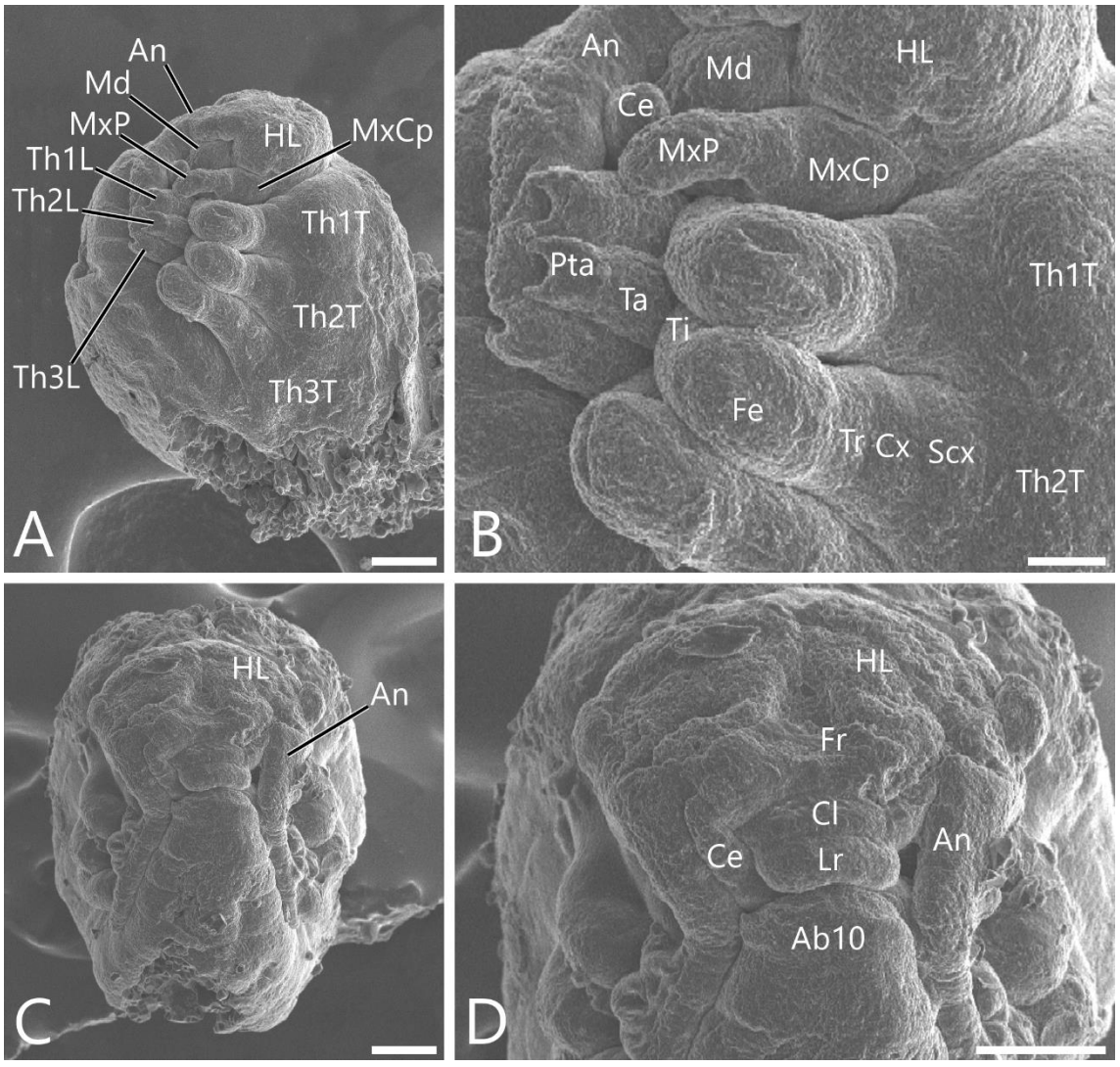
An
Md
MxP
HL
MxCp
Th1L
Th2L
Th1T
Th2T
Th3L
Th3T
A
An
Md
HL
Ce
MxP
MxCp
Pta
Th1T
Ta
Ti
Fe
Tr
Cx
Scx
Th2T
B
HL
An
C
HL
Fr
Cl
An
Ce
Lr
Ab10
D

Fig. 25. An embryo of *Scopura montana*, Stage 11, at which larval cuticle has been secreted, low-vacuum SEM. A, B: Lateral view of embryo (A) and the enlargement (B). C, D: Ventral view of embryo (C) and the enlargement (D).

Ab1, 5, 10, first, fifth and 10th abdominal segments; An, antenna; Ce, cercus; Cl, clypeus; Cx, coxa; ET, egg tooth; Fe, femur; Fr, frons; HC, head capsule; MxP, maxillary palp; Lr, labrum; Pta, pretarsus; Scx, subcoxa; Ta, tarsus; Th1-3L, pro-, meso- and metathoracic legs; Th1-3T, pro-, meso- and metathoracic terga; Ti, tibia; Tr, trochanter.

Scale bars = A–C, 50 μm; D, 20 μm.

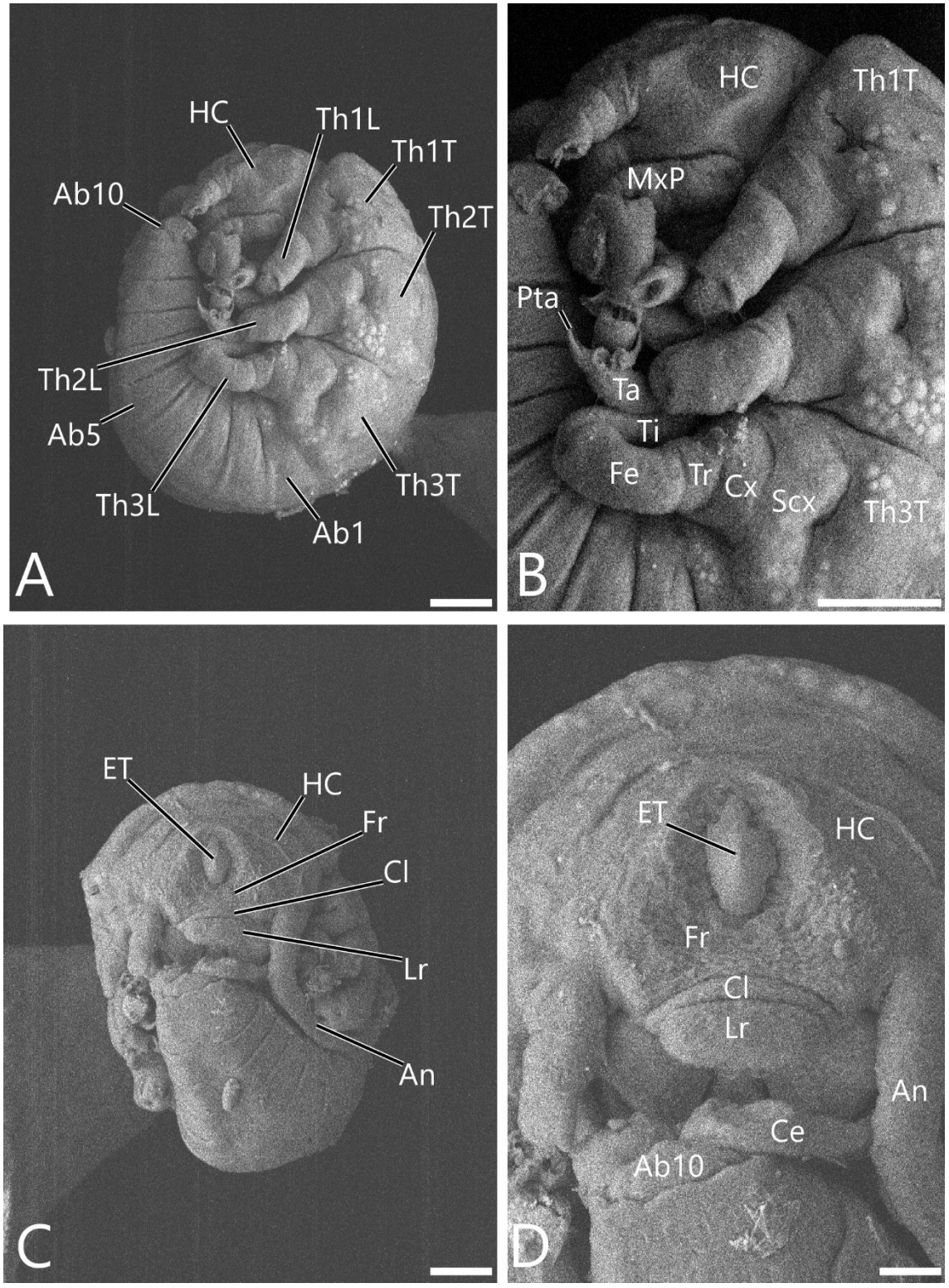
HC
Th1L
Th1T
Ab10
Th2T
Th2L
Ab5
Th3L
Th3T
Ab1
A
HC
Th1T
MxP
Pta
Ta
Ti
Fe
Tr
Cx
Scx
Th3T
B
ET
HC
Fr
Cl
Lr
An
C
ET
HC
Fr
Cl
Lr
An
Ce
Ab10
D

Fig. 26. A sagittal section of head of a *Scopura montana* embryo, Stage 11.

Br, brain; EmCt, embryonic cuticle; ET, egg tooth; FrG, frontal ganglion.

Scale bar = 20 μm.

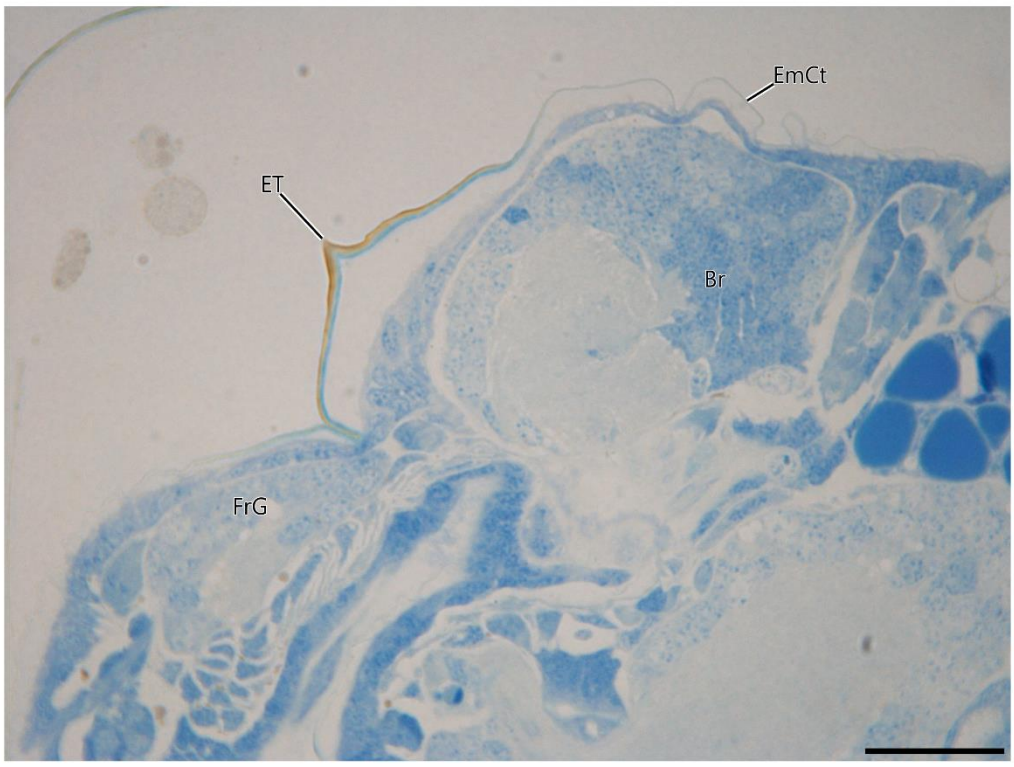
EmCt
ET
Br
FrG

Fig. 27. An embryo of *Scopura montana*, Stage 12, at which larval cuticle has been secreted, low-vacuum SEM. A, B: Lateral view of embryo (A) and the enlargement (B). C: Ventral view of embryo.

An, antenna; Cl, clypeus; Cx, coxa; ET, egg tooth; Epm, epimeron; Eps, episternum; Fe, femur; Fr, frons; HC, head capsule; Lr, labrum; PlS, pleural suture; Pta, pretarsus; Th1-3L, pro-, meso- and metathoracic legs; Th1-3T, pro-, meso- and metathoracic terga; Ti, tibia; Tr, trochanter.

Scale bars = 50 μm.

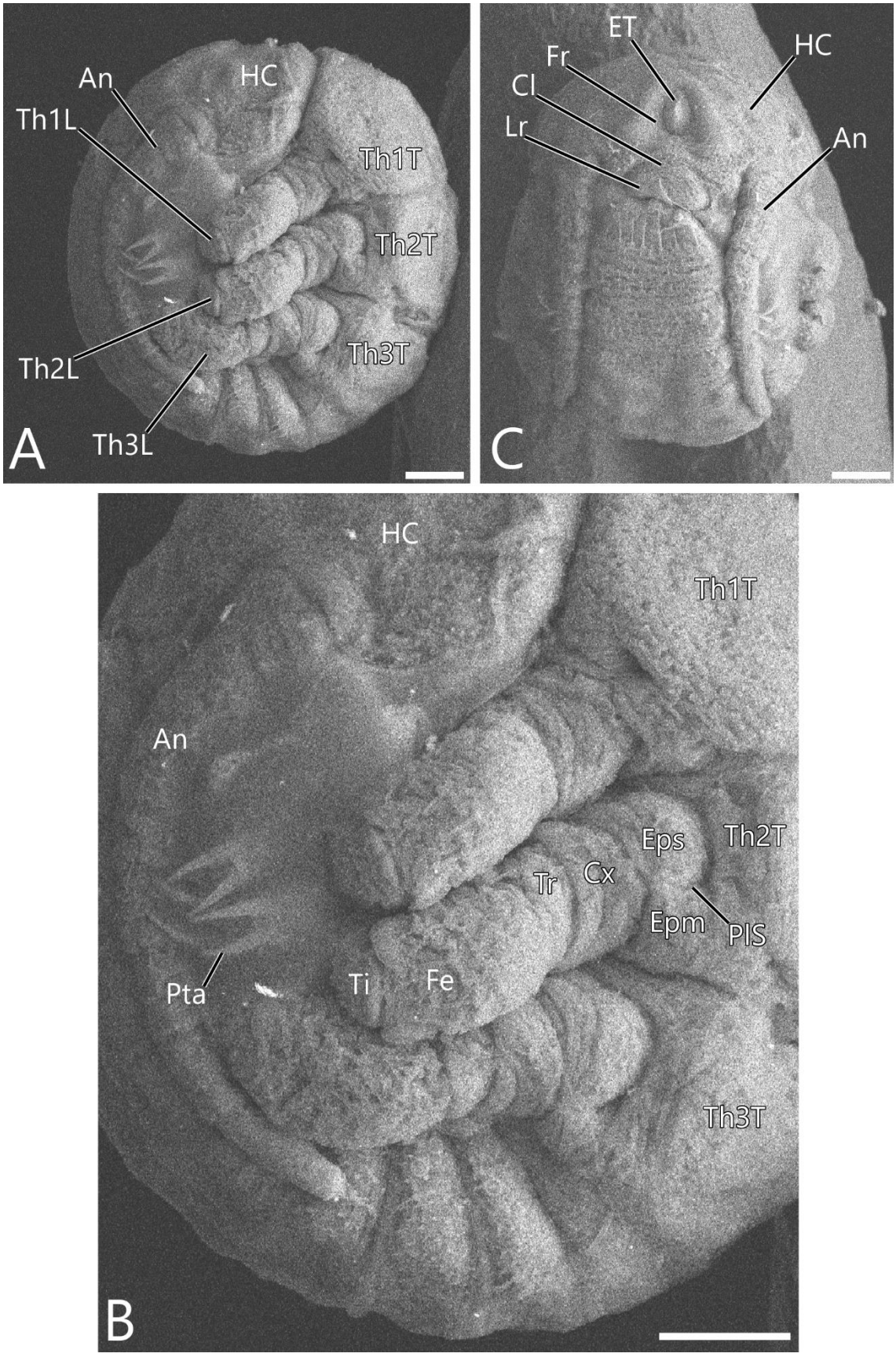
An
HC
Th1L
Th1T
Th2T
Th2L
Th3T
Th3L
A
ET
Fr
Cl
Lr
HC
An
C
HC
Th1T
An
Eps
Th2T
Tr
Cx
Epm
PIS
Pta
Ti
Fe
Th3T
B

Fig. 28. A first instar larva of *Scopura montana*, SEM, nano-suit method. A: Dorsal view of first instar larva. B, C: Dorsal (B) and ventral (C) views of the head. D, E: Ventral view of thoracic appendage (D) and abdominal region (E).

Ab, 9, 10, ninth and 10th abdominal segments; An, antenna; Ca, cardo; Ce, cercus; Cl, clypeus; Cx, coxa; Fe, femur; Fr, frons; Ga, galea, Gl, glossa; La, lacinia; LbP, labial palp; Lr, labrum; MxP, maxillary palp; Pgl, paraglossa; Pm, postmentum; Prm, prementum; Pta, pretarsus; Sba, subanal lobe; Spa, supraanal lobe; St, stipes; Ta, tarsus; Th1T, prothoracic targum; Ti, tibia; Tr, trochanter; Vx, vertex.

Scale bars = A–C, E, 100 μm; D, 50 μm.

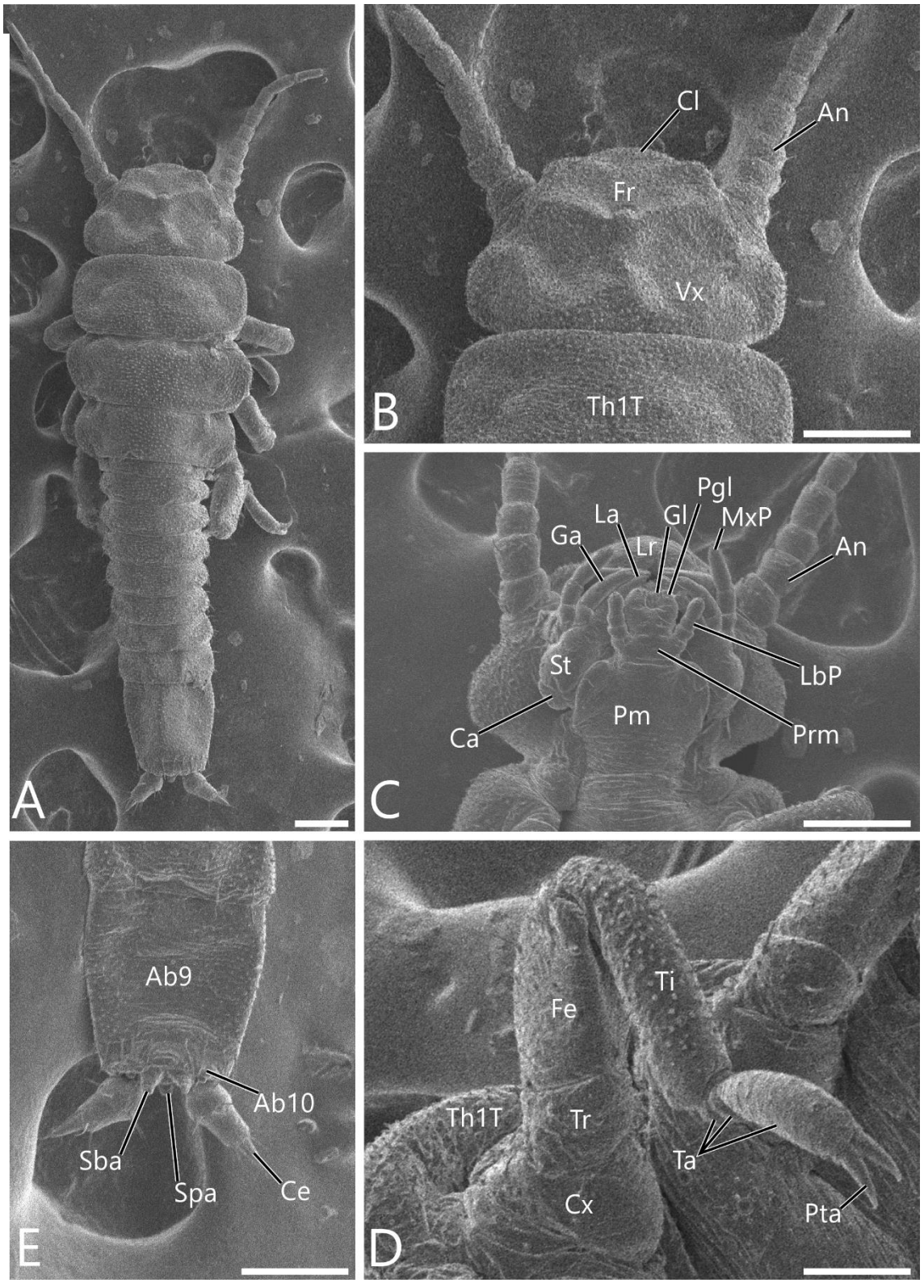
A
B
Cl
An
Fr
Vx
Th1T
C
Pgl
La
Gl
MxP
Ga
Lr
An
St
LbP
Pm
Ca
Prm
E
Ab9
Ab10
Sba
Spa
Ce
D
Ti
Fe
Th1T
Tr
Ta
Cx
Pta

Fig. 29. Details of the sternal and pleural sclerites of the first instar larva of *Scopura montana*, SEM, nano-suit method. A, B: Ventral (A) and ventrolateral (B) views of thoracic region. Arrowheads show the sternal apophyses.

Ab1, first abdominal segment, Bs1-3, pro-, meso- and metathoracic basisterna; Cx1, 2, pro- and mesocoxae; Epm1, 2, pro- and mesothoracic epimera; Eps1, 2, pro- and mesothoracic episterna; PlS1, 2, pro- and mesothoracic pleural sutures; Prs1-3, pro-, meso- and metathoracic presterna; Sps2, mesothoracic spinasternum; Th1, 2T, pro- and mesothoracic terga; Tn1, 2, pro- and mesotrochanters.

Scale bars = A–C, E, 100 μm; D, 50 μm.

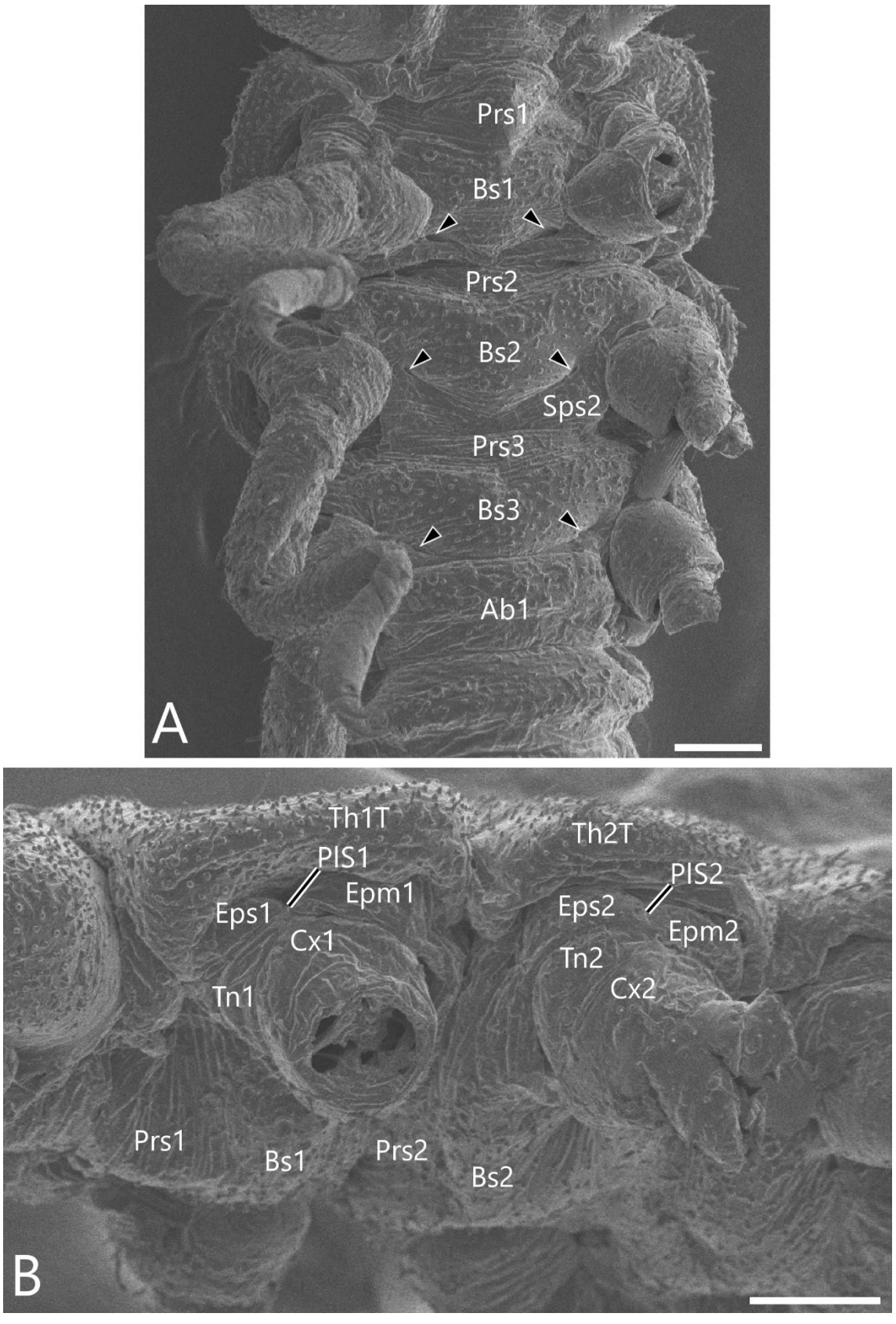
Prs1
Bs1
Prs2
Bs2
Sps2
Prs3
Bs3
Ab1
A
Th1T
PIS1
Eps1
Epm1
Cx1
Tn1
Th2T
PIS2
Eps2
Epm2
Tn2
Cx2
Prs1
Bs1
Prs2
Bs2
B

Fig. 30. Eggs of *Obipteryx* sp. SEM, lateral view, anterior to the top. A: Egg (lines on egg surface are artifacts). B: Enlargement of a micropylar area. Arrowheads show micropyles.

Scale bars = A, 50 µm; B, 10 µm.

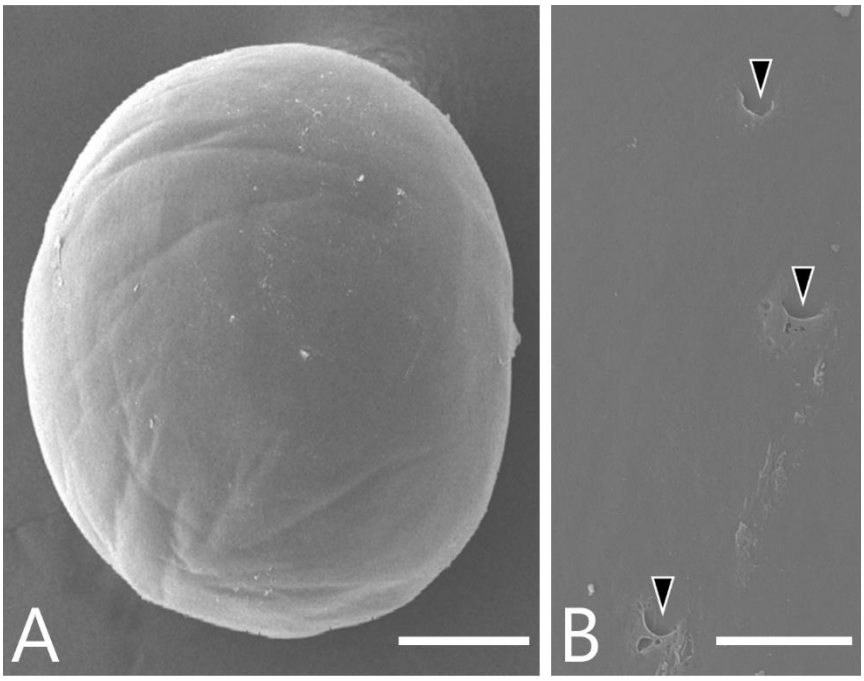
A
B

Fig. 31. Embryonic development of *Obipteryx* sp., DAPI staining, lateral view, anterior of the egg to the top, ventral of the egg to the left. A: Stage 1. B: Stage 2. C: Stage 3. D: Stage 4. E: Stage 5. F: Stage 6. G: Stage 7. H: Stage 8. I: Stage 9. J: Stage 10. K: Stage 11. L: Stage 12.

Am, amnion; An, antenna; Ce, cercus; CE, compound eye; Em, embryo; GD, germ disc; HC, head capsule; HL, head lobe; Md, mandible; MxP, maxillary palp; Pce, protocephalon; Pco, protocorm; SDO, secondary dorsal organ; Se, serosa; Th1L, prothoracic leg.

Scale bars = 100 µm.

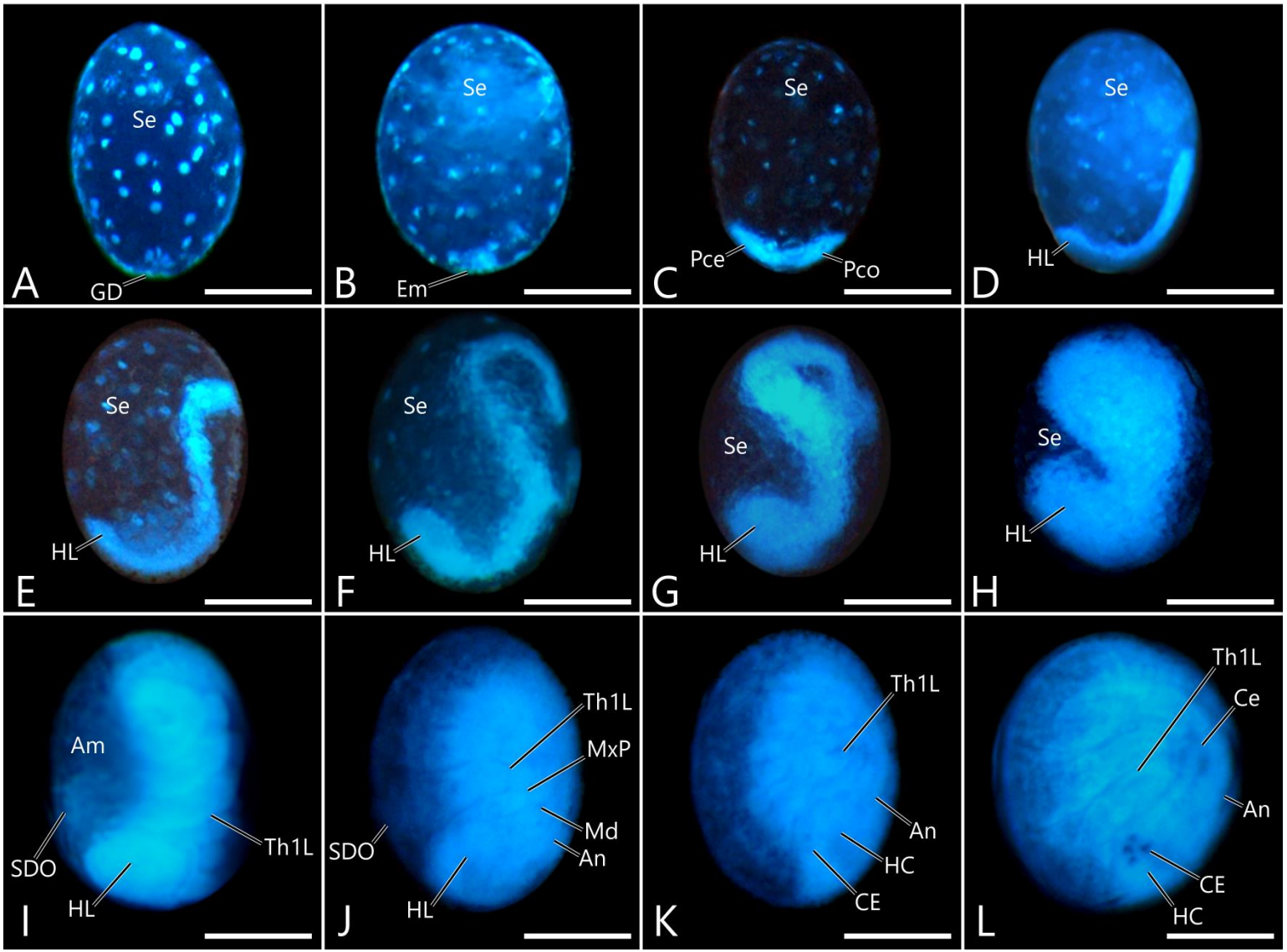
A
Se
GD
B
Se
Em
C
Se
Pce
Pco
D
Se
HL
E
Se
HL
F
Se
HL
G
Se
HL
H
Se
HL
I
Am
SDO
Th1L
HL
J
Th1L
MxP
SDO
Md
An
HL
K
Th1L
An
HC
CE
L
Th1L
Ce
An
CE
HC

Fig. 32. Thickened serosa and thickened serosal cuticle beneath the embryo of *Obipteryx* sp., Stages 2 (A) and 4 (B), anterior of the egg at the top. A: A vertical section of an embryo. B: A sagittal section of an embryo, ventral of the egg to the left.

Am, amnion; Em, embryo; Me, mesoderm; Se, serosa; SeCt, serosal cuticle; TSe, thickened serosa; TSeCt, thickened serosal cuticle; Y, yolk.

Scale bars = 20 μm.

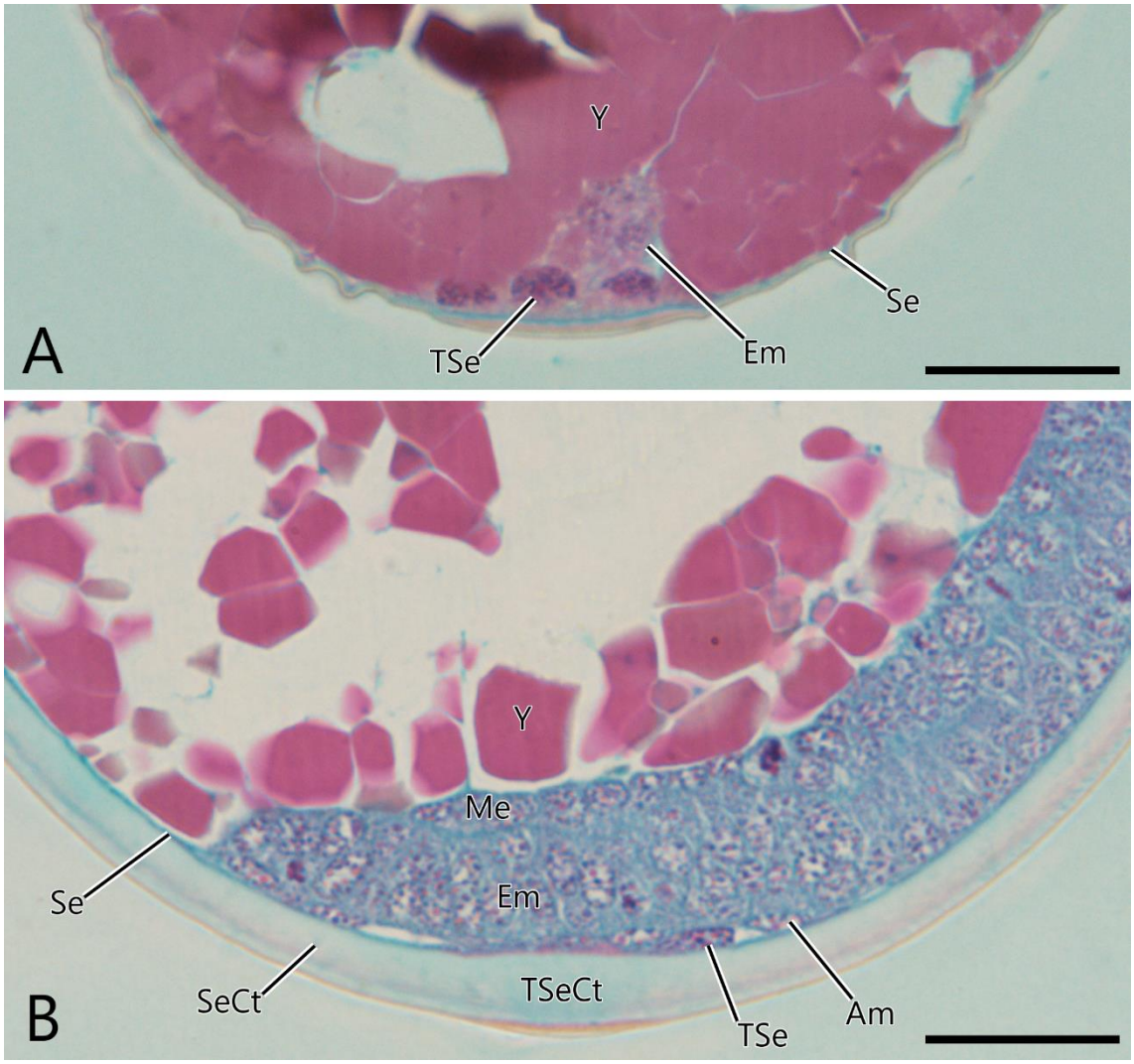
Y
Se
TSe
Em
A
Y
Me
Se
Em
SeCt
TSeCt
TSe
Am
B

Fig. 33. An egg of *Paraleuctra cercia*, which is artificially wrinkled during the drying for processing specimens, SEM, lateral view.

Scale bar = 50 μm.

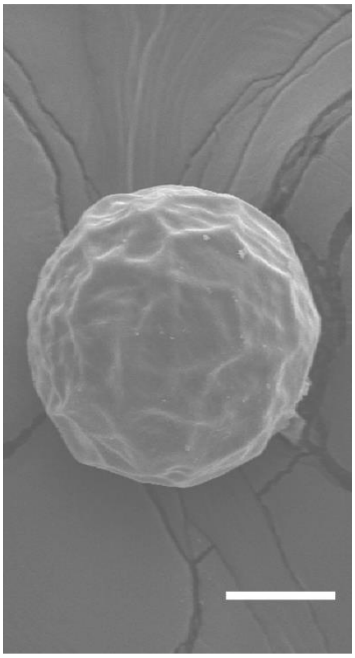

Fig. 34. Embryonic development of *Paraleuctra cercia*, DAPI staining, lateral view, anterior of the egg to the top, ventral of the egg to the left. A: Stage 1. B: Stage 2. C: Stage 3. D: Stage 4. E: Stage 5. F: Stage 6. G: Stage 7. H: Stage 8. I: Stage 9. J: Stage 10. K: Stage 11. L: Stage 12.

Am, amnion; An, antenna; Ce, cercus; CE, compound eye; Cllr, clypeolabrum; Em, embryo; Ga, galea; GD, germ disc; HC, head capsule; HL, head lobe; LbP, labial palp; Lr, labrum; Md, mandible; MxCp, maxillary coxopodite; MxP, maxillary palp; Pce, protocephalon; Pco, protocorm; SDO, secondary dorsal organ; Se, serosa; Th1L, prothoracic leg.

Scale bars = 50 μm.

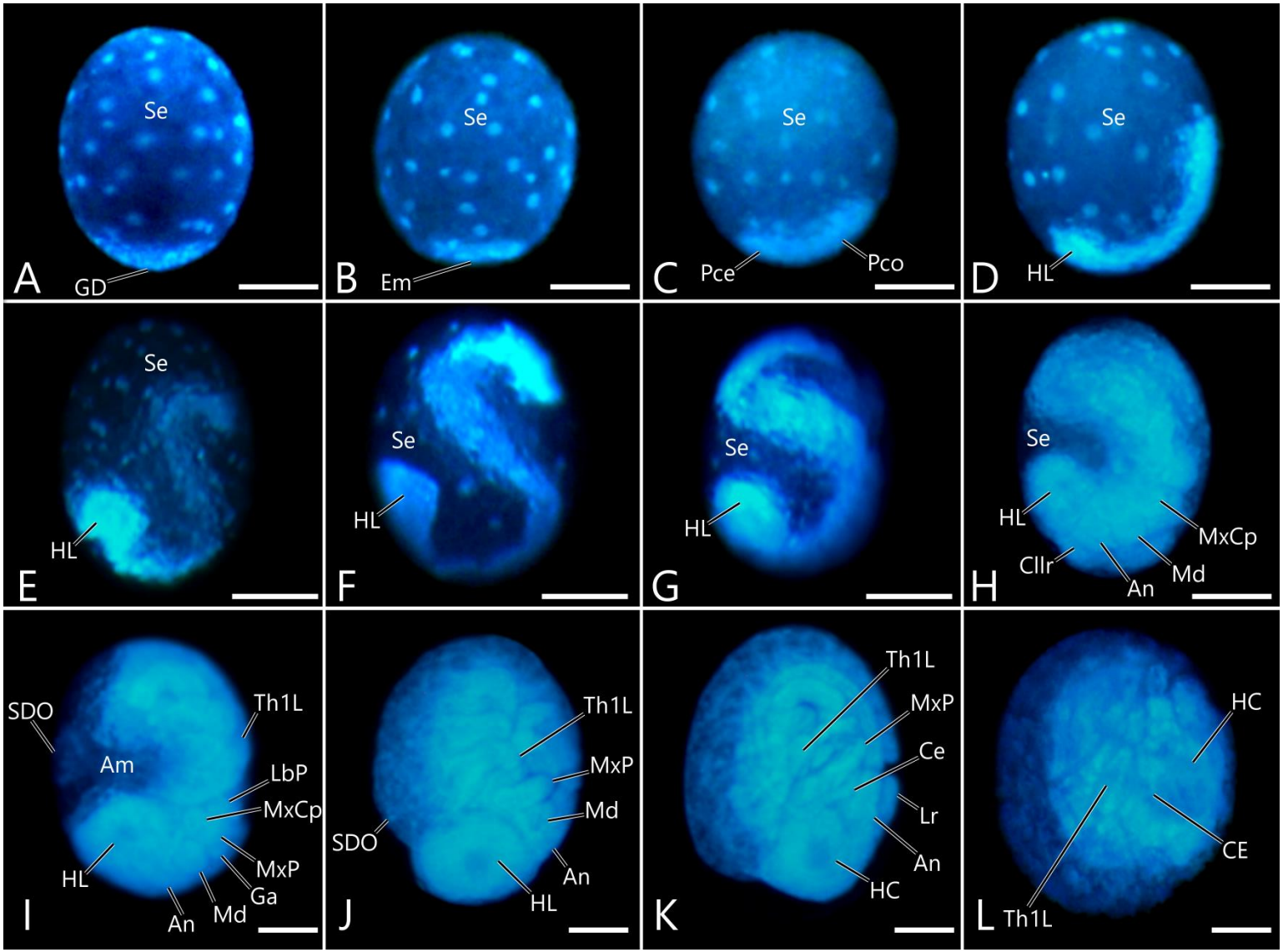
A
Se
GD
B
Se
Em
C
Se
Pce
Pco
D
Se
HL
E
Se
HL
F
Se
HL
G
Se
HL
H
Se
HL
MxCp
CIlr
An
Md
I
SDO
Th1L
Am
LbP
MxCp
HL
MxP
Ga
An
Md
J
Th1L
MxP
Md
SDO
An
HL
K
Th1L
MxP
Ce
Lr
An
HC
L
HC
CE
Th1L

Fig. 35. Thickened serosa and thickened serosal cuticle beneath the embryo of *Paraleuctra cercia*, Stages 3 (A) and 6 (B), anterior of the egg to the top. A: A vertical section of an embryo. B: A sagittal section of an embryo, ventral of the egg to the left.

Am, amnion; AmCv, amniotic cavity; Ch, chorion; Em, embryo; Me, mesoderm; Se, serosa; SeCt, serosal cuticle; TSe, thickened serosa; TSeCt, thickened serosal cuticle; Y, yolk.

Scale bars = 20 μm.

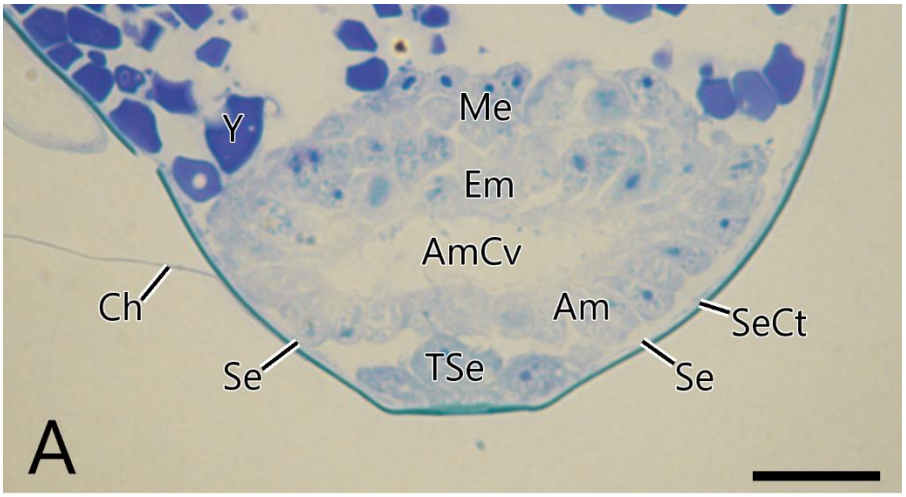
Y
Me
Em
AmCv
Ch
Am
SeCt
Se
TSe
Se
A

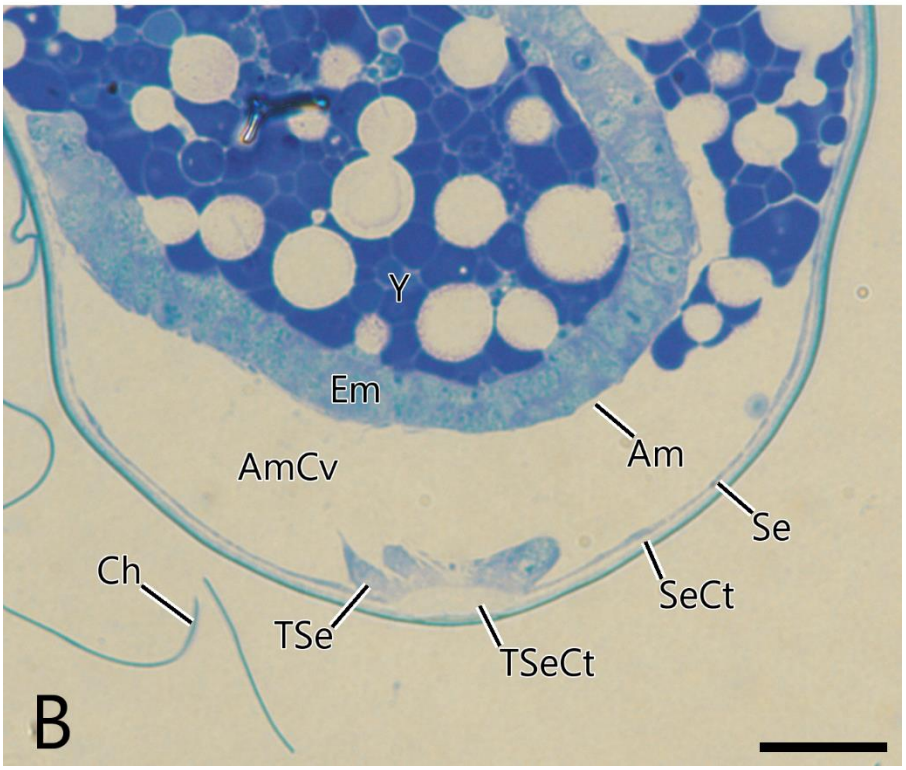
Y
Em
AmCv
Am
Se
Ch
SeCt
TSe
TSeCt
B

Fig. 36. An egg of *Apteroperla tikumana*, SEM, nano-sit method, lateral view, anterior to the top.

Scale bar = 50 μm.

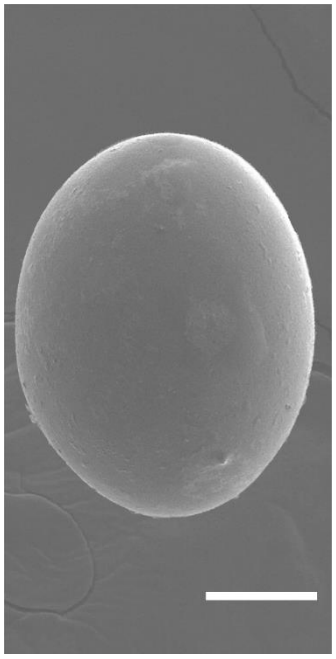

Fig. 37. Embryonic development of *Apteroperla tikumana*, DAPI staining, lateral view, anterior of the egg to the top, ventral of the egg to the left. A: Stage 1. B: Stage 2. C: Stage 3. D: Stage 4. E: Stage 5. F: Stage 6. G: Stage 7. H: Stage 8. I: Stage 9. J: Stage 10. K: Stage 11. L: Stage 12.

Am, amnion; An, antenna; Em, embryo; GD, germ disc; HC, head capsule; HL, head lobe; Lb, labium; Md, mandible; Mx, maxilla; MxP, maxillary palp; Pce, protocephalon; Pco, protocorm; SDO, secondary dorsal organ; Se, serosa; Th1L, prothoracic leg.

Scale bars = 50 μm.

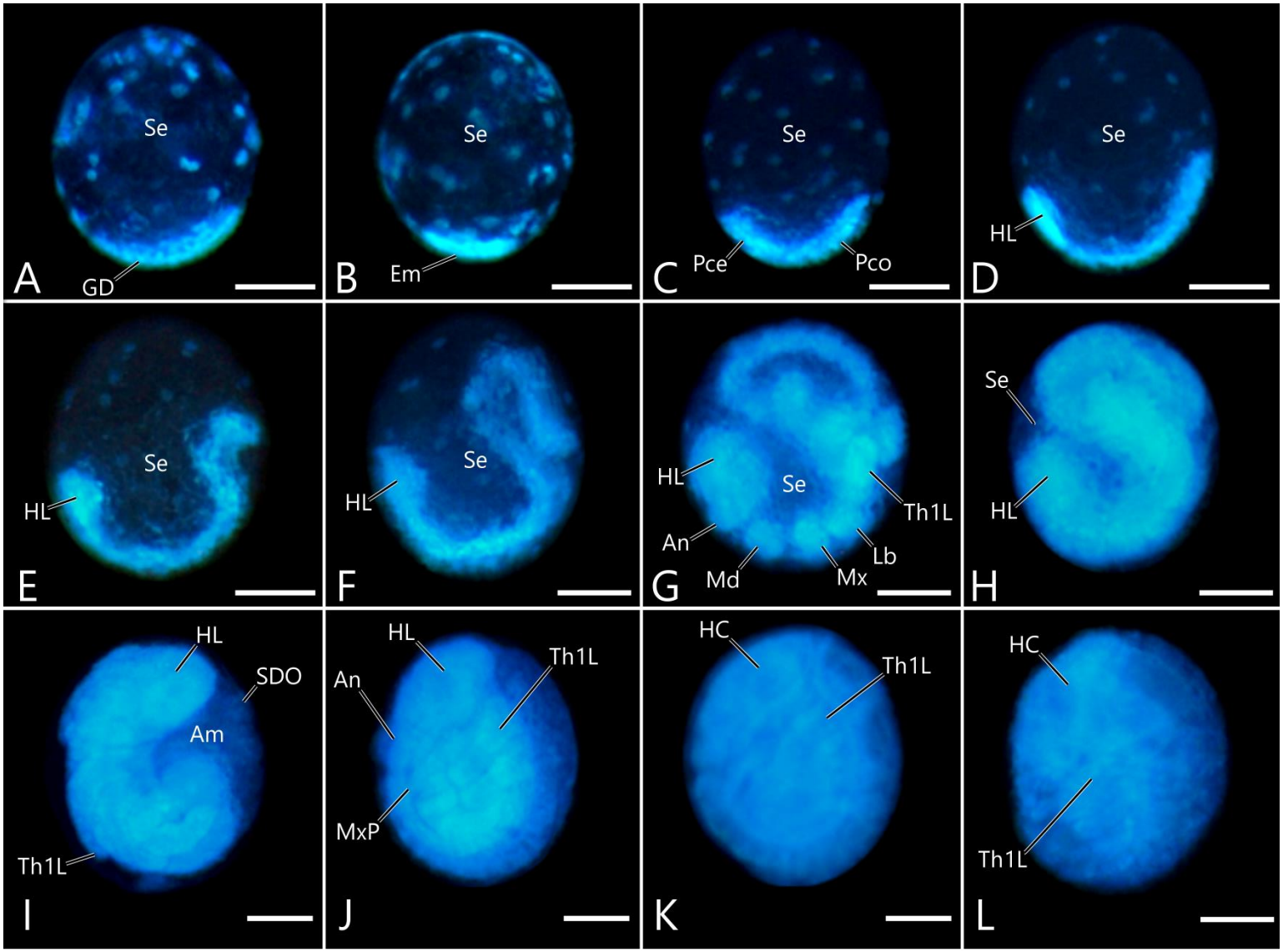
A
Se
GD
B
Se
Em
C
Se
Pce
Pco
D
Se
HL
E
Se
HL
F
Se
HL
G
HL
Se
Th1L
An
Lb
Md
Mx
H
Se
HL
I
HL
SDO
Am
Th1L
J
HL
Th1L
An
MxP
K
HC
Th1L
L
HC
Th1L

Fig. 38. A sagittal section of the thickened serosa and thickened serosal cuticle beneath the embryo of *Apteroperla tikumana*, Stage 3, anterior of the egg to the top, ventral of the egg to the left.

Am, amnion; Em, embryo; Me, mesoderm; Se, serosa; SeCt, serosal cuticle; TSe, thickened serosa; TSeCt, thickened serosal cuticle; Y, yolk.

Scale bar = 20 μm.

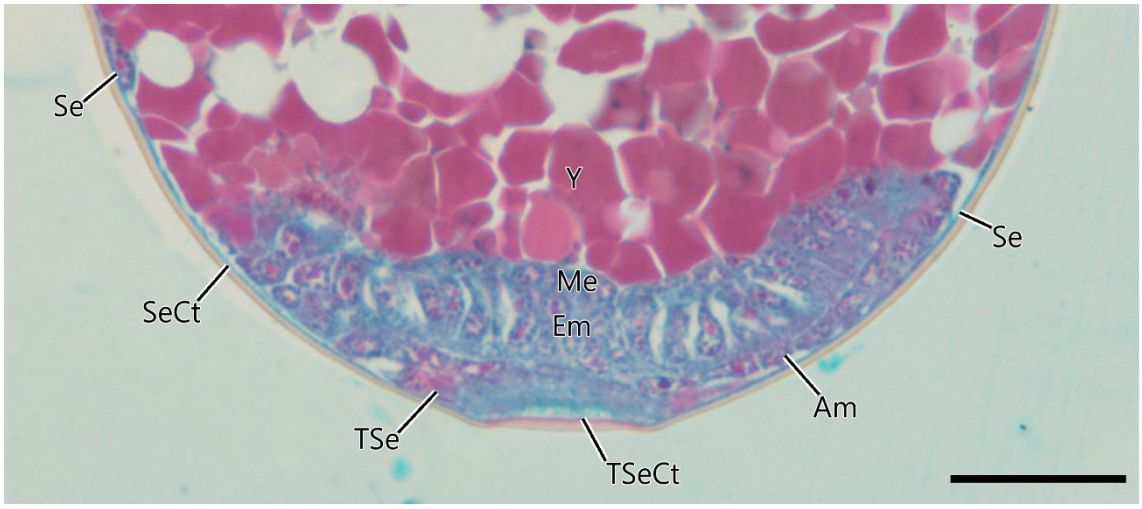
Se
Y
Se
Me
SeCt
Em
Am
TSe
TSeCt

Fig. 39. Eggs of *Protonemura towadensis*, SEM, lateral view, anterior to the top. A: Egg, which is artificially dented during the drying for processing specimens. B: Micropyles (arrowheads) (a white slanting line is an artifact).

Scale bars = A, 50 μm; B, 10 μm.

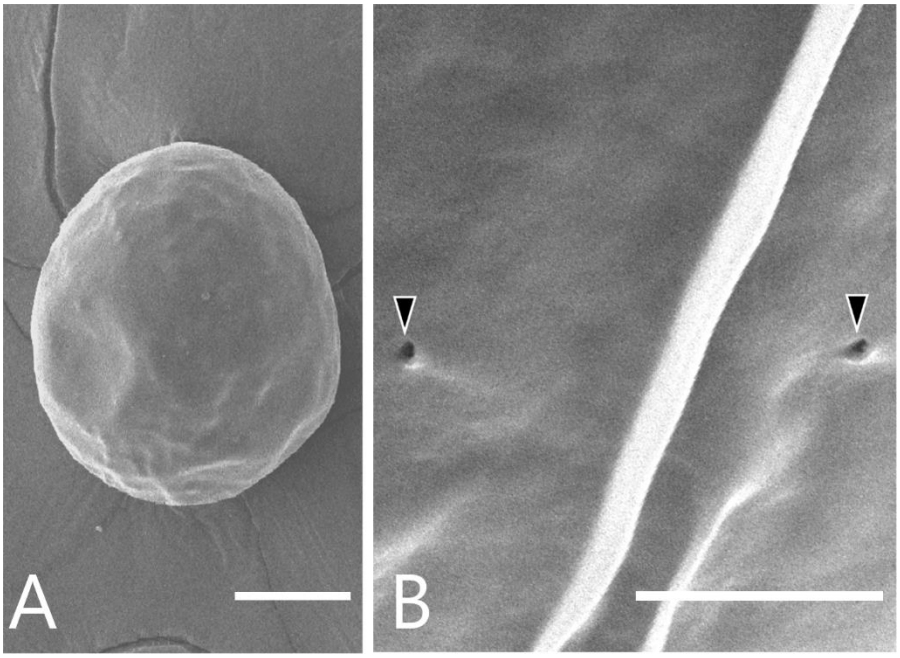
A
B

Fig. 40. Embryonic development of *Protonemura towadensis*, DAPI staining, lateral view, anterior of the egg to the top, ventral of the egg to the left. A: Stage 1. B: Stage 2. C: Stage 3. D: Stage 4. E: Stage 5. F: Stage 6. G: Stage 7. H: Stage 8. I: Stage 9. J: Stage 10. K: Stage 11. L: Stage 12.

Am, amnion; An, antenna; Ce, cercus; CE, compound eye; Em, embryo; GD, germ disc; HC, head capsule; HL, head lobe; Md, mandible; MxCp, maxillary coxopodite; MxP, maxillary palp; Pce, protocephalon; Pco, protocorm; SDO, secondary dorsal organ; Se, serosa; Th1L, prothoracic leg.

Scale bars = 50 μm.

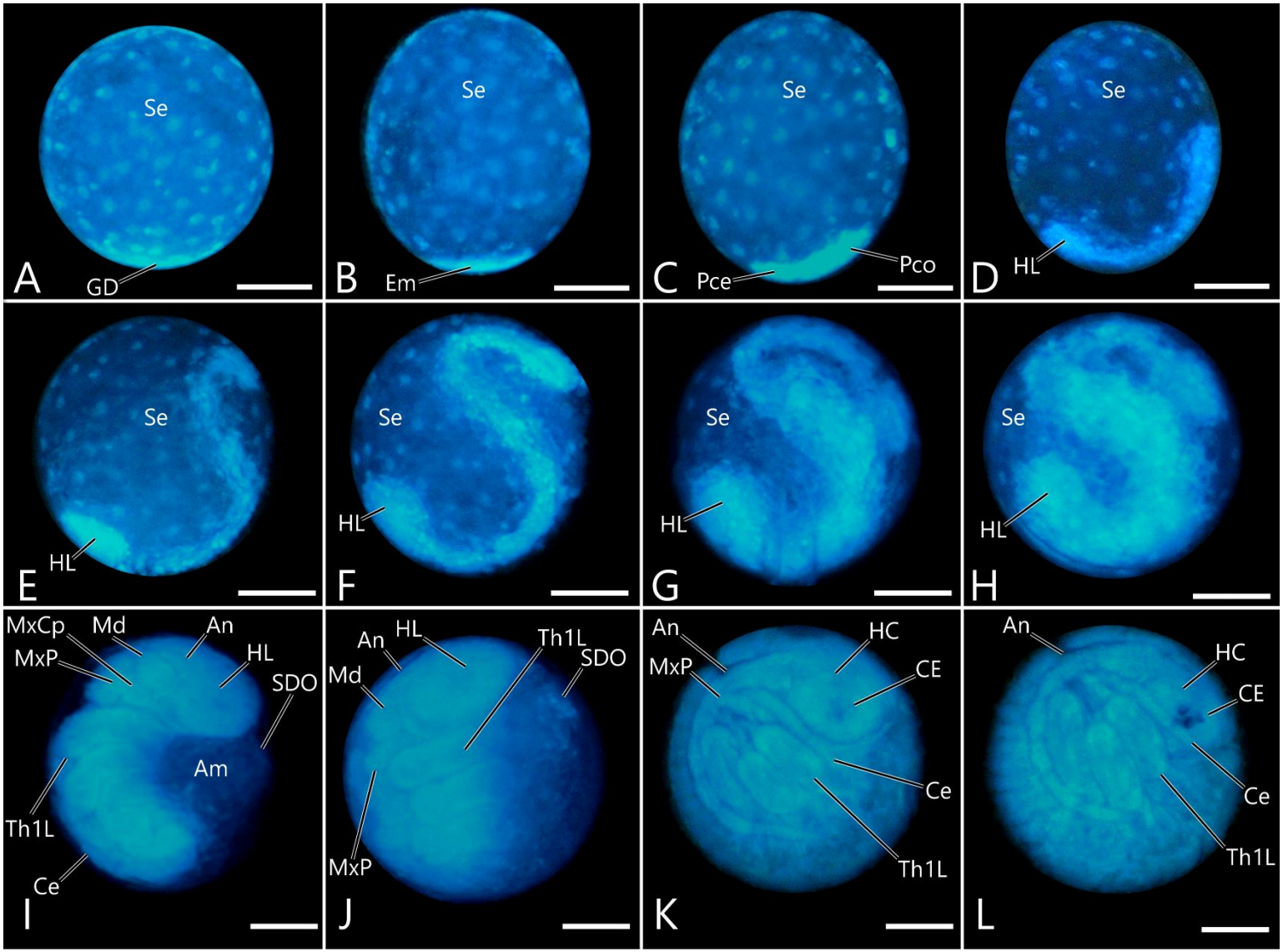
A
Se
GD
B
Se
Em
C
Se
Pce
Pco
D
Se
HL
E
Se
HL
F
Se
HL
G
Se
HL
H
Se
HL
I
MxCp
Md
An
MxP
HL
SDO
Am
Th1L
Ce
J
An
HL
Th1L
Md
SDO
MxP
K
An
HC
MxP
CE
Ce
Th1L
L
An
HC
CE
Ce
Th1L

Fig. 41. Sagittal sections of the thickened serosa and thickened serosal cuticle beneath the embryo of *Protonemura towadensis*, Stages 3 (A) and 7 (B), anterior of the egg to the top, ventral of the egg to the left.

Am, amnion; Ch, chorion; Em, embryo; Me, mesoderm; Sd, stomodaeum; Se, serosa; SeCt, serosal cuticle; TSe, thickened serosa; TSeCt, thickened serosal cuticle; Y, yolk.

Scale bars = 20 μm.

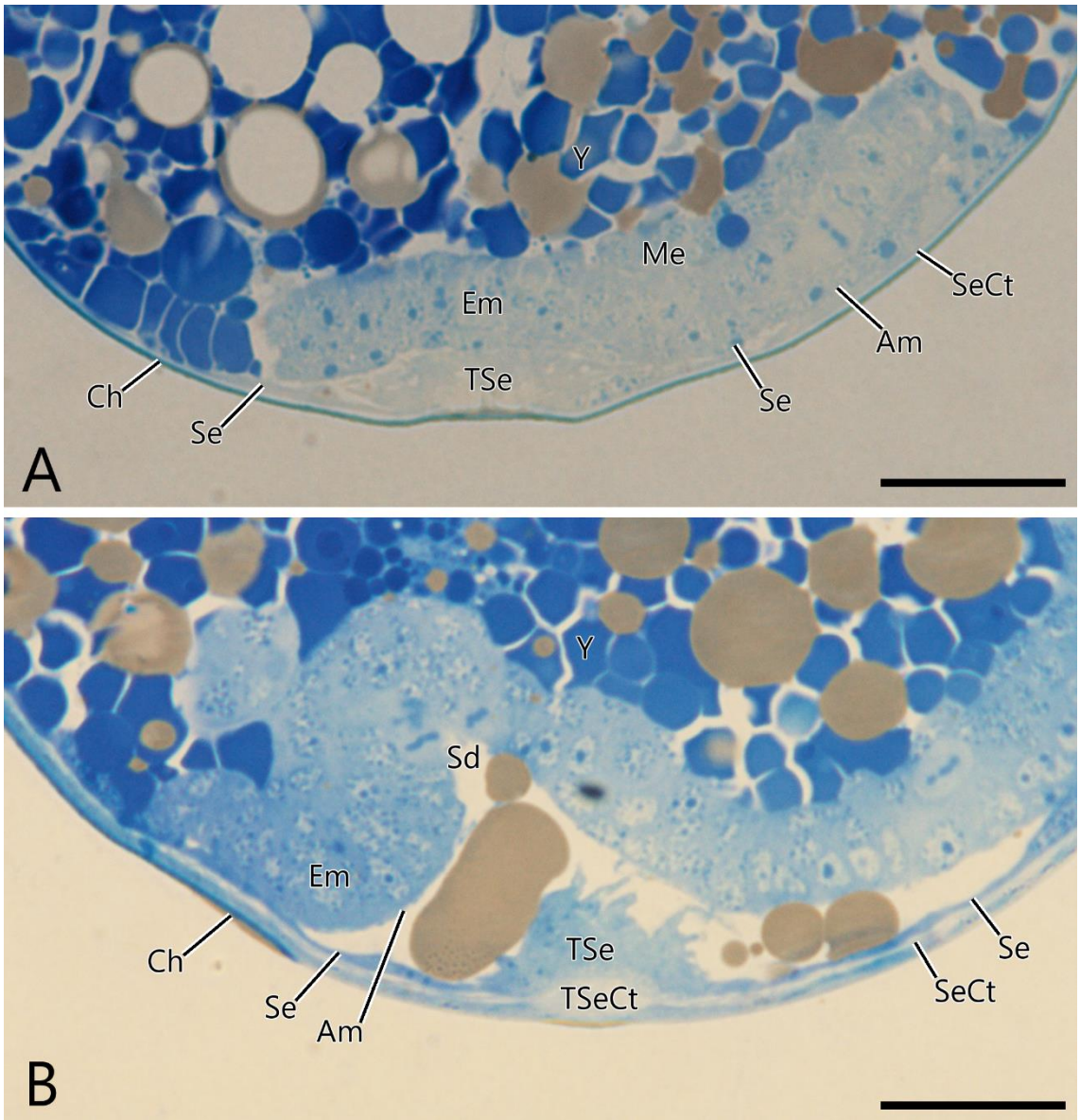
Y
Me
SeCt
Em
Am
TSe
Ch
Se
Se
A
Y
Sd
Em
Ch
TSe
Se
Se
Am
TSeCt
SeCt
B

Fig. 42. Eggs of *Calineuria stigmatica*, SEM, lateral view, anterior to the top. A: Egg, with the anchor plate resolved by soaking in bleach for a short time. B: Enlargement of the posterior pole with the intact anchor plate. C: Posterior pole, with the anchor plate resolved. D: Anterior half of egg, showing micropyles. E: Enlargement of micropyles. Arrowheads in (A) and (D) indicate micropyles.

AP, anchor plate; Co, collar.

Scale bars = A, D, 100 µm; B, C, 50 µm; E, 10 µm.

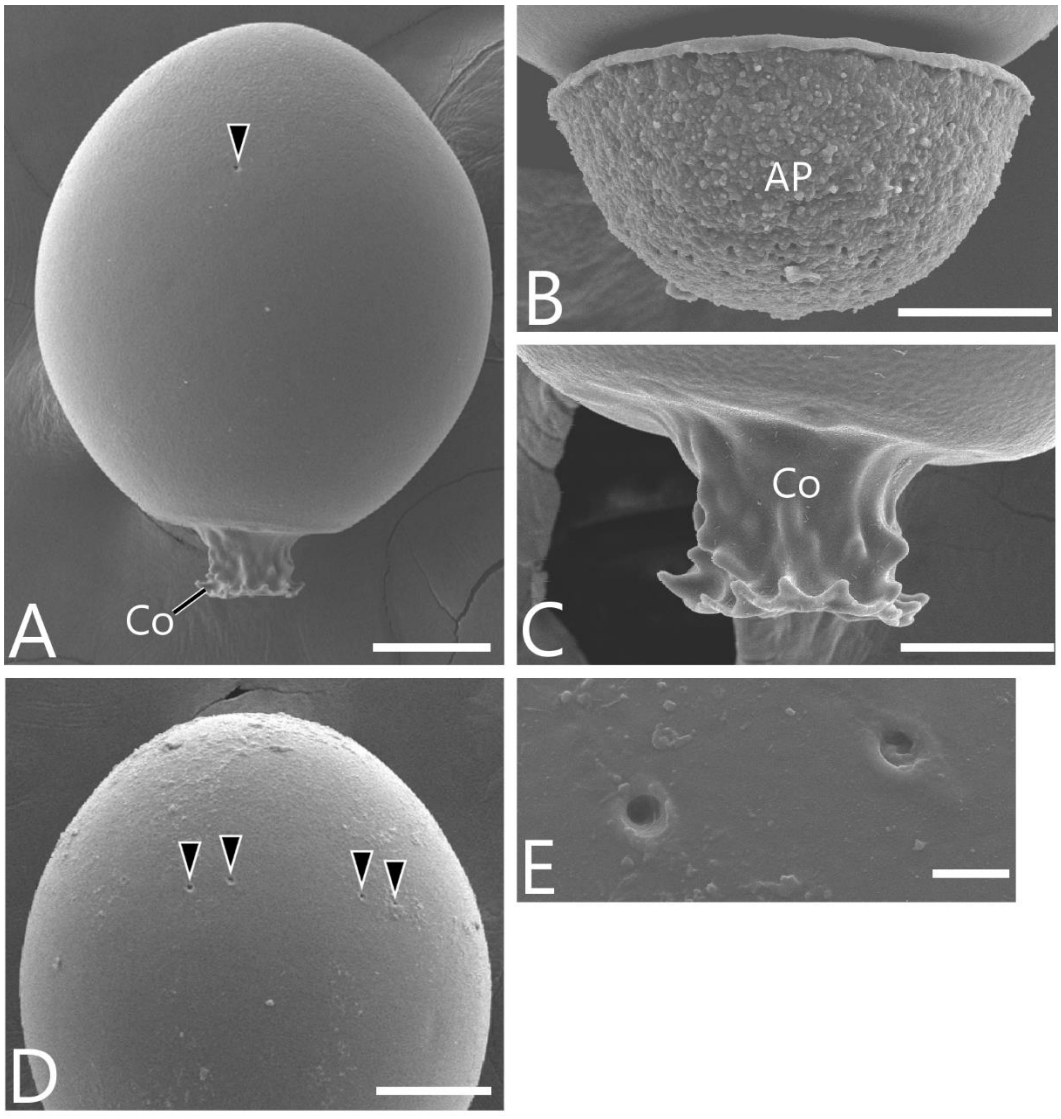
A
Co
B
AP
C
Co
D
E

Fig. 43. Embryonic development of *Calineuria stigmatica*, DAPI staining, lateral view, anterior of the egg to the top, ventral of the egg to the left. A: Stage 2. B: Stage 3. C: Stage 4. D: Stage 5. E: Stage 6. F: Stage 7. G: Stage 8. H: Stage 9. I: Stage 10. J: Stage 11. K: Stage 12.

Am, amnion; An, antenna; Ce, cercus; CE, compound eye; Em, embryo; Ga, galea; HC, head capsule; HL, head lobe; LbP, labial palp; Lr, labrum; Md, mandible; MxCp, maxillary coxopodite; MxP, maxillary palp; Pce, protocephalon; Pco, protocorm; SDO, secondary dorsal organ; Se, serosa; Th1L, prothoracic leg.

Scale bars = 100 μm.

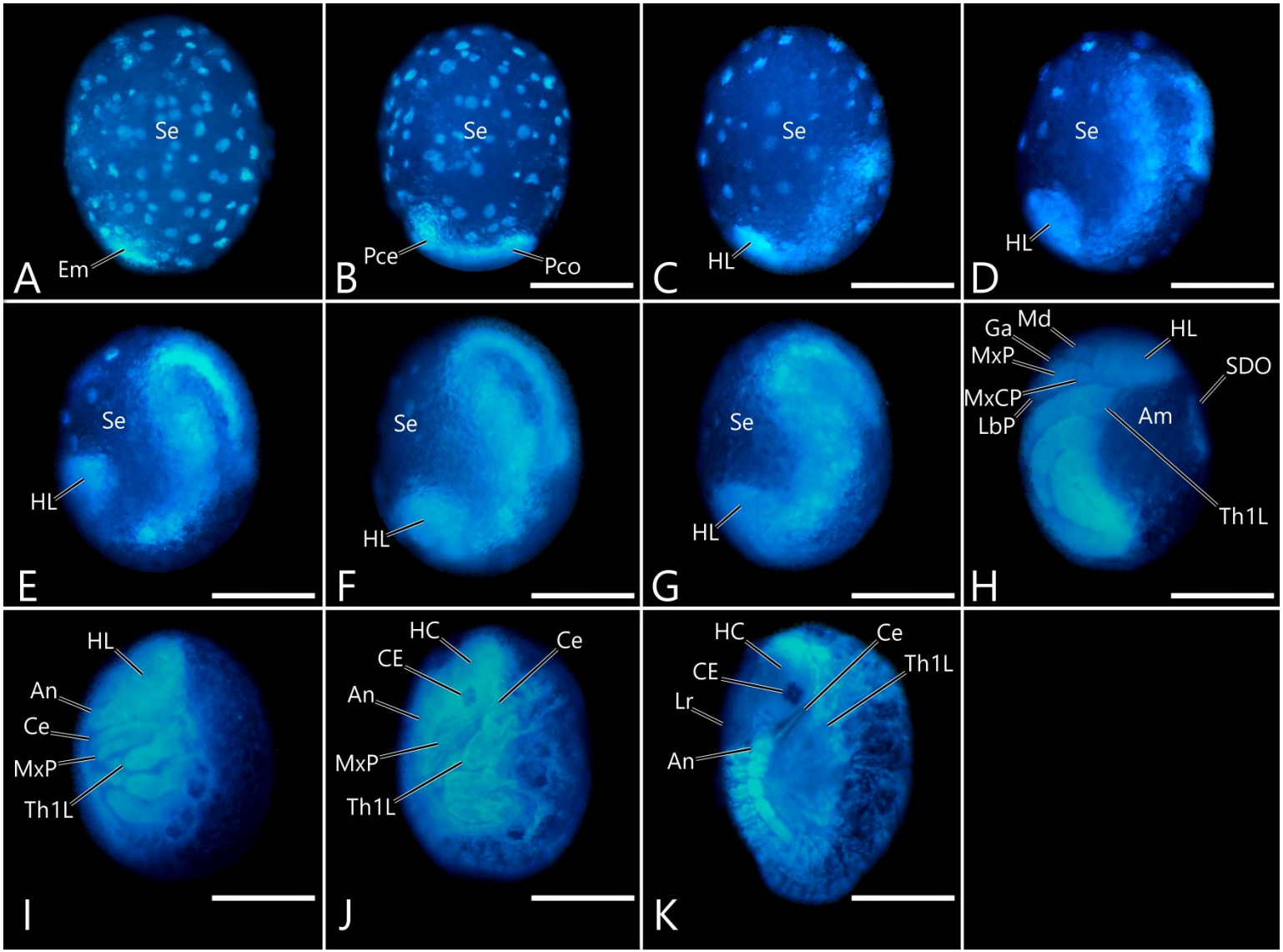
A
Em
Se
B
Pce
Pco
Se
C
HL
Se
D
HL
Se
E
HL
Se
F
HL
Se
G
HL
Se
H
Ga
Md
HL
MxP
SDO
MxCP
LbP
Am
Th1L
I
HL
An
Ce
MxP
Th1L
J
HC
CE
Ce
An
MxP
Th1L
K
HC
Ce
CE
Th1L
Lr
An

Fig. 44. A vertical section of the thickened serosa and thickened serosal cuticle beneath the embryo of *Calineuria stigmatica*, Stage 2, anterior of the egg to the top.

Ch, chorion; Em, embryo; Se, serosa; SeCt, serosal cuticle; TSe, thickened serosa; TSeCt, thickened serosal cuticle; Y, yolk.

Scale bar = 20 μm.


Y
Em
TSe
TSeCt
Ch
Se
Se
SeCt

Fig. 45. Eggs of *Sweltsa* sp., SEM, lateral view, anterior to the top. A: Egg. B: Anterior half of the egg. Arrowheads indicate micropyles. C: Enlargement of micropyles.

Scale bars = A, 100 µm; B, 50 µm; C, 10 µm.

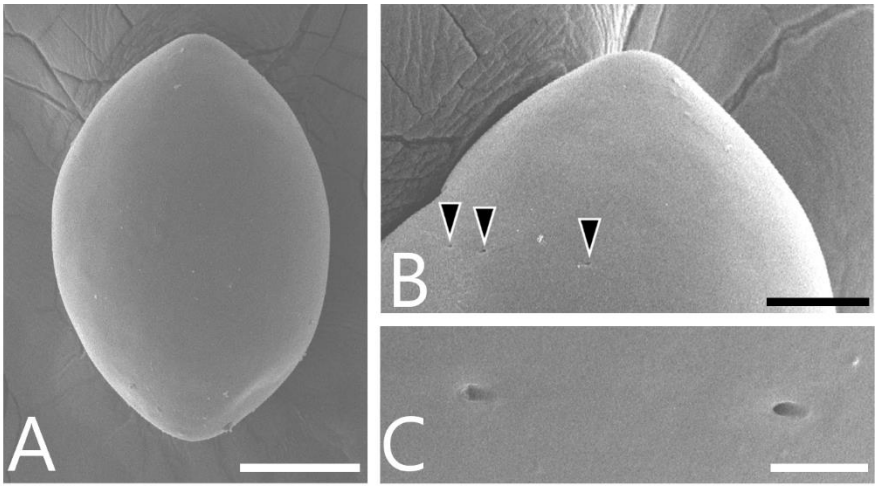
A
B
C

Fig. 46. Embryonic development of *Sweltsa* sp., DAPI staining, lateral view, anterior of the egg to the top, ventral of the egg to the left. A: Stage 2. B: Stage 3. C: Stage 4. D: Stage 5. E: Stage 6. F: Stage 7. G: Stage 8. H: Stage 9. I: Stage 10. J: Stage 11. K: Stage 12.

Am, amnion; An, antenna; Ce, cercus; CE, compound eye; Em, embryo; ET, egg tooth; Ga, galea; HC, head capsule; HL, head lobe; Lb, labium; LbP, labial palp; Lr, labrum; Md, mandible; Mx, maxilla; MxCp, maxillary coxopodite; MxP, maxillary palp; Pce, protocephalon; Pco, protocorm; SDO, secondary dorsal organ; Se, serosa; Th1, 3L, pro- and metathoracic legs.

Scale bars = 100 μm.

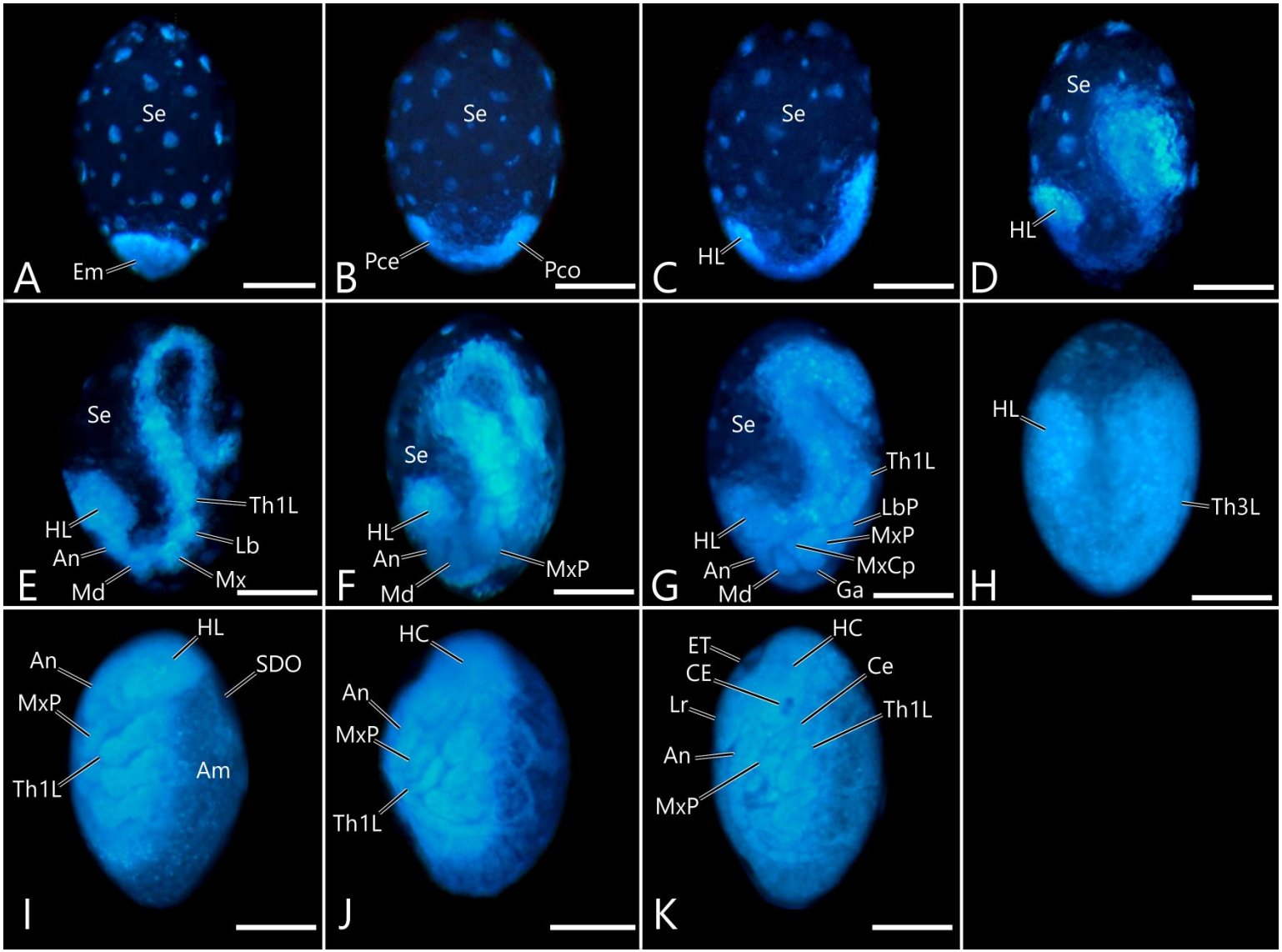
A
Se
Em
B
Se
Pce
Pco
C
Se
HL
D
Se
HL
E
Se
Th1L
HL
Lb
An
Md
Mx
F
Se
HL
An
Md
MxP
G
Se
Th1L
LbP
HL
MxP
An
MxCp
Md
Ga
H
HL
Th3L
I
HL
An
SDO
MxP
Am
Th1L
J
HC
An
MxP
Th1L
K
ET
HC
CE
Ce
Lr
Th1L
An
MxP

Fig. 47. A sagittal section of the thickened serosa and thickened serosal cuticle beneath the embryo of *Sweltsa* sp., Stage 4, anterior of the egg to the top, ventral of the egg to the left.

Am, amnion; Ch, chorion; Em, embryo; Se, serosa; SeCt, serosal cuticle; TSe, thickened serosa; TSeCt, thickened serosal cuticle; Y, yolk.

Scale bar = 20 μm.

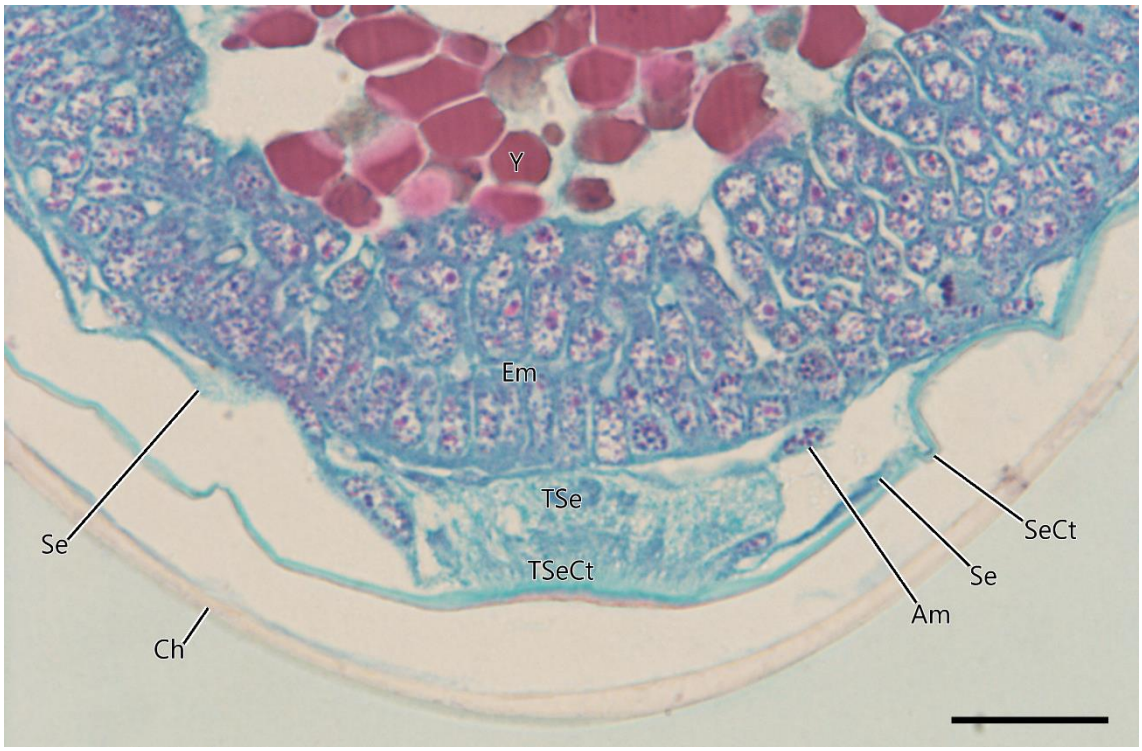
Y
Em
TSe
TSeCt
Se
Ch
Am
Se
SeCt

Fig. 48. Eggs of *Ostrovus* sp., SEM. A: Right side of the egg, anterior to the top. B: Left side of the egg. C: Newly laid egg, ventral view, left side to the top, anterior to the right. D: Egg just before hatching, ventral view. E: Posterior half of the left side of the egg. F: Enlargement of micropyles. Arrowheads in (B) and (E) indicate micropyles.

AP, anchor plate; Co, collar.

Scale bars = A–D, 100 μm; E, 50 μm; F, 10 μm.

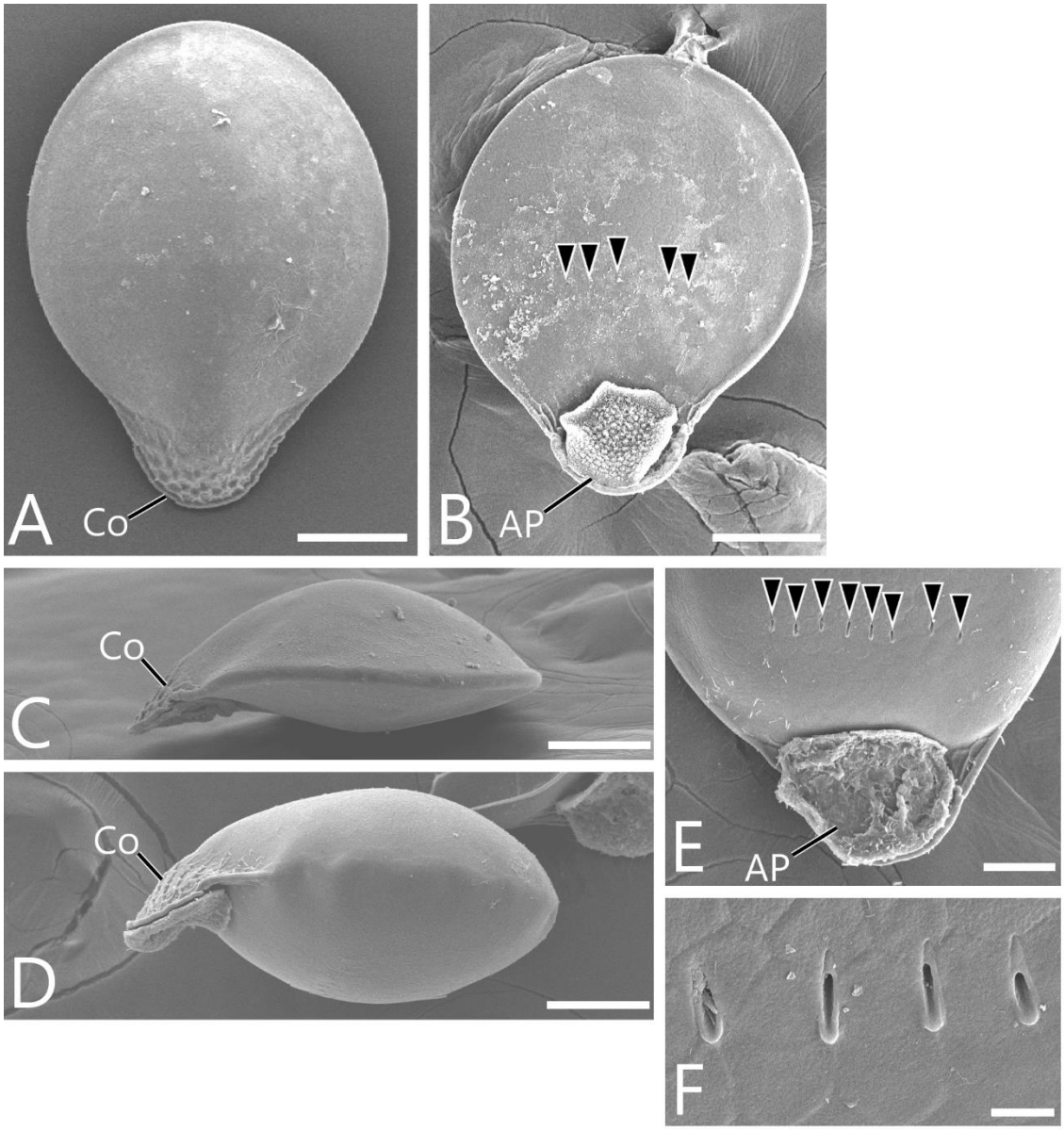
A
Co
B
AP
C
Co
D
Co
E
AP
F

Fig. 49. Embryonic development of *Ostrovus* sp., DAPI staining, lateral view from right side, anterior of the egg to the top, ventral of the egg to the right. A: Stage 2. B: Stage 3. C: Stage 4. D: Stage 5. E: Stage 6. F: Stage 7. G: Stage 8. H: Stage 9. I: Stage 10. J: Stage 11. K: Stage 12.

Am, amnion; An, antenna; Ce, cercus; CE, compound eye; Em, embryo; ET, egg tooth; Ga, galea; HC, head capsule; HL, head lobe; La, lacinia; Lr, labrum; Md, mandible; MxCp, maxillary coxopodite; MxP, maxillary palp; Pce, protocephalon; Pco, protocorm; SDO, secondary dorsal organ; Se, serosa; Th1L, prothoracic leg.

Scale bars = 100 μm.

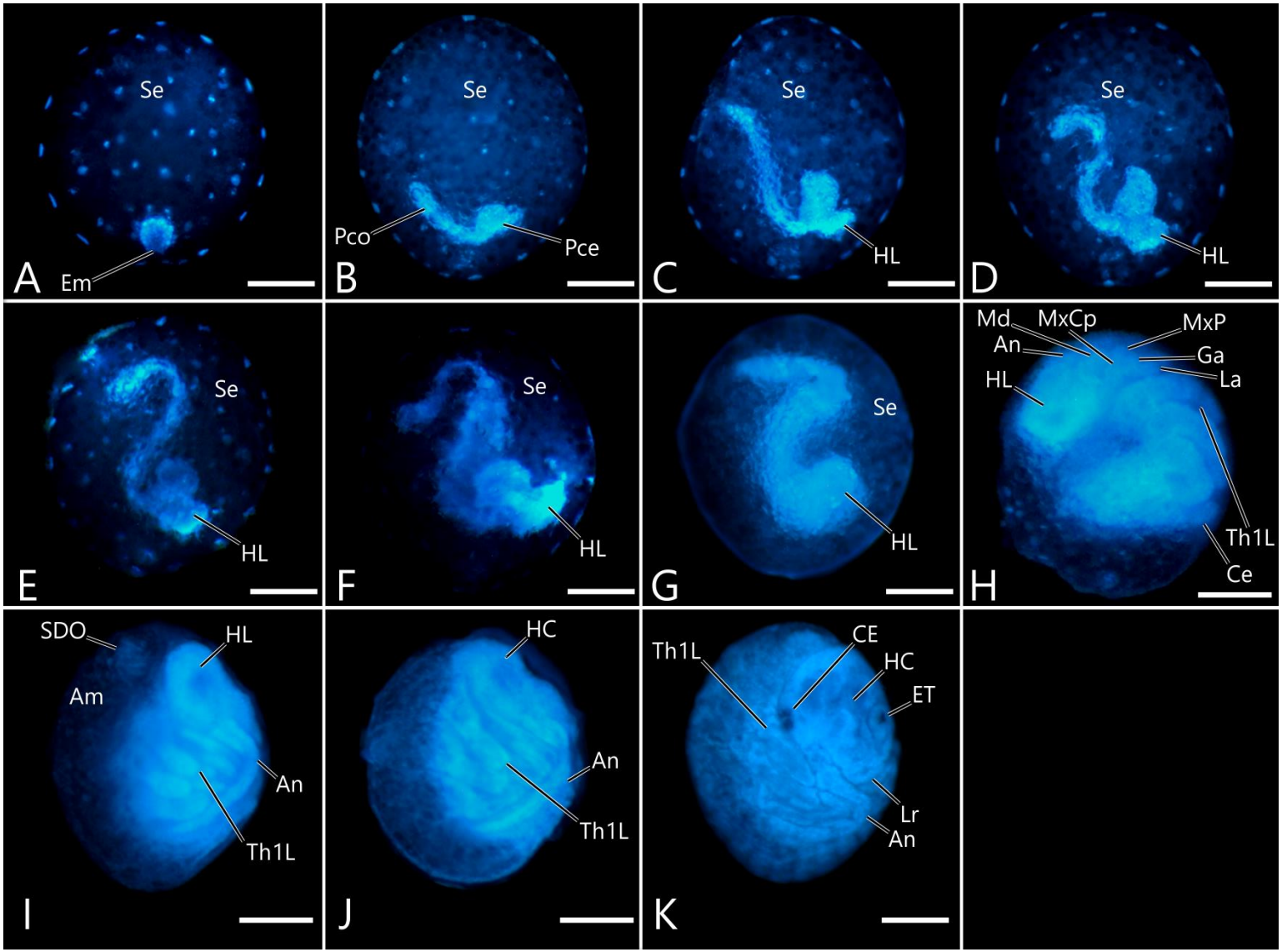
A
Se
Em
B
Se
Pco
Pce
C
Se
HL
D
Se
HL
E
Se
HL
F
Se
HL
G
Se
HL
H
Md
MxCp
MxP
An
Ga
HL
La
Th1L
Ce
I
SDO
HL
Am
An
Th1L
J
HC
An
Th1L
K
Th1L
CE
HC
ET
Lr
An

Fig. 50. Sagittal sections of the thickened serosa and thickened serosal cuticle beneath the embryo of *Ostrovus* sp., Stage 4, anterior of the egg to the top, ventral of the egg to the right. A, B: A sagittal section of an embryo (A) and the enlargement (B).

Am, amnion; Ch, chorion; Co, collar; Em, embryo; Se, serosa; SeCt, serosal cuticle; TSe, thickened serosa; TSeCt, thickened serosal cuticle; Y, yolk.

Scale bars = A, 50 μm; B, 20 μm.

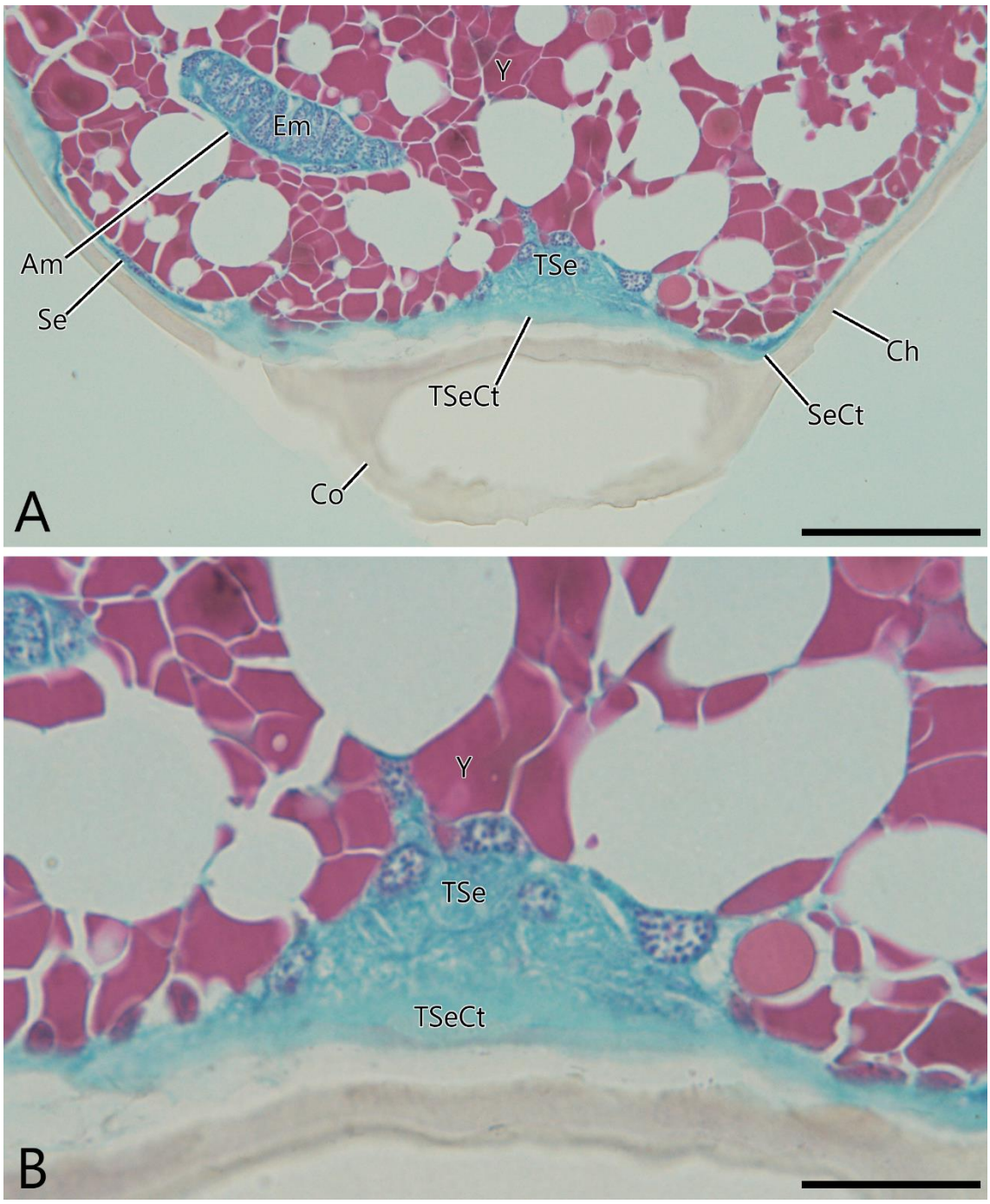
Y
Em
Am
Se
TSe
Ch
TSeCt
SeCt
Co
A
Y
TSe
TSeCt
B

Fig. 51. Eggs of *Yoraperla uenoi*, SEM. A: Egg, anterior view. Arrowheads indicate micropyles. B: Egg, posterior view. C: Egg, lateral view. D: Enlargement of micropyles.

AP, anchor plate.

Scale bars = A–C, 100 μm; D, 10 μm.

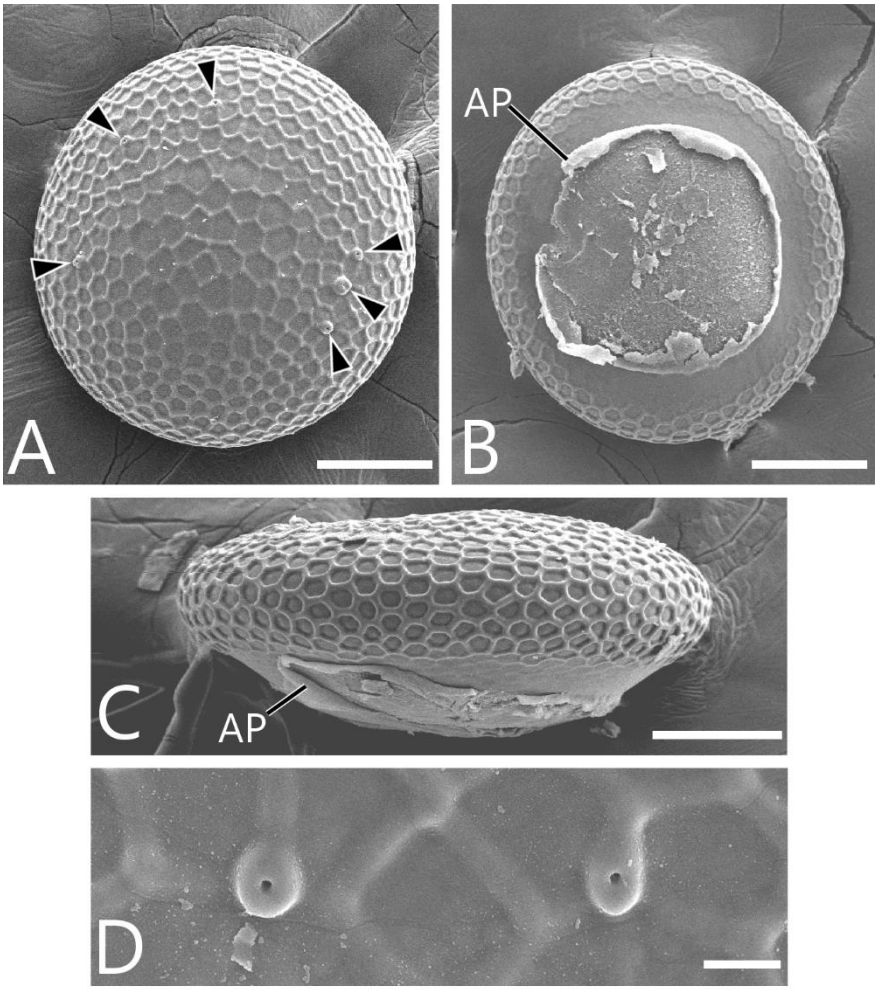
A
B
AP
C
AP
D

Fig. 52. Embryonic development of *Yoraperla uenoi*, DAPI staining, posterior view. A: Stage 1. B: Stage 2. C: Stage 3. D: Stage 4. E: Stage 5. F: Stage 6. G: Stage 7. H: Stage 8. I: Stage 9. J: Stage 10. K: Stage 11. L: Stage 12.

Ab, abdomen; Am, amnion; An, antenna; Ce, cercus; CE, compound eye; Em, embryo; Ga, galea; GD, germ disc; Gl, glossa; HC, head capsule; HL, head lobe; La, lacinia; Lb, labium; LbP, labial palp; Md, mandible; Mx, maxilla; MxP, maxillary palp; Pce, protocephalon; Pco, protocorm; Pgl, paraglossa; SDO, secondary dorsal organ; Se, serosa; Th1L, prothoracic leg.

Scale bars = 100 μm.

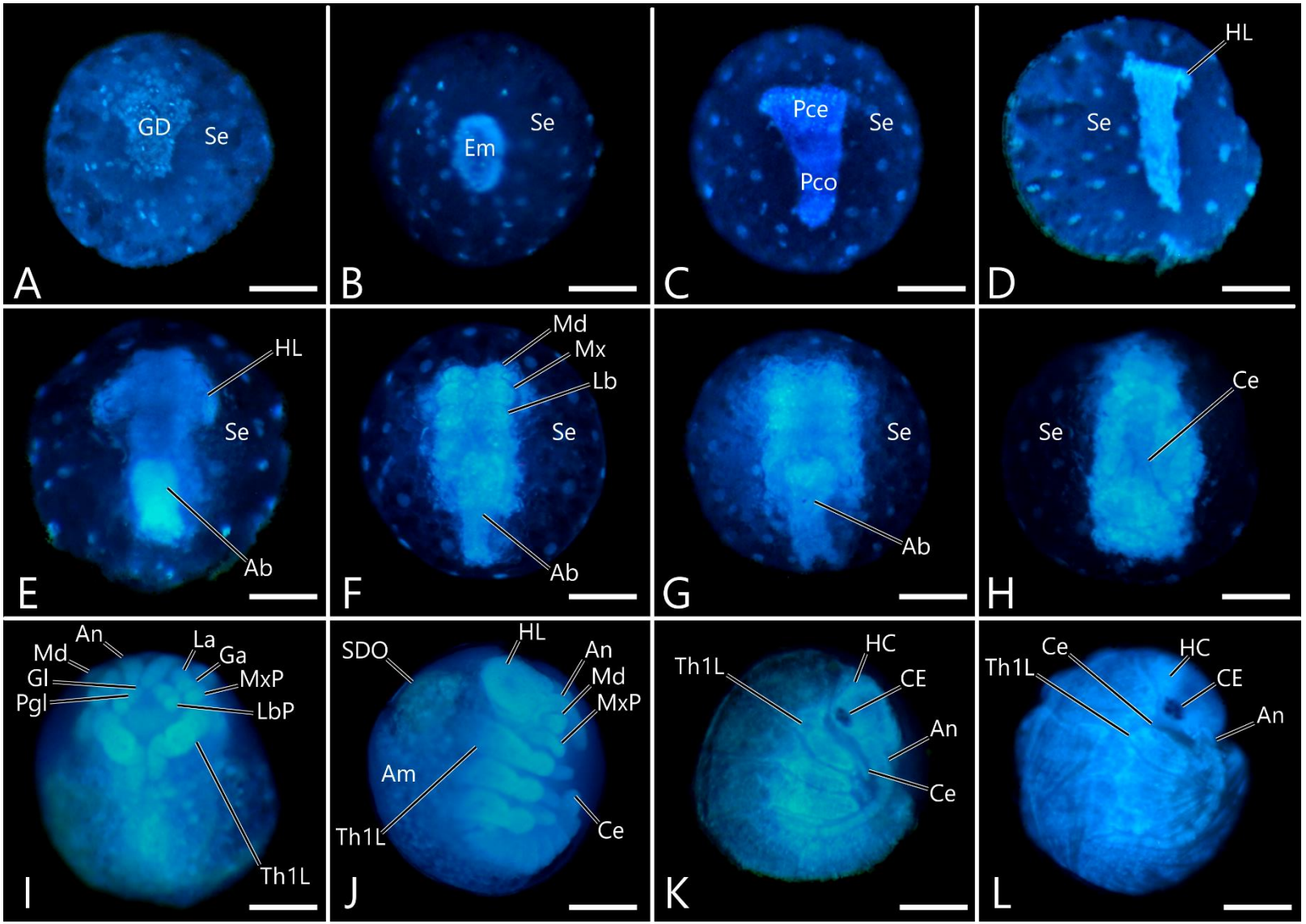
A
GD
Se
B
Em
Se
C
Pce
Se
Pco
D
HL
Se
E
HL
Se
Ab
F
Md
Mx
Lb
Se
Ab
G
Se
Ab
H
Se
Ce
I
An
Md
Gl
Pgl
La
Ga
MxP
LbP
Th1L
J
SDO
HL
An
Md
MxP
Am
Th1L
Ce
K
Th1L
HC
CE
An
Ce
L
Th1L
Ce
HC
CE
An

Fig. 53. Embryos of *Yoraperla uenoi*, Stages 2 (A), 5 (B, C), and 8 (D, E), anterior of the egg to the top. A: A sagittal section of an embryo, showing the thickened serosa is attached to it. B–E: Sagittal sections of embryos (B, D) and their enlargements (C, E), respectively, showing the thickened serosa and serosal cuticle beneath the embryo.

Am, amnion; AmCv, amniotic cavity; Ch, chorion; Em, embryo; Se, serosa; SeCt, serosal cuticle; TSe, thickened serosa; TSeCt, thickened serosal cuticle; Y, yolk.

Scale bars = A, C, E, 20 μm; B, D, 50 μm.

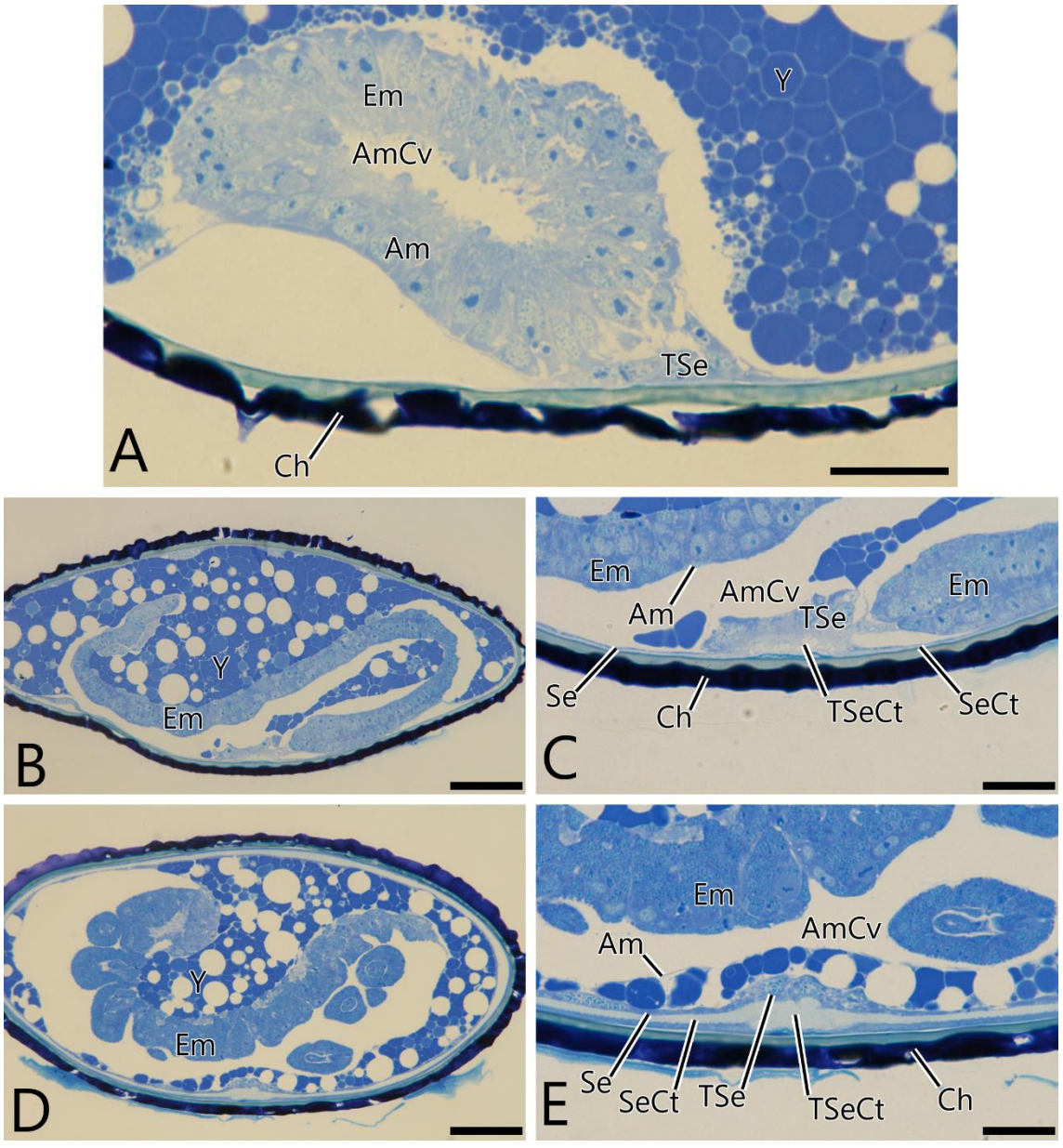
Em
AmCv
Am
Y
TSe
Ch
A
Y
Em
B
Em
Am
AmCv
TSe
Em
Se
Ch
TSeCt
SeCt
C
Y
Em
D
Em
AmCv
Am
Se
SeCt
TSe
TSeCt
Ch
E

Fig. 54. Time lapse images of katatrepsis in two plecopteran species, lateral view, anterior of the egg to the top, ventral of the egg to the left. A–C: *Scopura montana*; just before katatrepsis (A), in katatrepsis (B), and just after katatrepsis (C). D–F: *Protonemura towadensis*; just before katatrepsis (D), in katatrepsis (E), and just after katatrepsis (F).

Ab, abdomen; HL, head lobe; SDO, secondary dorsal organ; Y, yolk.

Scale bars = A–C, 100 μm; D–F, 50 μm.

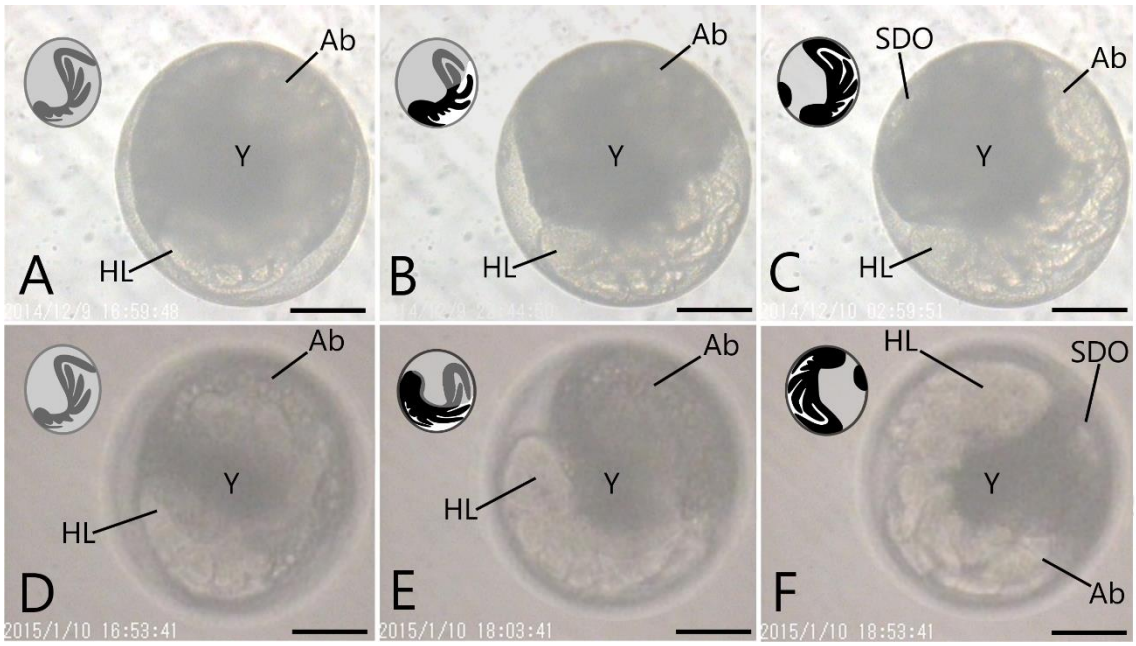
Ab
Y
HL
A
Ab
Y
HL
B
SDO
Ab
Y
HL
C
Ab
Y
HL
D
2015/1/10 16:53:41
Ab
HL
Y
E
2015/1/10 18:03:41
HL
SDO
Y
Ab
F
2015/1/10 18:53:41

Fig. 55. Evaluation of embryological features in Plecoptera, mapping them on the most reliable tree presented (e.g., Zwick, 2000, McCulloch et al., 2016), i.e., with the monophyly of each of Antarctoperlaria, Arctoperlaria, Euholognatha, and Systellognatha strongly suggested. See text.

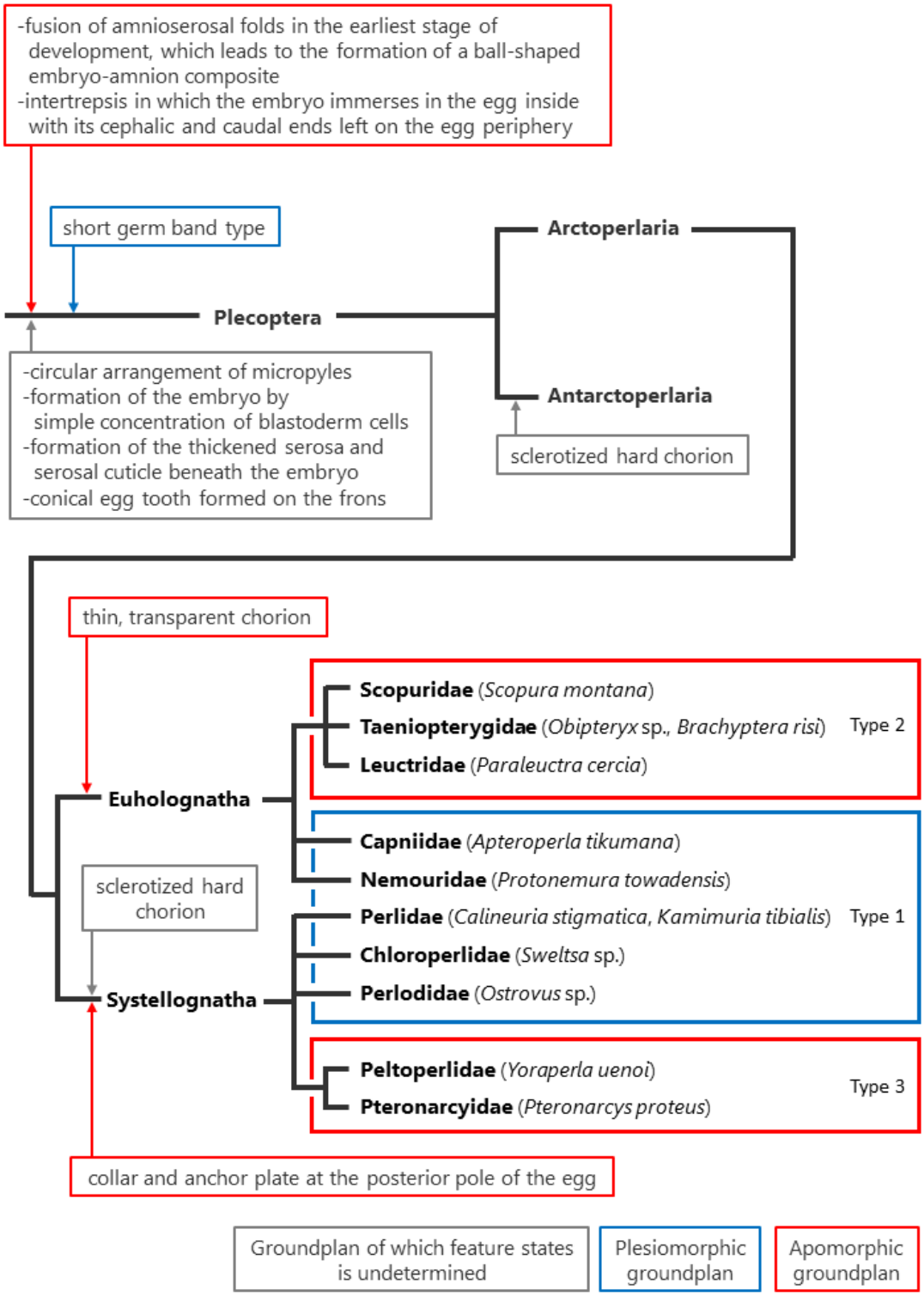
-fusion of amnioserosal folds in the earliest stage of development, which leads to the formation of a ball-shaped embryo-amnion composite
-intertrepsis in which the embryo immerses in the egg inside with its cephalic and caudal ends left on the egg periphery
short germ band type
Arctoperlaria
Plecoptera
-circular arrangement of micropyles
-formation of the embryo by simple concentration of blastoderm cells
-formation of the thickened serosa and serosal cuticle beneath the embryo
-conical egg tooth formed on the frons
Antarctoperlaria
sclerotized hard chorion
thin, transparent chorion
Scopuridae (Scopura montana)
Taeniopterygidae (Obipteryx sp., Brachyptera risi)
Type 2
Leuctridae (Paraleuctra cercia)
Euholognatha
Capniidae (Apteroperla tikumana)
Nemouridae (Protonemura towadensis)
Perlidae (Calineuria stigmatica, Kamimuria tibialis)
Type 1
sclerotized hard chorion
Chloroperlidae (Sweltsa sp.)
Perlodidae (Ostrovus sp.)
Systellognatha
Peltoperlidae (Yoraperla uenoi)
Pteronarcyidae (Pteronarcys proteus)
Type 3
collar and anchor plate at the posterior pole of the egg
Groundplan of which feature states is undetermined
Plesiomorphic groundplan
Apomorphic groundplan